SRDS Report Number
RD 64-160

FINAL REPORT

Contract Number FA-WA-4717
Project Number 206-003-R

METEOROLOGICAL ASPECTS OF THE SONIC BOOM

SEPTEMBER 1964

Prepared for

FEDERAL AVIATION AGENCY
Office of Supersonic Transport Development
and Systems Research & Development Service

by

THE BOEING COMPANY
AIRPLANE DIVISION
RENTON, WASHINGTON

"NOTICES"

The information contained herein is the result of a Federal Aviation Agency sponsored Contract No. FA-WA-4717.

When Government drawings, specifications, or other data are used for any purpose other than in connection with a definitely related Government procurement operation, the United States Government thereby incurs no responsibility nor any obligation whatsoever; and the fact that the Government may have formulated, furnished, or in any way supplied the said drawings, specifications, or other data, is not to be regarded by implication or otherwise as in any manner licensing the holder or any other person or corporation, or conveying any rights or permission to manufacture, use, or sell any patented invention that may in any way be related thereto.

For Sale by Clearinghouse for Federal Scientific and Technical Information
Springfield, VA. 22151 - Price $4.00

FINAL REPORT

Contract Number FA-WA-4717
Project Number 206-003-R
SRDS Report Number RD64-160

METEOROLOGICAL ASPECTS OF THE SONIC BOOM

September 1964

Prepared by

Edward J. Kane

Thomas Y. Palmer

"This report has been prepared by THE BOEING COMPANY under research and development sponsorship of the Office of Supersonic Transport Development and the Research Division, Systems Research and Development Service, Federal Aviation Agency by Contract No. FA-WA-4717, Arthur Hilsenrod, SRDS Project Manager. The contents of this report reflect the views of the contractor, who is responsible for the accuracy of the data presented herein, and do not necessarily reflect the official views or policies of the FAA. This report does not constitute a standard specification or regulation."

THE BOEING COMPANY
AIRPLANE DIVISION
RENTON, WASHINGTON

ABSTRACT

This report is a study of the effect of changing meteorological conditions on the sonic boom produced during steady level flight. The influence of variations in atmospheric temperature, pressure, and wind on this noise are investigated. Simplified methods are established for estimating the effect of these variations. Combinations of meteorological conditions which can produce anomalous propagation such as complete cut-off, focusing, and extreme lateral spread are discussed. The effect of air turbulence near the ground is considered. A number of comparisons with test data measured at Oklahoma City (1964) are presented, and recommendations for additional experimental and theoretical work are outlined.

TABLE OF CONTENTS

LIST OF ILLUSTRATIONS

SECTION I INTRODUCTION

It has been recognized for a number of years that the sonic boom generated during supersonic flight would be an important factor in the design and operation of a commercial supersonic transport airplane. Accordingly, research into the factors which effect the sonic boom have been actively pursued by industry and government agencies. Methods for predicting the influence of the airplane configuration have been established, and are well substantiated with both flight test and wind tunnel data. This approach however, is valid only in a homogeneous atmosphere with constant meterological properties between the airplane and the ground.

Until now, considerably less research has been devoted to developing an understanding of how an airplane's shock waves propagate through nonuniform atmospheric conditions. Some methods of analysis have been based on acoustic propagation through nonuniform temperature regions. Although this is acceptable for predicting shock-wave locations and patterns on the ground, this approach yields little useful information about the shock wave strength under, and to the side of, the flight track. Various correction factors such as the square root of the ratio of the ambient pressure at the ground to that at the airplane, $\sqrt{Pg/Pa}$, have been used to account for the effect of the variation in atmospheric properties between the airplane and the ground. These are based on approximate analysis of acoustic waves.

A more detailed approach to the problem was taken in Ref. 6. In this work the shock waves were assumed to propagate at velocities dictated by their strength, and the effect of pressure, temperature, and wind shear along the path of propagation was taken into account. An additional value of this approach is that it allows solutions of the shock wave strength in regions of focusing where the acoustic theory predicts totally unreal values. This work is expanded in Appendix II. It was also programmed for a digital computer (Refs. 8 and 83). The latter computer program is available from NASA.

The theory and method of Refs. 6 through 8 have been used in this report to predict variations in overpressure which would occur with variations in the atmospheric properties between the airplane and the ground. The purpose of this effort was to determine if variation in atmospheric properties could significantly influence the boom as it propagates between the airplane and the ground. Simplified methods for estimating the effect of such variations are established, and are summarized in Appendix VIII. Comparisons with experimental data are shown and recommendations for future work are also outlined.

The study was divided into investigations of the effects of variations of meteorological conditions in the atmosphere, and the effects of local turbulence. It has been found that:

- Variations in temperature, wind, and pressure can influence the boom strength on the ground.
- Variations in temperature and wind can influence the lateral distribution of the boom to the side of the flight track.
- Variations in temperature and winds can cause anomalous propagation such as complete cut-off (no boom heard on the ground), focusing (local intensification of boom strength), or extreme lateral spread (no cut-off to the side of the flight track).
- The above effects are significant only at Mach numbers below 1.3.
- Local turbulence may change the shape of the pressure wave on its way to the ground.

A number of horizontally stratified model atmospheres have been investigated. The results of the investigation have indicated that for flight at Mach numbers above 1.3 the largest influence of changing meteorological conditions on the sonic boom overpressure is generally no more than about ±5 percent from that generated in the still (no wind) standard atmosphere. For flight at Mach numbers between 1.0 and 1.3 the meteorological conditions between the airplane and the ground may result in more significant variations in the overpressure. The effect of temperature variations from the standard temperature-height curve, and of various winds is shown in Fig. 1. These results are typical of the type found throughout the investigation.

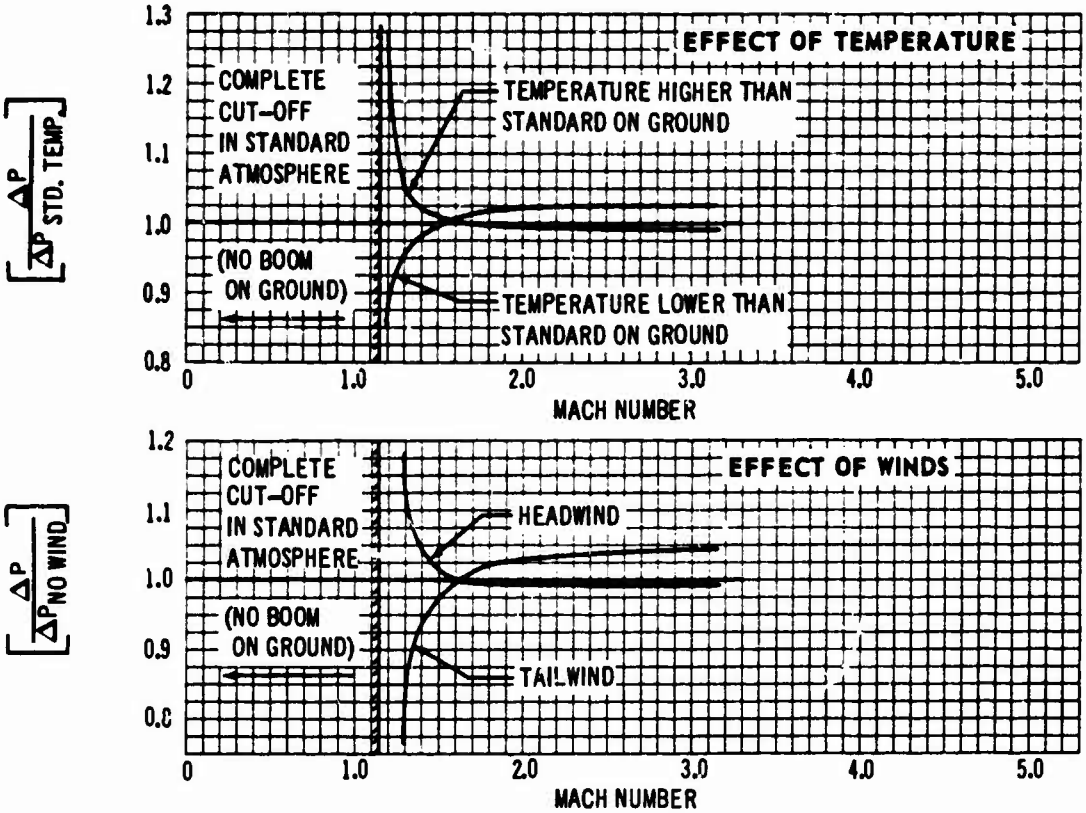

Fig. 1 Effect of Temperature and Winds on Sonic Boom Overpressure.

The figure shows that for Mach numbers less than 1.3, temperatures lower than standard at the ground generally reduce the overpressure, while higher temperatures generally increase the boom. For physically real conditions, this variation may be as much as ±15 percent at Mach 1.2. For Mach numbers less than 1.3, headwinds generally increase the boom while tailwinds and sidewinds decrease it. Winds may cause variation in the overpressure from that in a still atmosphere (no wind) of as much as ±20 percent at Mach 1.3.

Winds may also cause the overpressure, at the lateral cut-off, to be higher than that under the flight track for these low Mach numbers. However, the situation in this case is not fully understood because this phenomena accompanies cut-off where the shock front is locally normal to the ground. This precludes a reflection of the wave from the ground and the normal doubling of the free air overpressure assumed in most calculations (see Section III.D.1). Finally, winds may cause lateral distribution of the boom over much wider areas than normally predicted. This phenomena may occur at all Mach numbers. However, it need cause little concern for two reasons. First, the overpressure in the extended region drops off quite rapidly with distance. Second, it cannot occur if the airplane flies at altitudes above those where maximum winds exist. The contemplated supersonic flight altitudes for the supersonic transport are generally above these maximum winds.

The influence of local turbulence seems to be that of a distorting mechanism which deforms the incoming pressure signature on its way to the ground. Initial efforts to describe the deformation process were not successful, but the development of a more sophisticated approach is continuing. This work is presented, and the proposed steps for the completion of the theory are outlined. Present indications are that interactions of the shock waves with certain turbulent "eddies" result in a scattering of small portions of the incident wave energy to other parts of the wave. This process would lead to rounded signatures at some points on the ground and spiked (or very sharp peaks) signatures at others.

A limited amount of the measured data from the Oklahoma City flight test series was analyzed statistically. To avoid normalizing the data, the analysis considered data measured using the F-104A airplane, flying at Mach 1.5 at an altitude of 28,000 feet, at times when the cloud cover was less than 3/10. The observations were grouped for times near 0700, 0900, 1100 and 1300 Central Standard Time. Results from this work indicated that the important scattering parameters are the angle of the path of propagation of the shock wave, and the time of day (as related to the turbulent intensity). The data indicates that the upper and lower bounds of the overpressure of the front shock of a deformed pressure signature are respectively 2.0 and 0.3 times that for the undeformed measured signature. (The shapes of these signatures are indicated in Fig. 42.)

SECTION II EFFECTS OF VARIATIONS IN ATMOSPHERIC PROPERTIES

Considered in this section, are the effects of various horizontally stratified atmospheric models on the sonic boom produced in steady level flight. The results are presented in two categories; i.e., effects of the standard atmosphere, and effects of variations from the standard atmosphere. Consideration of these effects leads to simplified prediction of the influence of variations in atmospheric properties on the sonic boom and, in most cases, will make use of a computer program unnecessary for routine estimates of the boom strength. Special cases such as cut-off, focusing, etc. are considered in Section III.

(A) STANDARD ATMOSPHERE - The U.S. Standard Atmosphere, 1962 (Ref. 1), which forms the basis for calculations of the performance characteristics of any airplane configuration, has been used to establish the basis of the meteorological effects on the sonic boom. This model is representative of the mean atmospheric properties prevalent in the mid-latitudes. Boom strength, distribution, and extent on the ground has been established for the standard model.

(1) Sonic Boom Under the Flight Track - To predict the sonic boom strength in a nonhomogeneous atmosphere the Whitham theory (Ref. 2) has been modified to account for propagation of the shock wave through a region of varying density. The correction factor used, which yielded relatively close agreement with test data, was a geometric mean pressure given by $\sqrt{Pa\ Pg}$ (Refs. 3 through 5). This factor was used to replace the homogeneous ambient pressure used in the Whitham equation for the boom strength under the airplane. The Whitham equation may be written as shown below:

$$\Delta P_{Whitham} = K_R P_a \frac{(M^2-1)^{1/8}}{h^{3/4}} \frac{2^{1/4}\,\gamma}{(\gamma+1)^{1/2}} \left[\int_0^{Y_0} F(Y,\theta)dY\right]^{1/2} \qquad \text{Eq (1)}$$

where

K_R = Ground reflectivity factor

P_a = Ambient pressure at airplane

h = Airplane distance above ground

M = Airplane Mach number

γ = Ratio of specific heats (1.4 for air)

$\int_0^{Y_0} F(Y,\theta)dY$ = $I(Y_0,\theta)$ - function of airplane geometry and lateral location of the observer (Ref. 2)

To account for sonic boom propagation through the atmosphere, a factor may be applied to this equation which is a function of the atmospheric properties, namely ambient pressure, P , and temperature, T , airplane Mach number, and height above the ground. For $\theta = -90°$, i.e. under the flight track, Eq. (1) becomes:

$$\Delta P_{\text{under flt. track}} = K(P,T,M,H)\, K_R P_a \frac{(M^2-1)^{1/8}}{H^{3/4}} \frac{2^{1/4}\,\gamma}{(\gamma+1)^{1/2}} \left[I(Y_o, -90°) \right]^{1/2}$$

$$= K(P,T,M,H)\, \Delta P_{\text{Whitham}}$$

Specializing this for the properties in the standard atmosphere:

$$\Delta P_{\text{under flt. track}} = K(M,H)\, \Delta P_{\text{Whitham}} = K_A\, \Delta P_{\text{Whitham}} \qquad \text{Eq (2)}$$

The factor K_A is a function of airplane height above the ground and Mach number in the Standard Atmosphere. The variation of this factor was calculated by the method given in Refs. 6-8 and is shown in Fig. 2 for the ground located at sea level. It is compared with the usual correction factor $\sqrt{P_g/P_a}$. (This is equivalent to $\sqrt{P_a P_g}$ when multiplied by the P_a from Eq. (1).)

It can be seen that K_A and $\sqrt{P_g/P_a}$ are very close at the lower altitudes which accounts for the agreement with the early flight test data.

Location of the ground above mean sea level will affect the variation of K_A with height above the ground. This is primarily due to the change in ambient pressure at the ground from that at sea level. Curves, similar to those in Fig. 2, have been prepared for the standard atmosphere with the ground located at 2000, 4000, and 6000 feet above mean sea level. These curves are presented in Appendix I and may be used when the boom is being calculated for areas which are above mean sea level.

Each time the atmospheric properties vary from those in the standard atmosphere, the variation of $K(P, T, M, H)$ with Mach number and height above the ground changes. Generation of a number of charts similar to Fig. 2 for every conceivable variation would be a

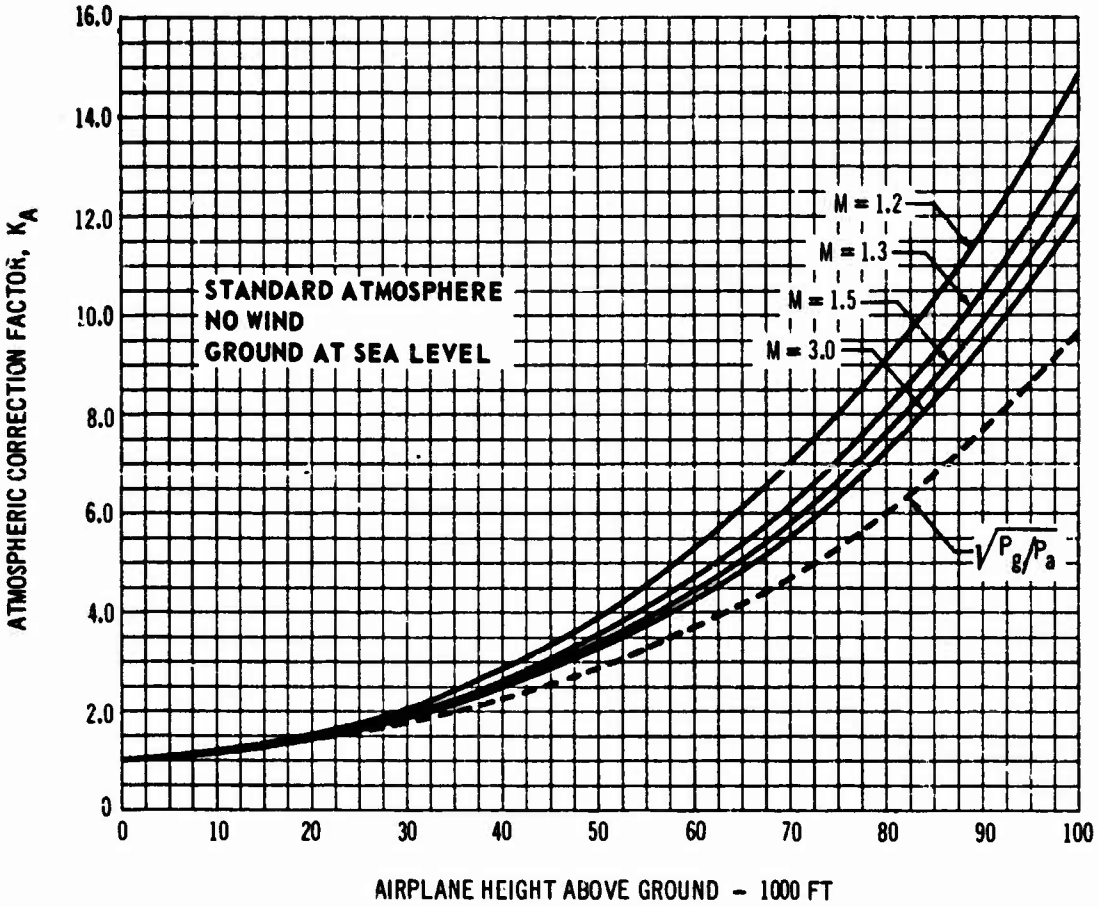

Fig. 2 Atmospheric Correction Factor for U. S. Standard Atmosphere, 1962.

huge task of little value, in that numerous possible combinations exist. The problem of accounting for small variations from the standard atmosphere is covered in Section II.B.

(2) Lateral Distribution of Boom Strength – The lateral distribution of sonic boom strength, as given by Whitham (Ref. 2) varies inversely as the 3/4 power of the distance from the airplane to the point of the observer on the ground. In many cases the airplane configuration is such that the lateral variation of boom strength is also dependent on the variation of $I(Y_o, \theta)$ with θ. The combination of these effects is given below:

$$\Delta P = \Delta P_{\text{under flt. track}} \left[\frac{H}{D}\right]^{3/4} \left[\frac{I(Y_o, \theta)}{I(Y_o, -90°)}\right]^{1/2}$$

where

H = airplane altitude

D = distance from airplane to observer at lateral distance Y from flight track = $(H^2 + Y^2)^{1/2}$

$\theta \doteq -\tan^{-1}(H/Y)$

Rearranging this expression so that the right side is independent of the airplane geometry:

$$\frac{\Delta P}{\Delta P_{\text{under flt. track}}} \left[\frac{I(Y_o, -90°)}{I(Y_o, \theta)}\right]^{1/2} = \left[1+\left(\frac{Y}{H}\right)^2\right]^{-3/8} \qquad \text{Eq. (3)}$$

The variation of boom strength with lateral distance, as computed by the method of Refs. 6-8, is shown in Fig. 3 compared to the prediction obtained by using Eq. (3).

This comparison shows that agreement with Eq. (3) is quite close. The maximum differences are less than ±10 percent and are confined to the very low Mach number points ($M \leqslant 1.2$).

The above results indicate that in the standard atmosphere the variation of boom strength with lateral distance may be very closely approximated by Eq. (3) with $\Delta P_{\text{under flt. track}}$ being obtained by the methods of Section II.A.1. The lateral distribution of sonic boom strength predicted by this method should be suitable for most routine calculations.

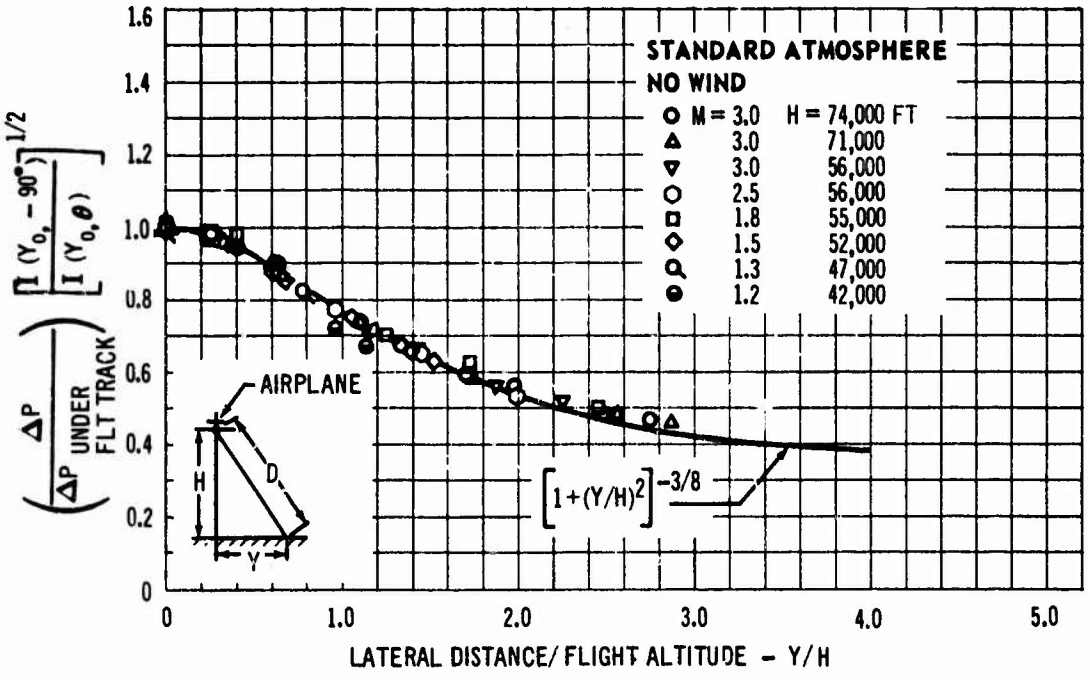

Fig. 3 Variation of Boom Strength with Lateral Distance for U. S. Standard Atmosphere, 1962.

(3) **Lateral Extent of Boom Strength** – Temperature variations in the atmosphere will cause the rays, describing the path of the shock wave from the airplane to the ground, to be distorted. Under some circumstances certain of these rays will not reach the ground but will be refracted back into the atmosphere. It is possible to determine mathematically the lateral extent of the boom by determining the lateral location of the last ray to reach the ground. This has been done by specifying that the direction cosine of the shock front at the ground where lateral cut-off occurs is equal to unity. The location of the lateral cut-off in the standard atmosphere for the ground at mean sea level is shown in Fig. 4 for various airplane Mach numbers and altitudes.

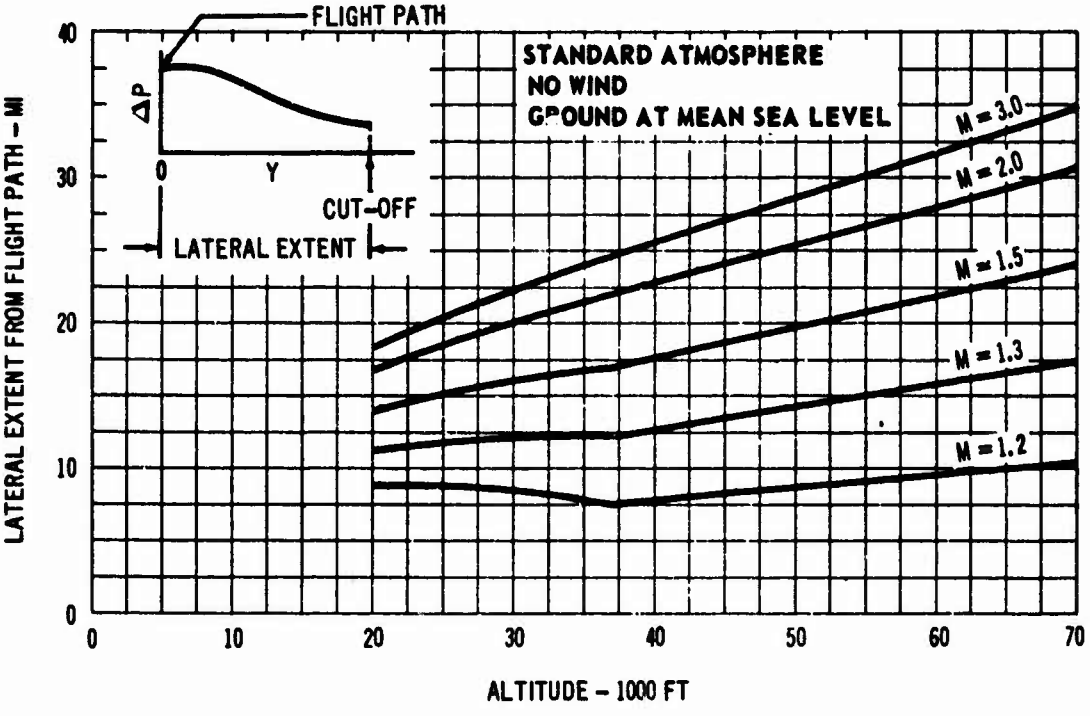

Fig. 4 Lateral Location of Sonic Boom Cut-Off in U. S. Standard Atmosphere, 1962.

Details of the calculations and a general equation for the determination of the lateral location of cut-off on the ground for a general atmosphere are given in Section II.B.6.

The location of the lateral cut-off point defines the point at which the shock front begins to degenerate. Beyond this point noise may be heard as a low rumble. Data from the Oklahoma City flight tests, for instance, indicate that the pressure-time trace recorded beyond the lateral cut-off location is similar to a sine wave. There is no evidence of the sharp pressure rise which is produced by a shock. Thus, beyond the location of lateral cut-off the shock front has degenerated into something similar to an acoustic noise front. This is illustrated by comparing the pressure-time records reproduced in Fig. 5.

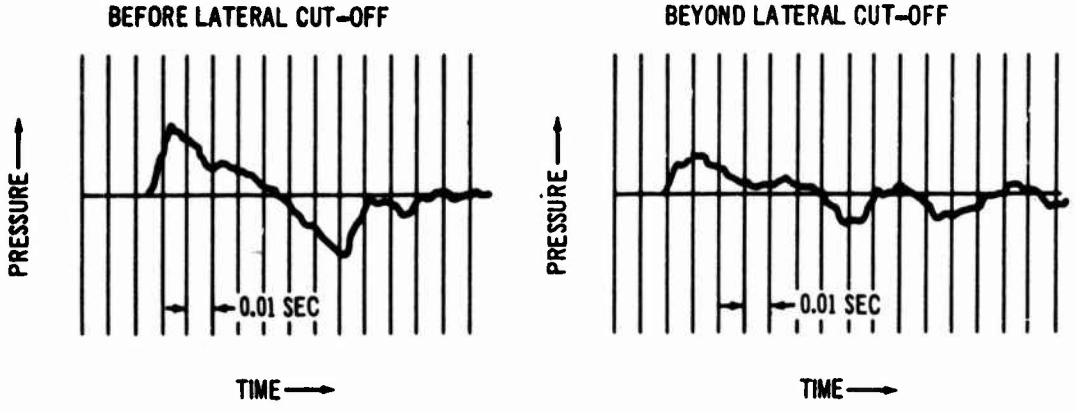

Fig. 5 Pressure-Time Traces Near Lateral Cut-Off.

At the present time there are no data which indicate the rate at which the acoustic noise decays to zero, but the maximum pressure difference above the local ambient pressure is quite small and the pressure rise time is quite large. This should cause little annoyance. For practical purposes, then, the lateral cut-off location would define the boundary of shock wave noise which would be produced by a supersonic airplane.

(4) Routine Calculation of Sonic Boom in the Standard Atmosphere – Once the airplane geometry inputs, $I(Y_o, \theta)$, (see Eq. (1)) have been established for each altitude and Mach number of interest, routine calculations of sonic boom strength, lateral distribution, and lateral extent for steady level flight in the U. S. Standard Atmosphere, 1962 may be obtained in the following manner:

(a) Compute $\Delta P_{\text{under flt. track}}$ from Eq. (2) and Fig. 2 for each Mach number and altitude.

(b) Compute lateral distribution of the boom strength from Eq. (3) for each Mach number and altitude.

(c) Obtain the location of lateral cut-off from the curves in Fig. 4 for each Mach number and altitude, and terminate the lateral distribution of boom strength at this point.

The above method is represented schematically in Fig. 6, and may be used for $M \geq 1.2$ with relatively good accuracy.

(B) VARIATIONS FROM STANDARD ATMOSPHERE – Variations in temperature, pressure, and wind in the atmosphere will produce variations in the sonic boom strength received at the ground. The effect of some typical changes in atmospheric properties from those in the standard atmosphere model are considered in this section. Methods of approximately accounting for these influences are presented, and where approximations are not possible the importance of the resulting effects are discussed. In most cases

involving routine calculations it is possible to make estimates of the boom strength, lateral distribution, and lateral extent without using complex computer calculations.

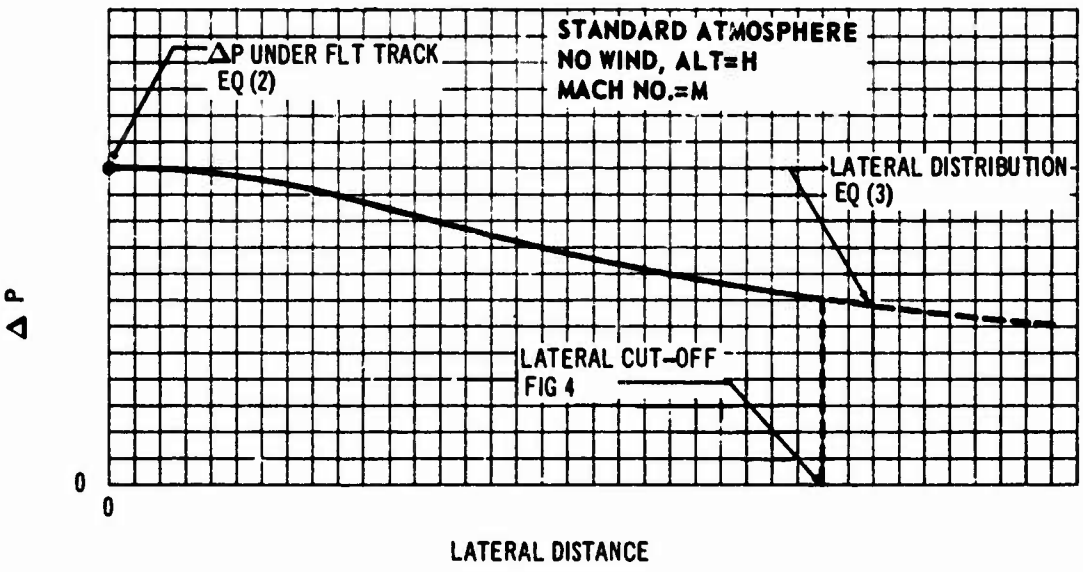

Fig. 6 Routine Calculation of Sonic Boom in U. S. Standard Atmosphere, 1962.

(1) **Temperature** – Atmosphere temperature variations between the airplane and the ground will cause the ray path, which describes the motion of the shock wave through the atmosphere, to be deformed. In general, increasing temperatures along the path of propagation (negative lapse rates) will cause the ray to bend up while decreasing temperatures (positive lapse rates) will cause it to bend down. This distortion of the ray path will influence the boom strength received on the ground. The effect of temperature variations, on the boom strength under the airplane, have been studied for a number of model atmospheres. These models (Refs. 9-16) characterize the following meteorological conditions:

- Various tropopause heights and associated temperature gradients.
- Temperature inversions near the ground caused by nocturnal radiation, snow cover, and coastal stratus.
- Multiple temperature inversions due to mixing and advection.
- Frontal temperature inversions.
- Combinations of the above.

They are summarized in Fig. 7, which shows the standard atmosphere, for reference.

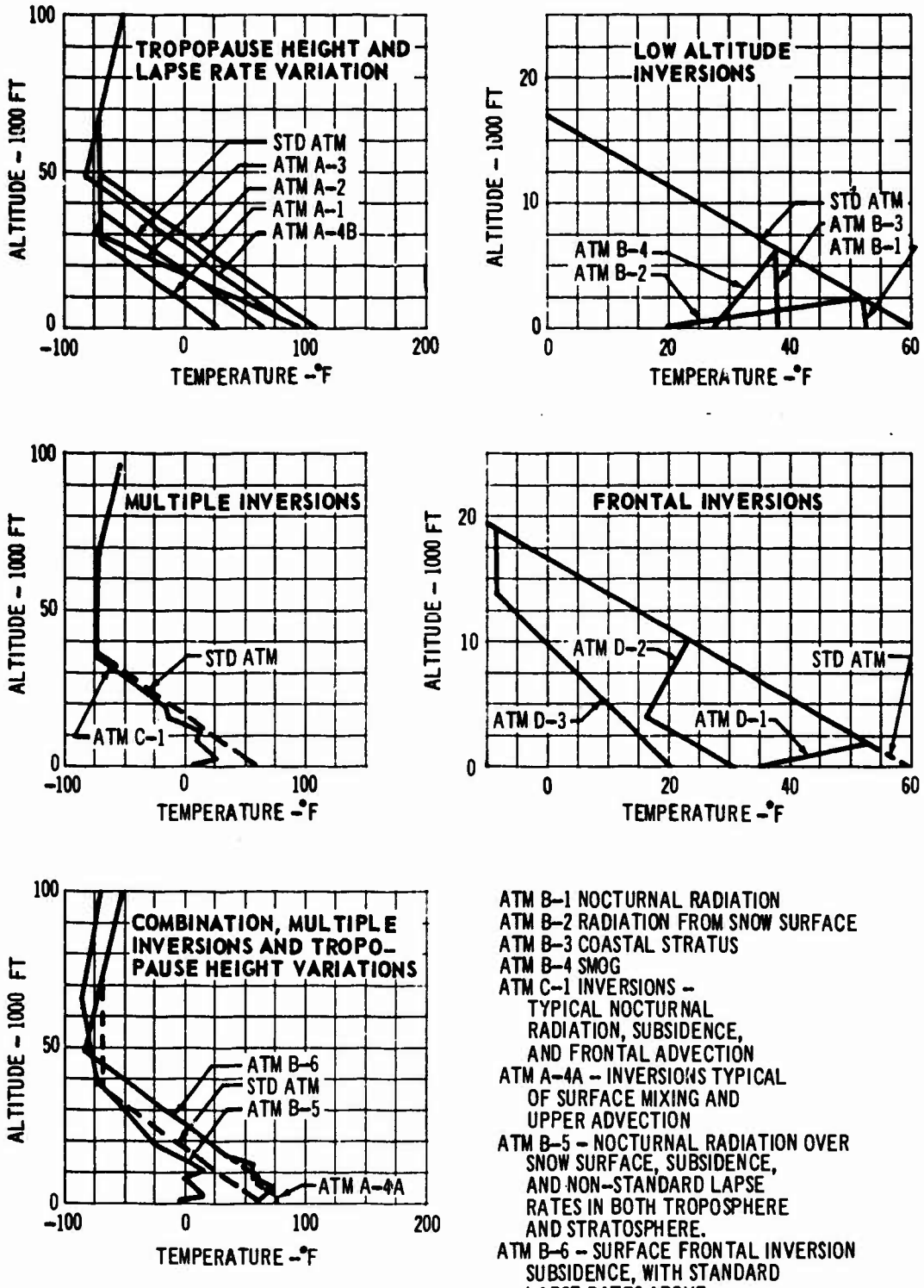

Fig. 7 Summary and Key of Atmospheric Models.

The effect of these variations on boom strength was studied in each temperature model. It was found that the temperature effect was primarily a function of airplane Mach number and the ratio of the absolute temperature at the airplane to that at the ground. This is illustrated in the summary of the calculated data shown in Fig. 8. To better

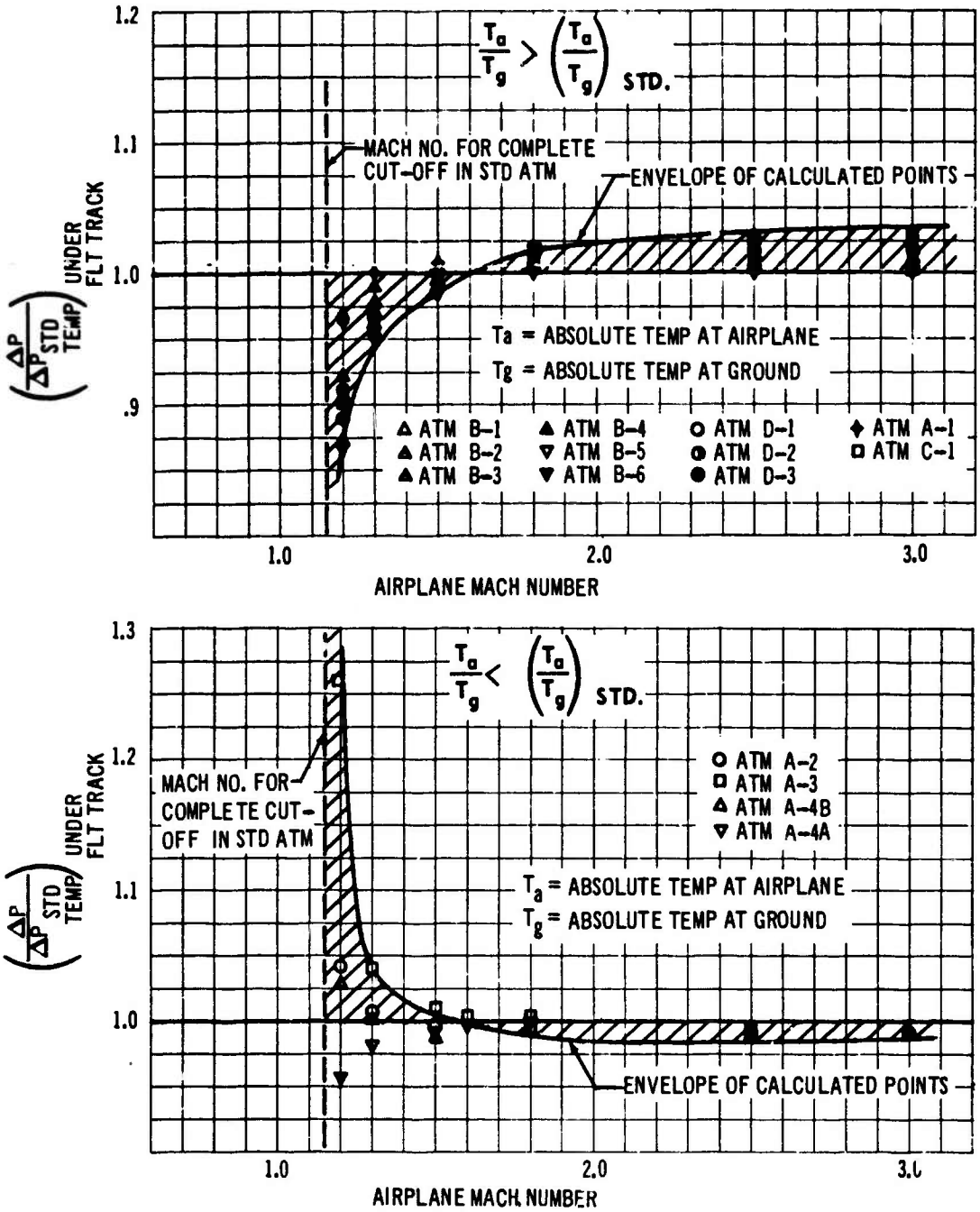

Fig. 8 Effect of Temperature Variations on Sonic Boom Produced Under the Flight Track.

display the variation in boom strength, the overpressure produced under the airplane in each atmospheric model has been divided by the overpressure generated in the standard atmosphere for the corresponding Mach number and altitude.

The data presented in Fig. 8 indicate that significant changes in the overpressure, caused by temperature variations from the standard atmosphere, are mainly confined to the Mach number range between that required for complete cut-off (no boom heard on the ground) and about Mach 1.2. For Mach numbers greater than 1.2 the effect is relatively small. The influence of temperature variations for Mach 1.2 is shown in Fig. 9. This figure presents the data shown in Fig. 8 for Mach 1.2, plotted against the airplane Mach number based on the speed of sound at the ground, M_g ($M_g = Ma_a/a_g = M(T_a/T_g)^{1/2}$).

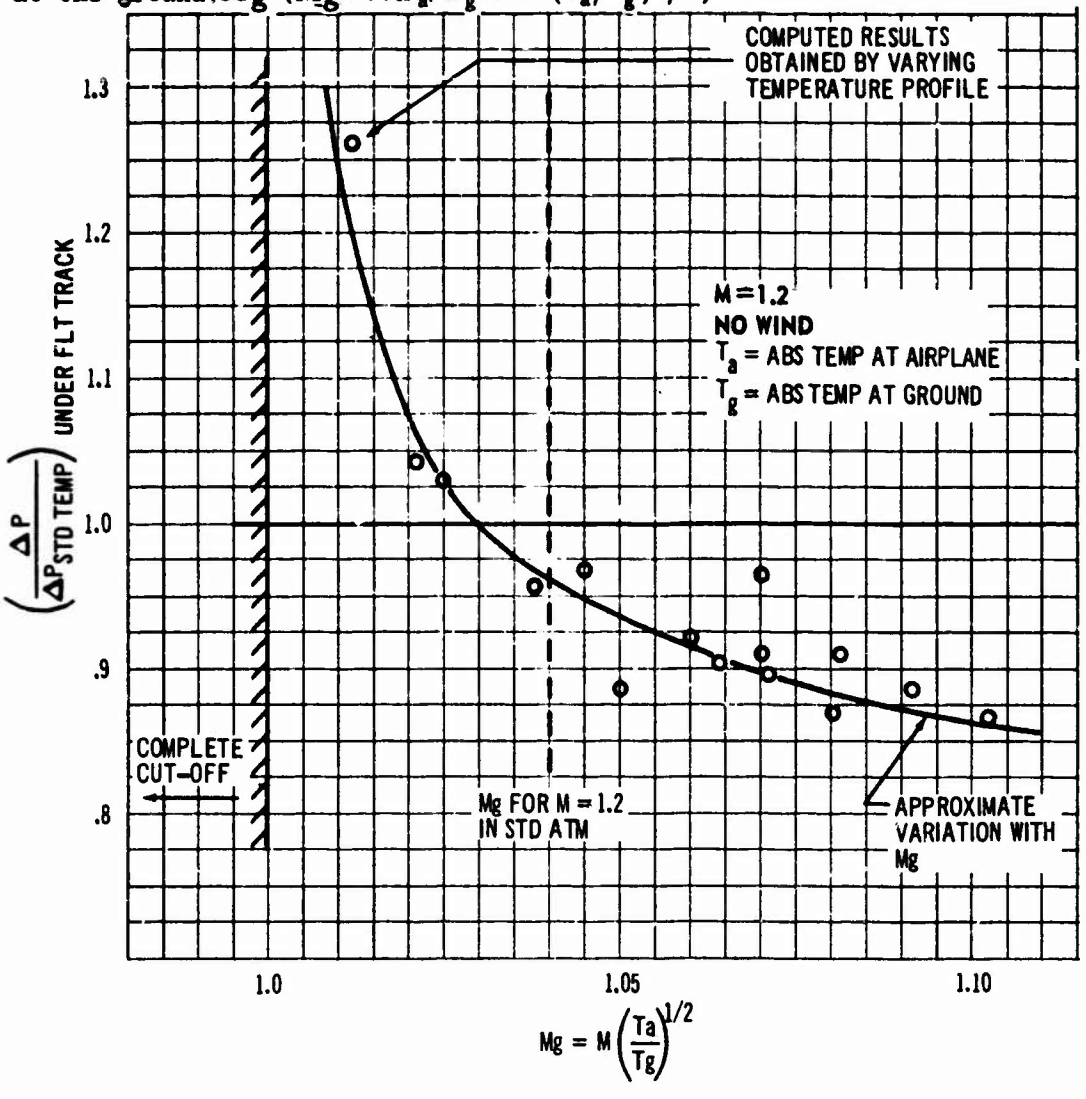

Fig. 9 Approximate Variation of Overpressure with Temperature for Mach 1.2.

When the airplane Mach number is less than or approximately equal to 1.2 extreme care must be used in estimating the boom strength generated under the airplane. Because all the meteorological factors involved may significantly affect the boom strength, simple approximations are not possible in most cases. A more complete discussion of these effects in the low Mach number range is given in Section III. However, for routine analysis it may be possible to approximately estimate the effect of temperature variations on the boom strength by referring to Figs. 8 and 9. The change at Mach 1.2 would be estimated from Fig. 9 and the variations for the rest of the Mach number range would be estimated from Fig. 8. As the variations in boom strength for Mach 1.5 do not usually exceed ±2 percent, the effect of temperature in this range might be neglected for routine calculations.

(2) Pressure - Pressure variations between the airplane and the ground will influence the boom intensity received on the ground. Investigation of the equations describing the propagation of a shock wave through a nonhomogeneous horizontally stratified media (Refs. 6 and 7) indicate that the influence of small variations from an established pressure-height curve can be described by a relationship between the ambient pressures at the airplane and the ground. If the established pressure-height curve is taken as the one for the standard atmosphere the influence of variations from it can be estimated from Eq. (4). (This equation is developed in Appendix III.)

$$\left(\frac{\Delta P}{\Delta P_{\substack{\text{std.}\\ \text{press.}}}}\right)_{\substack{\text{under}\\ \text{flt. track}}} = \left[\frac{Pg}{(Pg)_{std.}}\right]^{1/2} \left[\frac{Pa}{(Pa)_{std.}}\right]^{1/4} \qquad \text{Eq. (4)}$$

where

Pg = Ambient pressure at ground in model

$(Pg)_{std.}$ = Ambient pressure at ground in standard atmosphere

Pa = Ambient pressure at airplane (tapeline) altitude

$(Pa)_{std.}$ = Ambient pressure in standard atmosphere at airplane (tapeline) altitude

The influence of pressure on sonic boom strength is independent of airplane Mach number. This is because the path of propagation (i.e. the ray path) is primarily a function of the temperature variation and airplane Mach number, and is generally independent of the pressure variation in the atmosphere.

This expression has been checked by making a number of comparisons with results obtained using the method of Refs. 6-8. The atmospheric temperature models shown in Fig. 7 were used for the comparison. First, the sonic boom was computed in each model assuming the U.S.

Standard Atmosphere, 1962 (Ref. 1) pressure-height curve. Boom strength was then recomputed assuming a pressure-height curve which was developed by using the hypsometric equation for each temperature model (Ref. 17). These two results were then ratioed to obtain the effect of pressure variations from the standard pressure-height curve on the sonic boom, i.e., $\left(\Delta P / \Delta P_{\substack{\text{std.} \\ \text{temp.}}} \right)_{\substack{\text{under} \\ \text{flt. track}}}$. The comparison between Eq. (4) and the computed results is shown in Fig. 10, for each group of temperature models.

These data show that agreement between Eq. (4) and the computed results is quite close. This equation should be adequate to allow estimation of the effect of normal pressure variations, from the standard atmosphere, on the sonic boom produced under the flight path.

(3) Combined Temperature and Pressure - Variations of both temperature and pressure, in the atmosphere, will affect the strength of the sonic boom received on the ground. The influence of these variations on the sonic boom is a function of airplane Mach number, altitude, and atmosphere thermodynamic properties. In Section II.B.1 it was observed that the influence of temperature variations from the standard temperature-height profile was a function of airplane Mach number, altitude, and the absolute temperature profile. This could be put in the functional form:

$$\left(\frac{\Delta P}{\Delta P_{\substack{\text{std.} \\ \text{temp.}}}} \right)_{\substack{\text{under} \\ \text{flt. track}}} = K(M,T,H)$$

Furthermore, it was observed, in Section II.B.2, that the effect of pressure variations from the standard pressure-height profile was primarily a function of that profile and airplane altitude. This could be put in the functional form:

$$\left(\frac{\Delta P}{\Delta P_{\substack{\text{std.} \\ \text{press.}}}} \right)_{\substack{\text{under} \\ \text{flt. track}}} = K(P,H)$$

The combined effects of pressure and temperature variations from the standard atmosphere can be obtained by the product of the above two functional quantities.

Specifically, if the first of these functional quantities is noted as K_T (temperature correction factor) and the second is put in the form given by Eq. (4), the product of these is:

$$\left(\frac{\Delta P}{\Delta P_{\text{std.}}} \right)_{\substack{\text{under} \\ \text{flt. track}}} = K_T \left[\frac{Pg}{(Pg)_{\text{std.}}} \right]^{1/2} \left[\frac{Pa}{(Pa)_{\text{std.}}} \right]^{1/4}$$

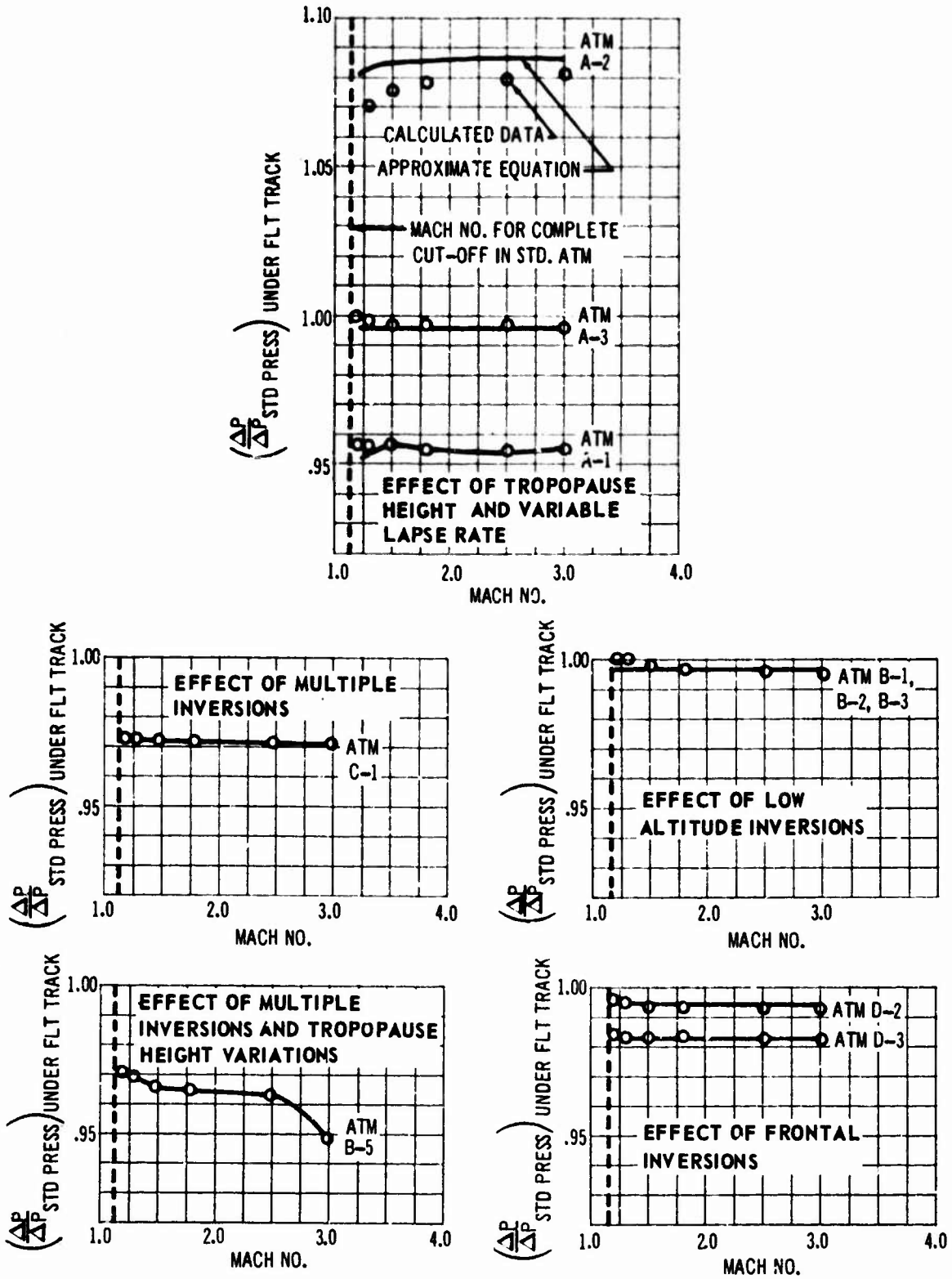

Fig. 10 Effect of Pressure Variations on Sonic Boom Produced Under the Flight Track.

Thus, for a nonstandard atmosphere the overpressure under the flight track would be given by Eq. (5).

$$\Delta P_{\text{under flt. track}} = K_T \left[\frac{Pg}{(Pg)_{std.}}\right]^{1/2} \left[\frac{Pa}{(Pa)_{std.}}\right]^{1/4} K_A \, \Delta P_{\text{Whitham}} \qquad \text{Eq. (5)}$$

where

K_T = Temperature correction factor

Pg = Ambient pressure at ground

$(Pg)_{std.}$ = Ambient pressure at ground in standard atmosphere

Pa = Ambient pressure at airplane tapeline altitude above ground

$(Pa)_{std.}$ = Ambient pressure at airplane tapeline altitude above ground in standard atmosphere

K_A = Atmospheric correction factor for standard atmosphere (see Section II.A.1, and Appendix I)

$\Delta P_{\text{Whitham}}$ ≈ Eq. (1) (See Section II.A.1)

For most routine calculations, the temperature correction factor, K_T, may be determined by the method outlined in Section II.B.1. In some special cases, such as for Mach numbers less than 1.2, special methods may be required in order to make estimates. However, these situations would fall into the special class of problems which are discussed in Section III. Thus, use of the correction factors outlined in Eq. (5) eliminates the need to generate a number of K_A curves (Fig. 2), to allow estimation of the effect of normal atmospheric variations from standard conditions.

(4) Winds - Variation in wind speed and direction (i.e. wind shear) between the airplane and the ground will tend to distort the ray path in much the same manner as variations in temperature. In general, headwinds cause the rays to bend up away from the ground, while tailwinds cause them to bend down. Distortion of the ray paths will cause some variation in sonic boom strength. This variation was investigated by constructing a set of model wind profiles (Refs. 18-35) and calculating the resulting overpressures on the ground. The wind models were selected to be characteristic of:

- Gradients in zonal and meridonal wind components
- High-speed jet streams near the tropopause
- Low-level jet streams over the great plains

Each model was assumed to be omnidirectional, i.e. no lateral shear. The wind models are summarized in Fig. 11 for each of the above categories.

The effect of winds on the overpressures received at the ground was studied by assuming that the wind velocities were aligned parallel and perpendicular to the airplane flight path. In this manner, the influence of headwinds, tailwinds and sidewinds were studied. The overpressures computed by the method of Refs. 6-8 under the flight track

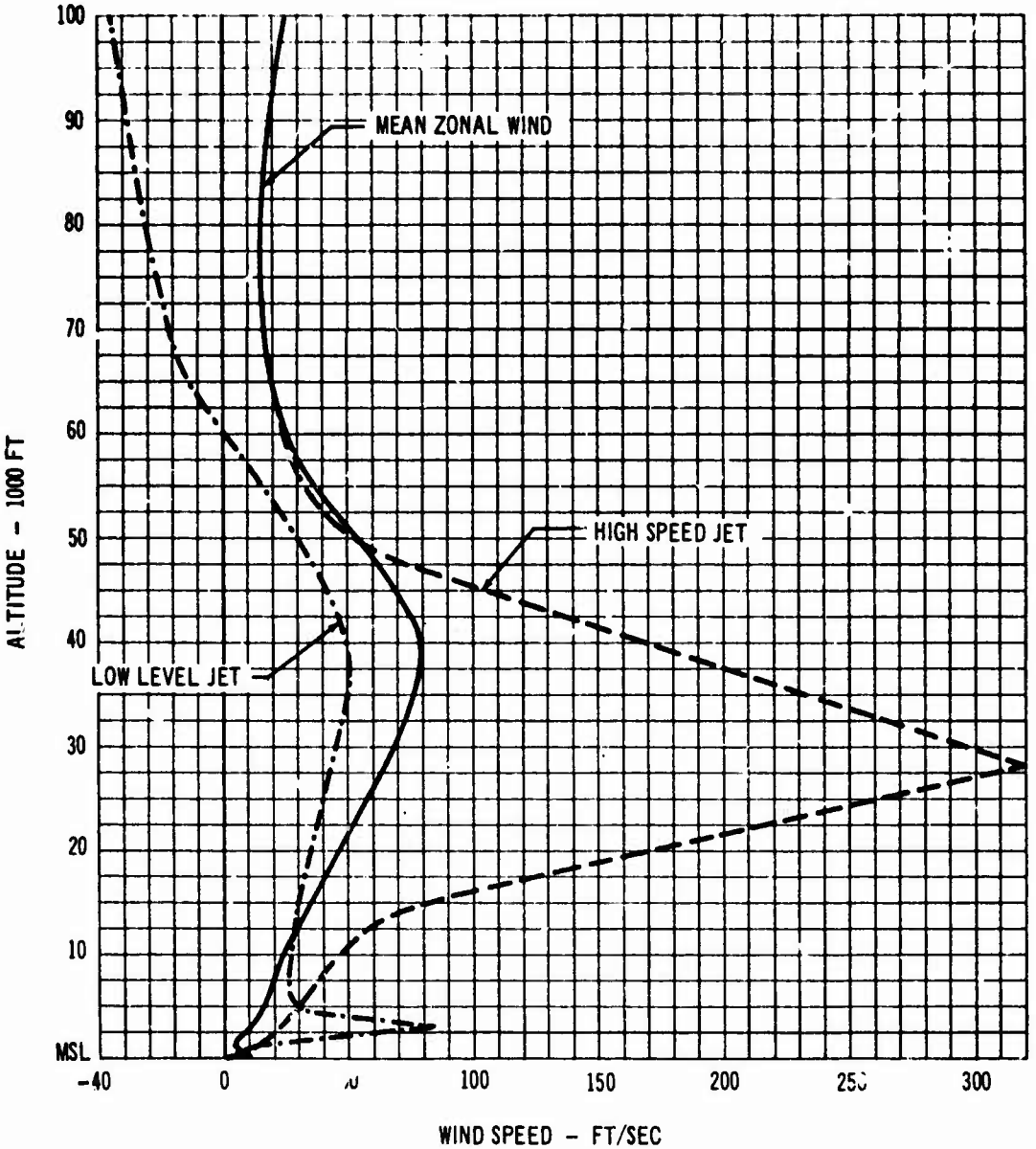

Fig. 11 Summary of Model Wind Profiles.

with wind were divided by the overpressures in the same model atmosphere with no wind, to better indicate the influence of each profile. These results are shown in Fig. 12 for the various assumed wind directions.

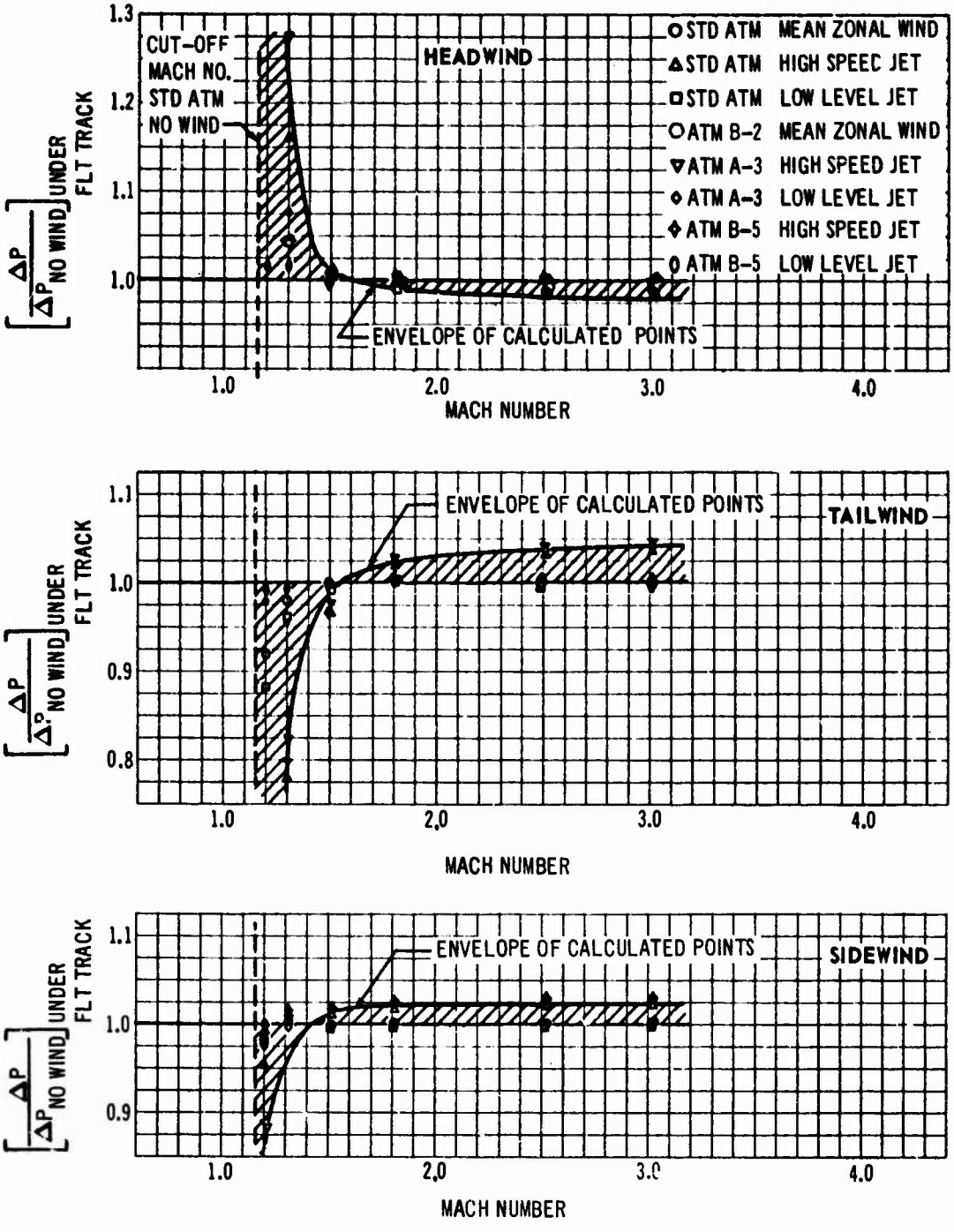

Fig. 12 Effect of Wind on Sonic Boom Under the Flight Track.

This figure illustrates that the headwinds and tailwinds exert the most powerful influence on the overpressure under the flight path for Mach numbers less than about 1.5. Sidewinds seem to have relatively little influence on the sonic boom under the airplane regardless of Mach number. The results for winds parallel to the flight track are similar to those obtained by varying the temperature profile (Section II.B.1). For Mach numbers above 1.5, the effect of winds is relatively small (of the order of ±2 percent). In the Mach number range between 1.2 and 1.5 the wind components parallel to the flight path may have a significant effect. In some cases, especially at low Mach numbers, winds may cause focusing of the sonic boom under or to the side of the flight track. These situations represent a special set of cases which are considered in detail in Section III.B.

Care must be taken in estimating the influence of wind on the boom under the flight track for Mach numbers less than about 1.3, but for Mach 1.3 and moderate winds the effect may be estimated from a cross plot of some of the data in Fig. 12. This is shown in Fig. 13 where the data at Mach 1.3 has been plotted against the sum of the speed of sound ratio (a_g/a_a) and the relative wind component (U^*/a_a) parallel to the flight path.

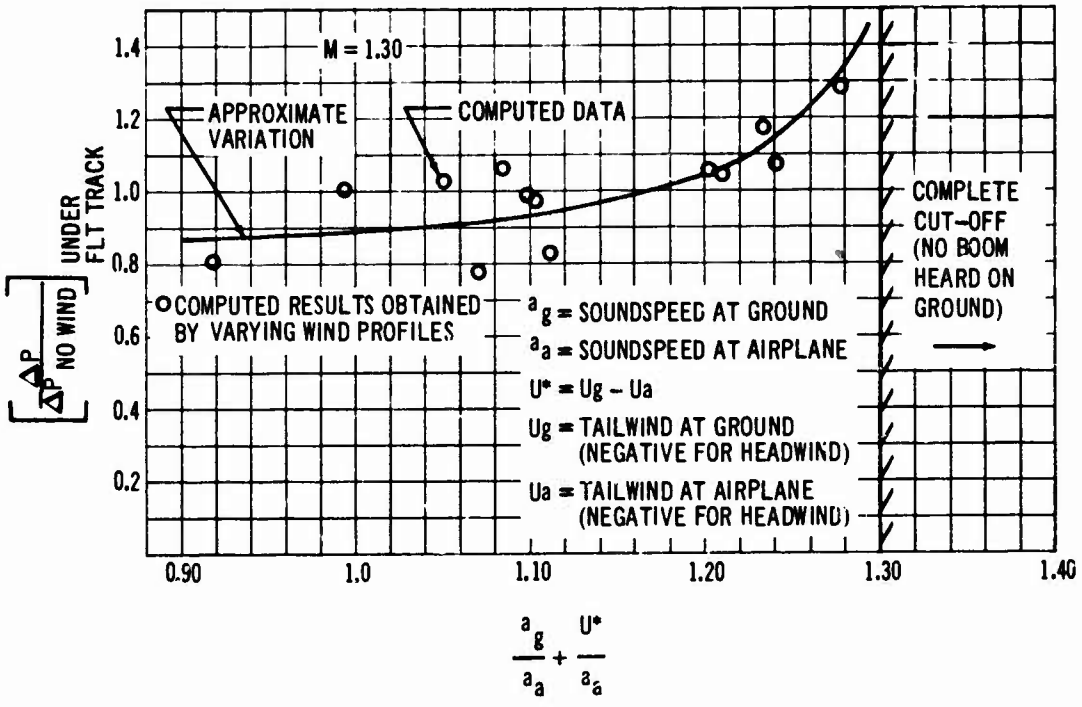

Fig. 13 Approximate Variation of Overpressure with Wind Along Flight Path for Mach 1.3.

The data from this figure may be used to estimate the influence of headwinds and tailwinds at Mach 1.3. Figure 12 data may be used to estimate the effect over the remainder of the Mach number range, for most routine calculations. In routine calculations, the effect of sidewind components could probably be ignored since the most extreme winds cause less than a 5 percent change in the overpressure under the flight path at Mach 1.2, and less than ±2 percent at higher Mach numbers.

(5) Lateral Distribution of Boom Strength – It was shown in Section II.A.2 that according to theory the lateral distribution of the sonic boom strength varied inversely as the 3/4 power of the distance from the airplane to any point on the ground. The expression developed in that section, Eq. (3), was compared to data computed using the method of Refs. 6 through 8 for each of the nonstandard atmospheric models shown in Fig. 7. This comparison is shown in Fig. 14 for several Mach numbers. No wind shear is assumed.

The figure shows that the maximum deviation from the approximate equation, Eq. (3), is about 8 percent for Mach 1.2. The majority of the computed points show very close agreement, especially at the Mach numbers above 1.2. The results of this comparison would indicate that Eq. (3) should yield a relatively good approximation for both standard and nonstandard atmospheric models.

The presence of wind shears will also influence the lateral distribution of the boom strength. In some cases the approximation obtained by using Eq. (3) may not be sufficient and more complicated methods must be used. The validity of the simple approximation was checked in the standard atmosphere with the mean zonal and high-speed jet wind profiles (Fig. 11). The wind directions were taken individually as tailwinds, headwinds, and sidewinds and the distribution of boom strength under the airplane was computed for each case. The computed results are compared to Eq. (3) in Fig. 15(a) for the mean zonal wind profile and in Fig. 15(b) for the high-speed jet wind profile.

The figure shows that for the mean zonal wind profile (Fig. 15(a)), the agreement with Eq. (3) is quite good at all Mach numbers above 1.2. In the case of high-speed jet profile (Fig. 15(b)) agreement is not quite as good, especially at low Mach numbers. From this comparison, it appears that estimates computed using the approximate equation, Eq. (3), are sufficient in cases of moderate winds (with maximum wind speeds less than about 100 feet per second) at all Mach numbers, and for high winds at Mach numbers greater than about 1.5. The results at low Mach numbers for the high-speed jet profile illustrate some of the special cases discussed in Section III.B. For instance, at Mach 1.2 both the headwind and tailwind cause complete cut-off so that no boom would be heard on the ground. However, as a sidewind the high-speed jet would cause lateral focusing off the flight track (i.e. overpressures to the side of the flight track higher than those under it). In the cases of high wind speeds in the vicinity of the airplane altitude, extreme care must be exercised when estimating the boom strength and

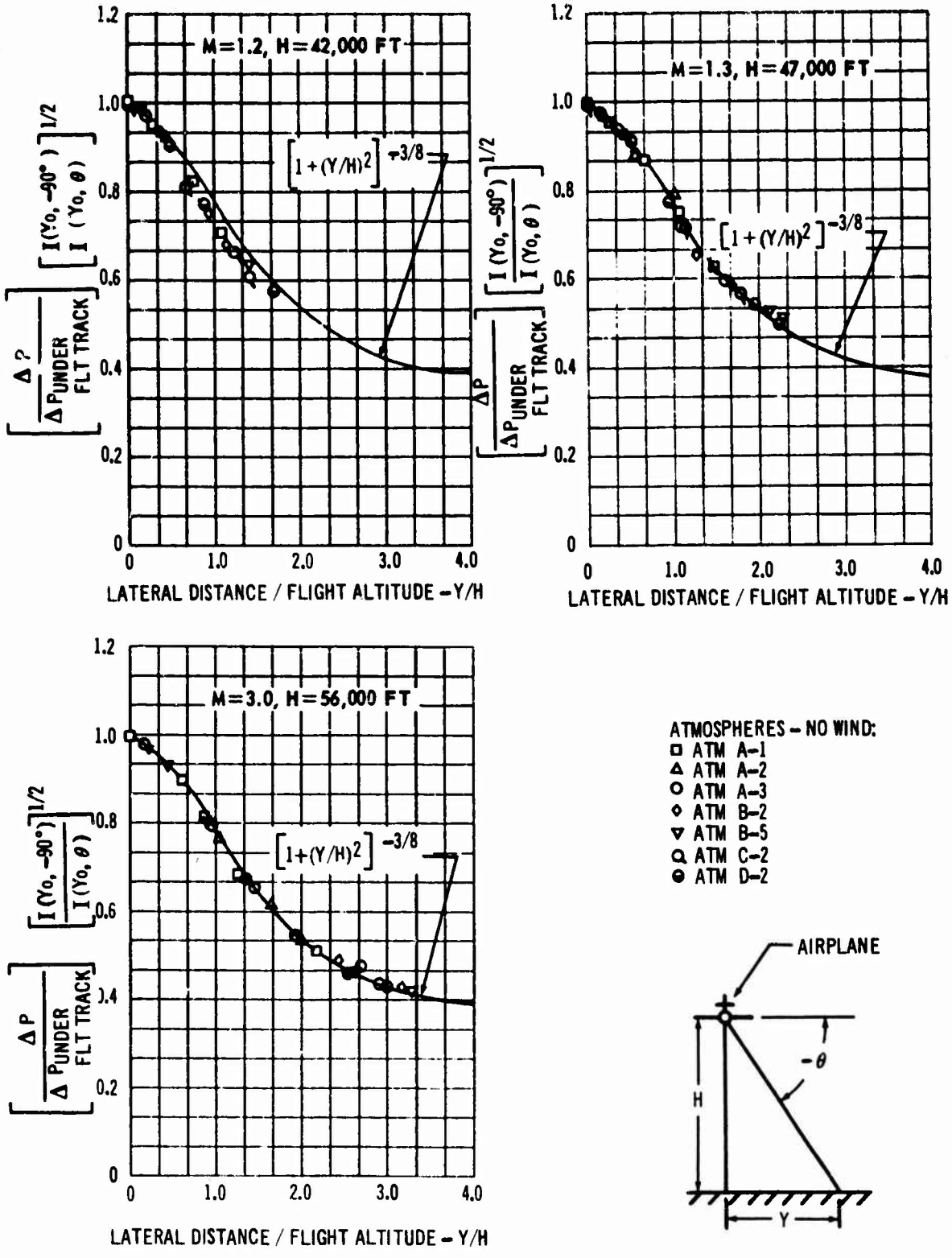

Fig. 14 Variation of Sonic Boom Strength with Lateral Distance for Non-Standard Model Atmospheres (No Wind).

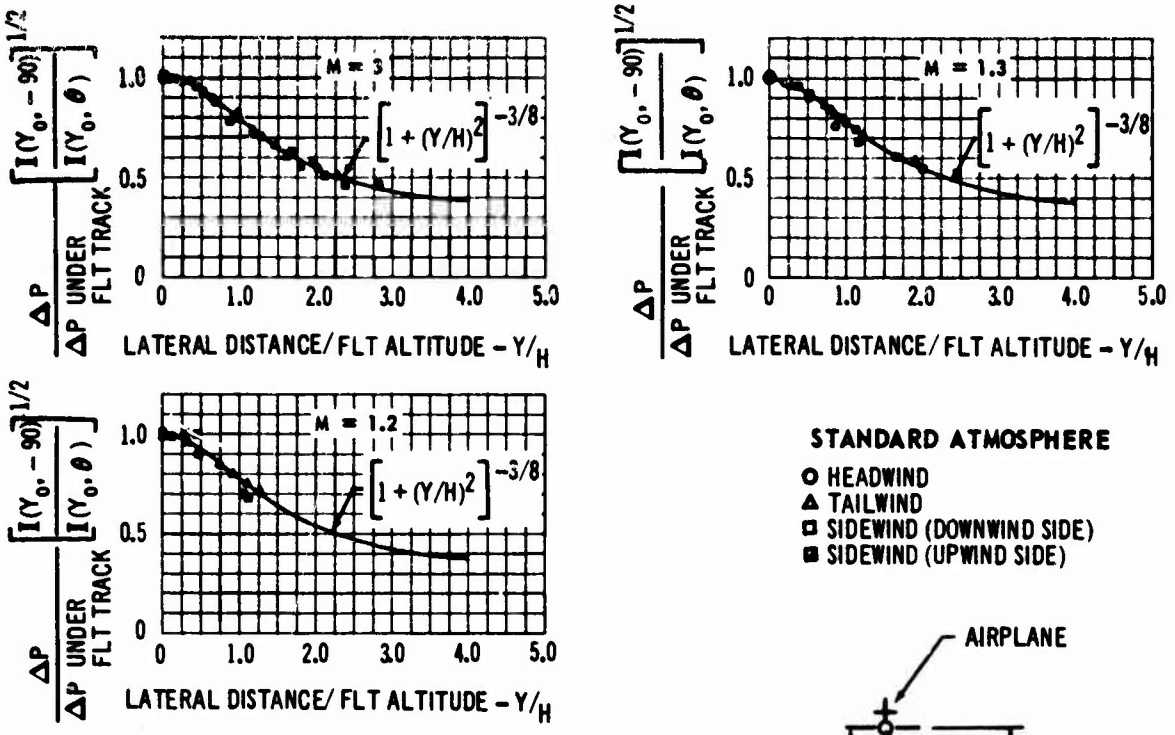

(A) MEAN ZONAL WIND PROFILE (FIG. 11)

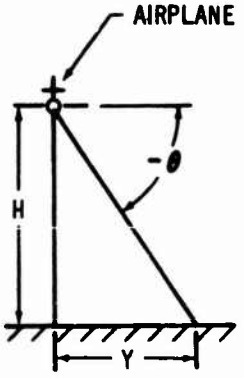

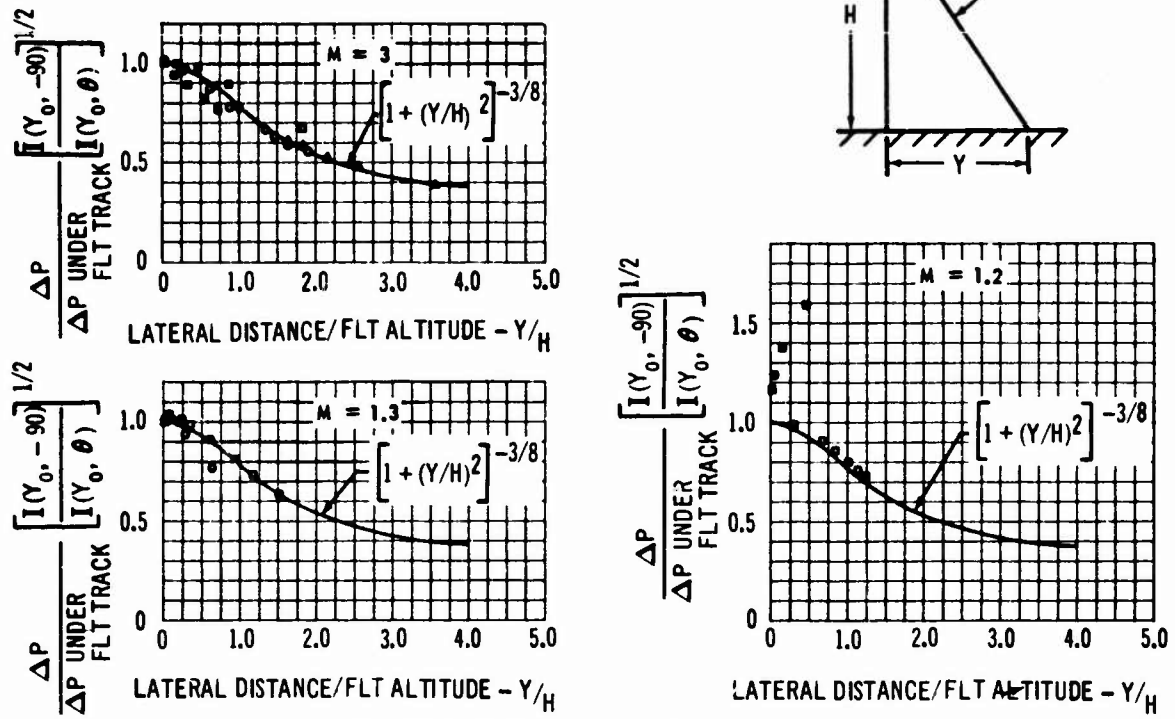

(B) HIGH SPEED JET PROFILE (FIG. 11)

Fig. 15 Effect of Wind on Loterol Distribution of Sonic Boom Strength.

distribution on the ground. This situation represents a set of special cases which are covered in more detail in Section III.B. Criteria are established in that section so that these special situations may be isolated and investigated separately if necessary. For ordinary meteorological conditions the approximation established previously should be sufficient in making routine estimates of the lateral distribution of the boom strength on the ground.

(6) Lateral Extent of Boom Strength – The lateral extent of the boom strength to the side of the flight track in a still atmosphere is determined primarily by the temperature distribution between the airplane and the ground, the flight altitude, and airplane Mach number. The location of the lateral cut-off point does not necessarily define the location beyond which no noise will be heard as noted in Section II.A.3. It is possible to theoretically determine the lateral extent of noise by investigating the equations describing the path of the shock front from the airplane to the ground. These paths are commonly called ray paths and their lateral extent is found by determining the location of the last ray to reach the ground.

Consider a general temperature profile such as that shown in Fig. 16, where the temperature is assumed to vary linearly between significant levels.

The lateral location of the last ray to reach the ground for this profile is given by (this equation is developed in Appendix IV):

$$Y_{max} = \pm\left[1-\left(\frac{1}{M}\frac{a_{max}}{a_{apl}}\right)^2\right]^{1/2} \sum_{n=1}^{n=4} \frac{[a_{max}^2-a_n^2]^{1/2}-[a_{max}^2-a_{n+1}^2]^{1/2}}{a_{n+1}-a_n}(z_{n+1}-z_n) \quad \text{Eq. (6)}$$

In some cases the temperature between two levels is constant, such as in the stratosphere of the standard atmosphere. Assuming this occurs between levels z_m and z_{m+1} (i.e. $a_m = a_{m+1}$) the term in Eq. (6) involving $(z_{m+1}-z_m)$ becomes:

$$\frac{a_{m+1}}{(a_{max}^2-a_{m+1}^2)^{1/2}}(z_{m+1}-z_m) \quad \text{Eq. (7)}$$

This is further illustrated in Appendix IV where Eq. (6) is expanded for the standard atmosphere.

The assumptions involved in deriving Eq. (6) are that the speed of sound varies linearly between levels, and that the shock front travels at speeds nearly equal to the local speed of sound. The influence of these assumptions has been checked by comparing results computed by the method of Refs. 6-8 with those computed using the above equations. A typical example of this comparison is shown in Fig. 17 for the model temperature profile B-5 (Fig. 7), at several Mach numbers and altitudes.

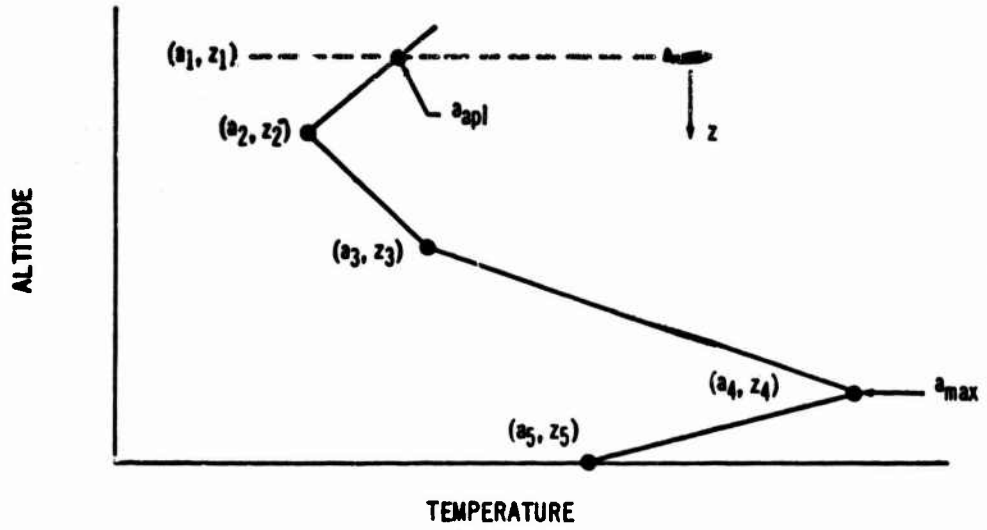

Fig. 16 General Temperature Profile

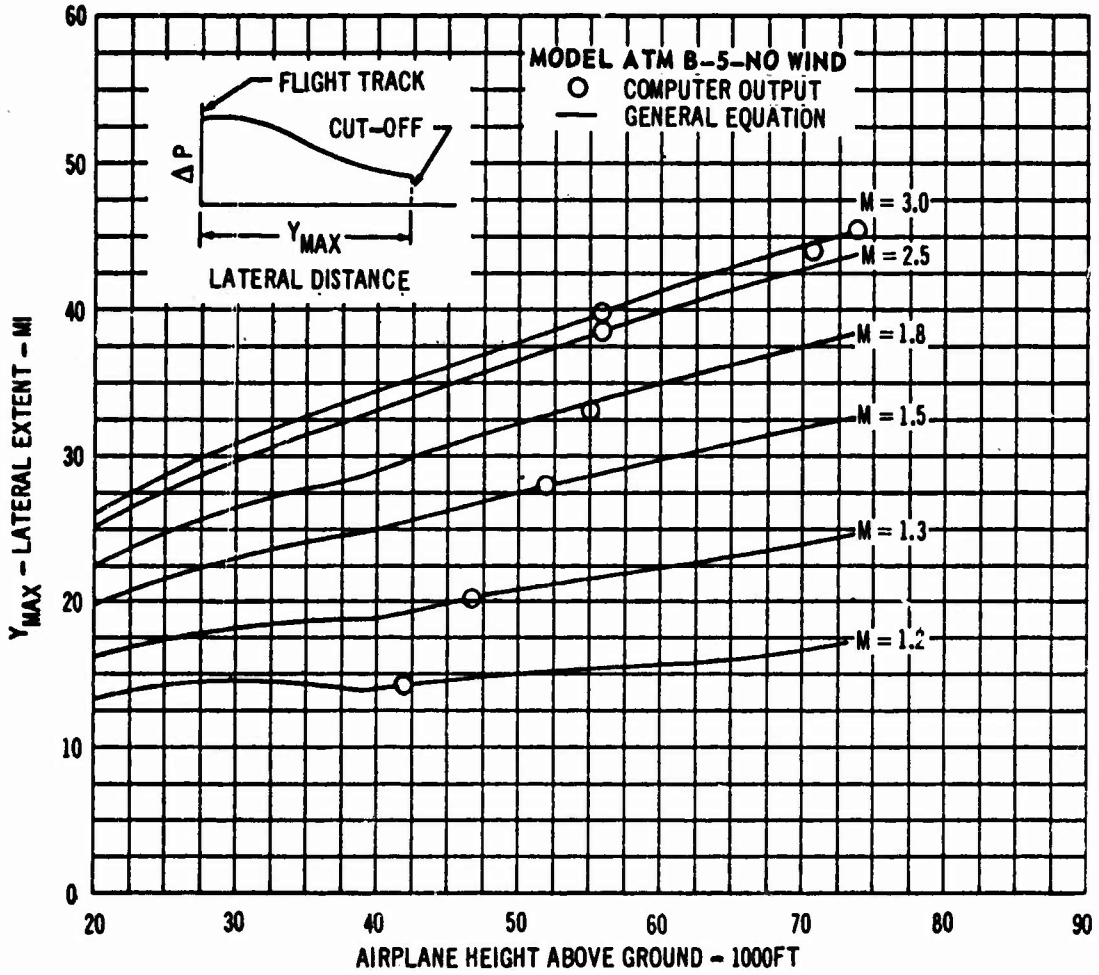

Fig. 17 Comparison of Computed Location of Lateral Cut-Off.

The figure shows that the effect of the assumptions is not very significant, as the results computed by both methods are quite close.

Variations in the temperature profile will cause variations in the location of the lateral cut-off. The extent of the lateral distribution of sonic boom strength was computed for each of the atmospheric models shown in Fig. 7.

The variation in lateral extent is shown in Fig. 18 for the two models which produced the widest deviations from the values in the standard atmosphere. The extent in the standard atmosphere is shown for reference.

The figure shows that, in the extreme cases, variations from the standard atmosphere locations 5 to 10 miles may occur. In general, temperatures lower than standard on the ground will increase the lateral extent, Y_{max}, while ground temperatures higher than standard will decrease Y_{max}.

Wind shears will also affect the location of lateral cut-off off. The magnitude of the variation caused by moderate winds was studied in the standard atmosphere with the mean zonal wind profile (Fig. 11.). The value of Y_{max} was computed by the method of Refs. 6-8, for a headwind, tailwind, and sidewind. For the purposes of comparison these values were divided by the value of Y_{max} with no wind for the same Mach number and altitude and are shown plotted in Fig. 19 against airplane Mach number.

The figure shows that for moderate winds the maximum variation occurs at Mach numbers near 1.2. For Mach numbers greater than about 1.5 the variation is of the order of ±5 percent. In general, tailwinds and sidewinds (on the downwind side) increase the value of Y_{max}, while headwinds and sidewinds (on the upwind side) decrease Y_{max}. In some cases strong winds may substantially increase the magnitude of Y_{max}. The conditions required for this to occur are described more fully in Section III.B.4. For purposes of routine calculation the influence of moderate winds on the location of the lateral cut-off point might be ignored or estimated from Fig. 19.

(7) Routine Calculations of Sonic Boom in General Atmosphere – The method for calculating sonic boom distribution on the ground was outlined in Section II.A.4, for the U.S. Standard Atmosphere, 1962, with no wind. A similar procedure would be used in making routine estimates for a general atmosphere with wind. The following method should be used with extreme care for Mach numbers between 1.0 and 1.3, especially in cases when wind shears are to be considered. Criteria for meteorological conditions which may cause anomalies in the overpressure and distribution of the sonic boom are developed in Section III. These should be checked when making calculations in the above Mach number range.

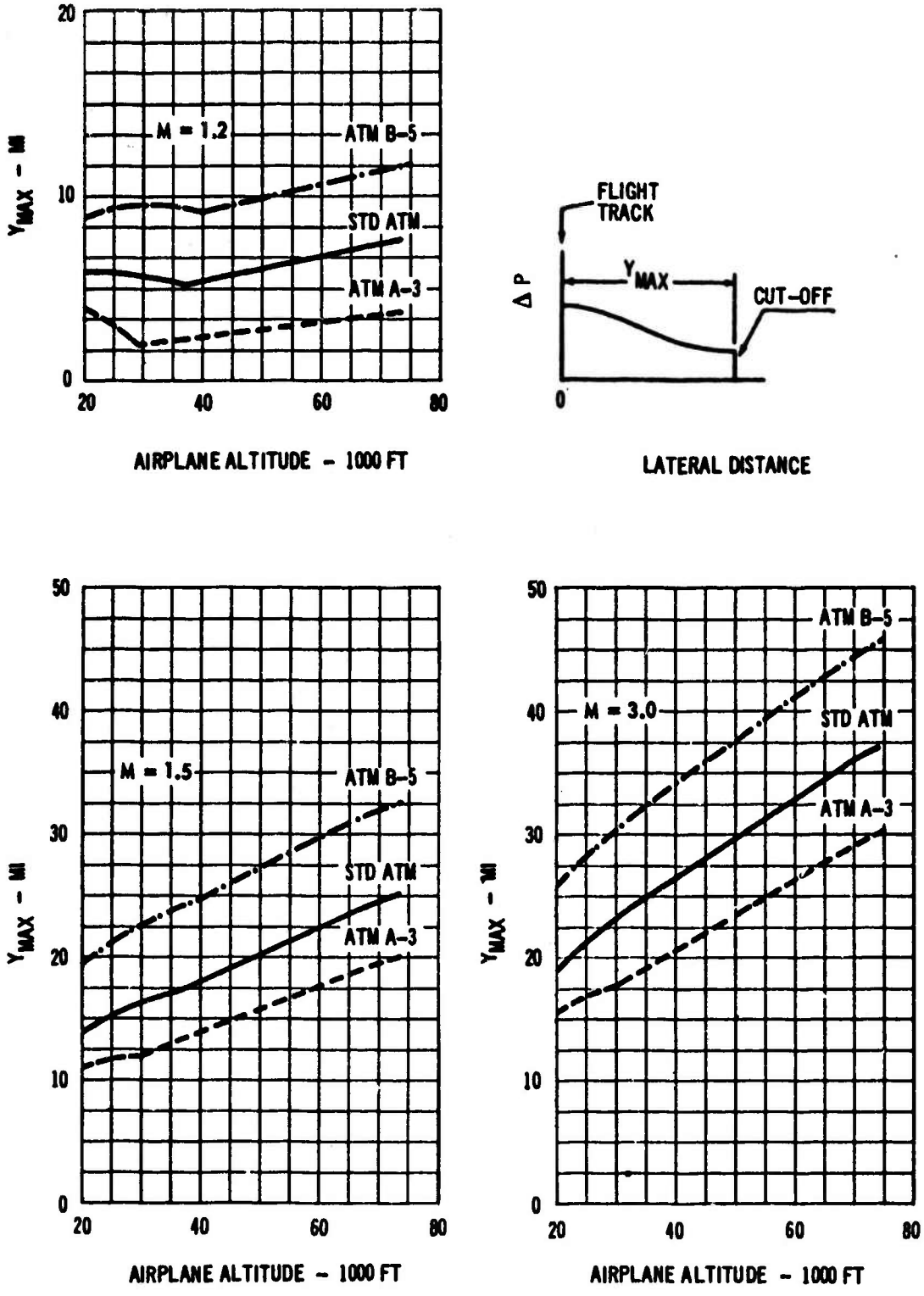

Fig. 18 Variation of Lateral Extent With Temperature Profile.

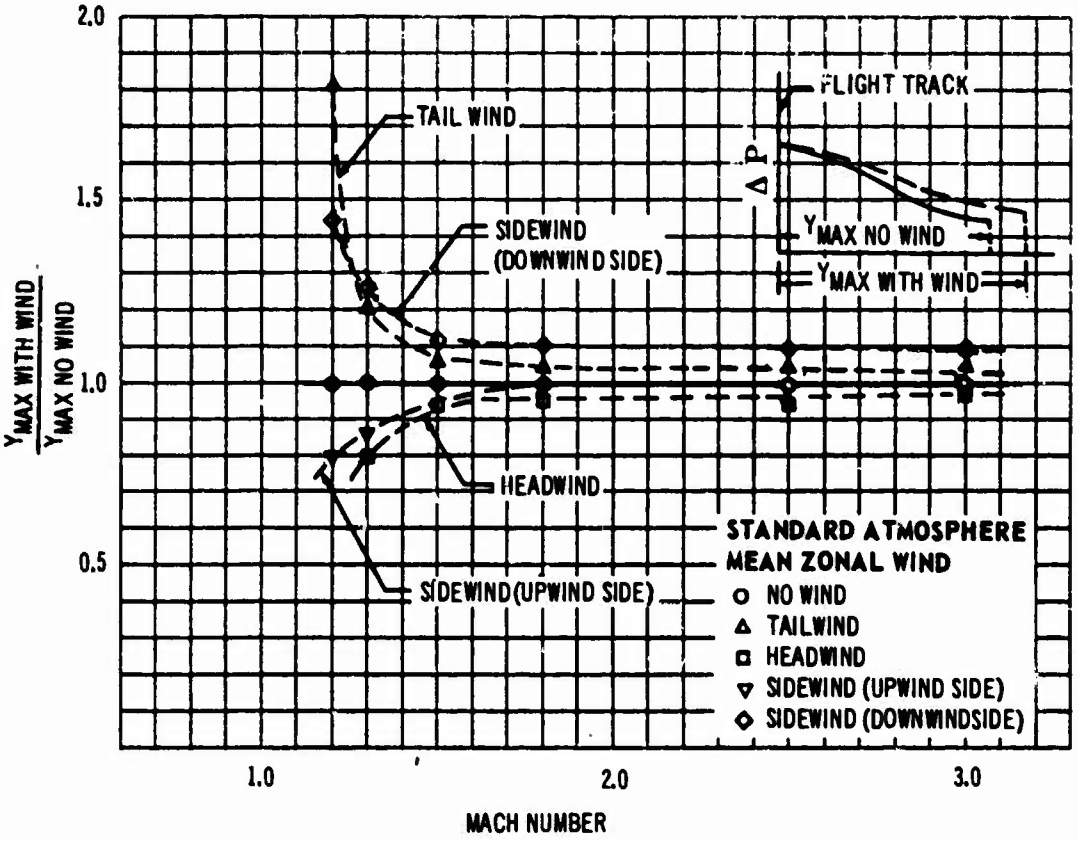

Fig. 19 Variation of Location of Lateral Cut-Off With Wind

Once the airplane geometry influence, $I(Y_o, \theta)$, (see Eq. (1)) has been determined for each Mach number and altitude of interest the calculation of sonic boom strength and distribution may proceed as follows:

(a) Calculate $\Delta P_{\text{under flt. track}}$ from Eq. (5) and Fig. 2 (or Appendix Figs. I-1, I-2, or I-3 for the ground located above 0 MSL) for each altitude and Mach number

- The variation of the temperature correction factor, K_T , with Mach number may be estimated from Fig. 8, with the value at Mach 1.2 estimated from Fig. 9.
- The variation of the correction for wind shears with Mach number may be estimated from Fig. 12 with the value at Mach 1.3 taken from Fig. 13.

(b) Compute the lateral distribution of sonic boom strength from Eq. (3) for each altitude and Mach number. (Caution must be exercised when estimating the lateral distribution for low Mach numbers and high winds, Fig. 15.)

(c) Obtain the location of lateral cut-off from Eq. (6) and Eq. (7) for each Mach number and altitude, and terminate the lateral distribution at that point. (Effect of moderate winds on the lateral cut-off location may be estimated from Fig. 19.)

The above procedure was generally illustrated in Fig. 6, which may be referred to as a guide for performing routine calculations of the sonic boom intensity and distribution on the ground in a nonstandard atmosphere.

(C) SUMMARY OF RESULTS -The effect of variations in temperature and pressure on the sonic boom intensity and lateral distribution were established in this section for the U. S. Standard Atmosphere, 1962. Variations in these properties from the standard conditions and the presence of winds were also investigated. Simplified methods for predicting the influence of these changes were developed. Further, these investigations indicated that the effect of varying meteorological conditions for flight at Mach numbers above 1.3 on the sonic boom intensity is generally no more than ±5 percent from that generated in the still, standard atmosphere. Flight at Mach numbers below 1.3 may result in more significant variations in the overpressure.

SECTION III A REVIEW OF CONDITIONS WHICH MAY CAUSE ANOMALOUS PROPAGATION

Various meteorological conditions may exist between the airplane and the ground which will cause unusual influences on the sonic boom intensity and its lateral distribution at the ground. It is the purpose of this section to discuss these conditions, their effect on the overpressure, and when possible, to present criteria for determining the conditions necessary to produce the anomaly. The presence of the required conditions may result in focusing (local intensification of the boom), complete cut-off (no boom heard on the ground), extreme lateral spread (boom heard at extremely large distances to the side of the flight track), and distortion of the wave form due to interaction with turbulence. Variations in temperature alone can cause focusing or cut-off, while variations in both wind and temperature can cause focusing, cut-off, or extreme lateral spread. For purposes of simplicity it is convenient to consider these in terms of temperature and wind produced anomalies. The effects of low altitude turbulence, the shock wave history near cut-off, and the effect of high altitude turbulence and shower clouds are also discussed.

(A) TEMPERATURE PRODUCED ANOMALIES - The primary influence of temperature variations in the atmosphere is to distort the ray path, which describes the path of the shock front from the airplane to the ground. In some situations, the temperature variation can be such that the rays are refracted so completely that the boom will not reach the ground. This condition is known as "complete cut-off" of the sonic boom. On the other hand the conditions may be such that the boom will be focused (i.e. locally intensified) at a point on the ground. Both of these phenomena occur at very low Mach numbers where the speed of the airplane relative to the ground is nearly equal to the local sound speed at the ground.

(1) Complete Cut-off - Investigation of the ray path equations (Eqs. II.1a) through (II.1f) in the Appendix) indicates that for conditions of no wind the sonic boom will be prevented from reaching the ground if the velocity of the airplane relative to the ground is less than the maximum speed of sound at any altitude between the airplane and the ground. Stated in terms of the airplane Mach number, $M < a_{max}/a_a$. The limiting value of Mach number, $M_{cut\text{-}off}$, is determined by putting this in the form of an equality which is expressed in Eq. (8) below.

where

$$M_{cut\text{-}off} = \frac{a_{max}}{a_a} \qquad \text{Eq. (8)}$$

$M_{cut\text{-}off}$ = Largest airplane Mach number at which complete cut-off will occur.

a_{max} = Largest value of sound speed between the airplane and the ground.

a_a = sound speed at the airplane.

This relationship also defines the meteorological conditions required for no boom to reach the ground. It has been applied in Fig. 20 to several examples to illustrate the application to the standard and nonstandard atmospheres. The model atmospheres considered are illustrated in Fig. 7. The figure shows that for altitudes above 36,000 feet, the limiting Mach number lies generally between 1.1 and 1.2. No boom would be heard on the ground for flights in a still atmosphere at Mach numbers less than the $M_{cut\text{-}off}$ at the airplane altitude.

(2) Focusing on the Ground – Focusing or intensification of the sonic boom overpressure will occur if a set of adjacent ray paths describing the propagation of a portion of the shock front tend to come together. This leads to cusping or folding over of the shock front at a point where the area between the adjacent rays (i.e. ray tube area) tends to go to zero. This phenomena is discussed in more detail in Ref. 36. A general expression for the variation of the area between the adjacent rays is given in the Appendix (Eq. (II-6)). This expression has been investigated to determine the meteorological conditions required for the ray tube area to approach zero. It was found that if focusing takes place, it can occur only at the location of a cut-off of the sonic boom (either lateral or under the flight track). For a still atmosphere focusing can occur only under the airplane and takes place simultaneously with the complete cut-off at that point. The Mach number at which focusing may occur on the ground is given by Eq. (9) which is derived in Appendix V.

$$M_{Focus} = \frac{a_g}{a_a} \quad \text{if and only if} \quad a_g = a_{max} \qquad \text{(Eq. 9)}$$

where

a_g = sound speed at the ground

a_a = sound speed at airplane

a_{max} = largest value of sound speed between the airplane and the ground

If a temperature inversion exists near the ground such that $a_g < a_{max}$ the boom cannot be focused at the ground because the cut-off, if it exists, will occur at the top of the inversion. Thus, in an atmosphere such as B-5 (Fig. 7) the boom will not be focused at the ground, regardless of Mach number. Referring to Fig. 20, the $M_{cut\text{-}off}$ line shown for the Standard Atmosphere, and model A-3 would also represent the M_{focus} line. The effect of approaching the Mach number at which focusing may occur is shown in Fig. 21 where the variation in overpressure produced at a fixed altitude by varying the Mach number is shown for the Standard Atmosphere and Model A-3. The data for these curves were computed using the method of Refs. 6-8.

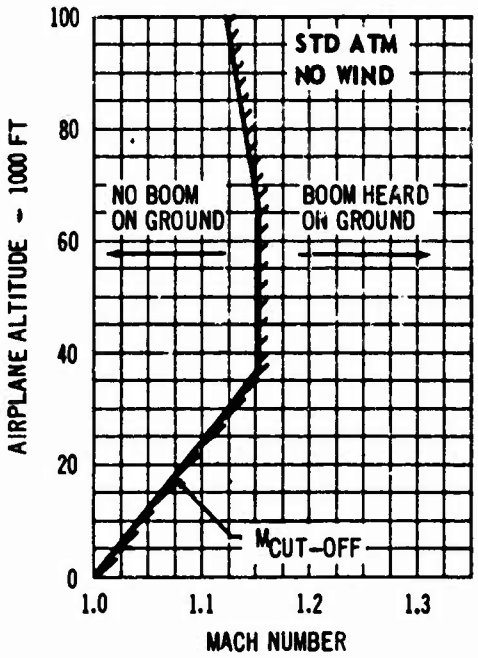

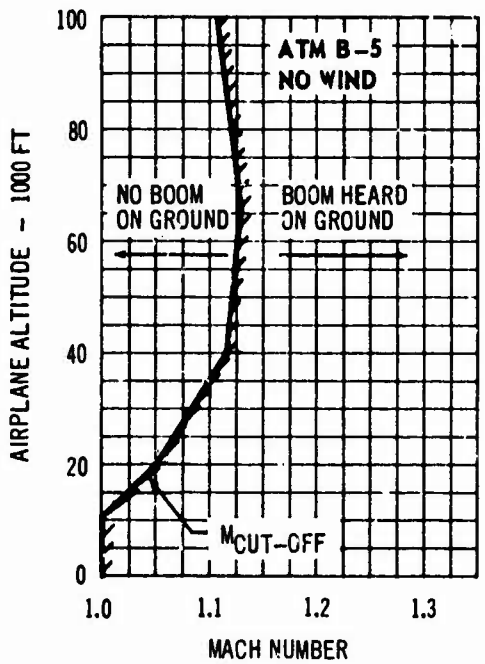

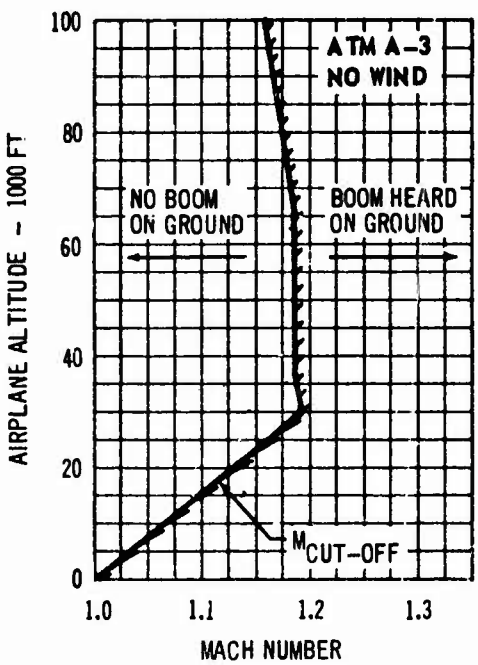

Fig. 20 Airplane Mach Number for Complete Cut-Off in Several Model Atmospheres.

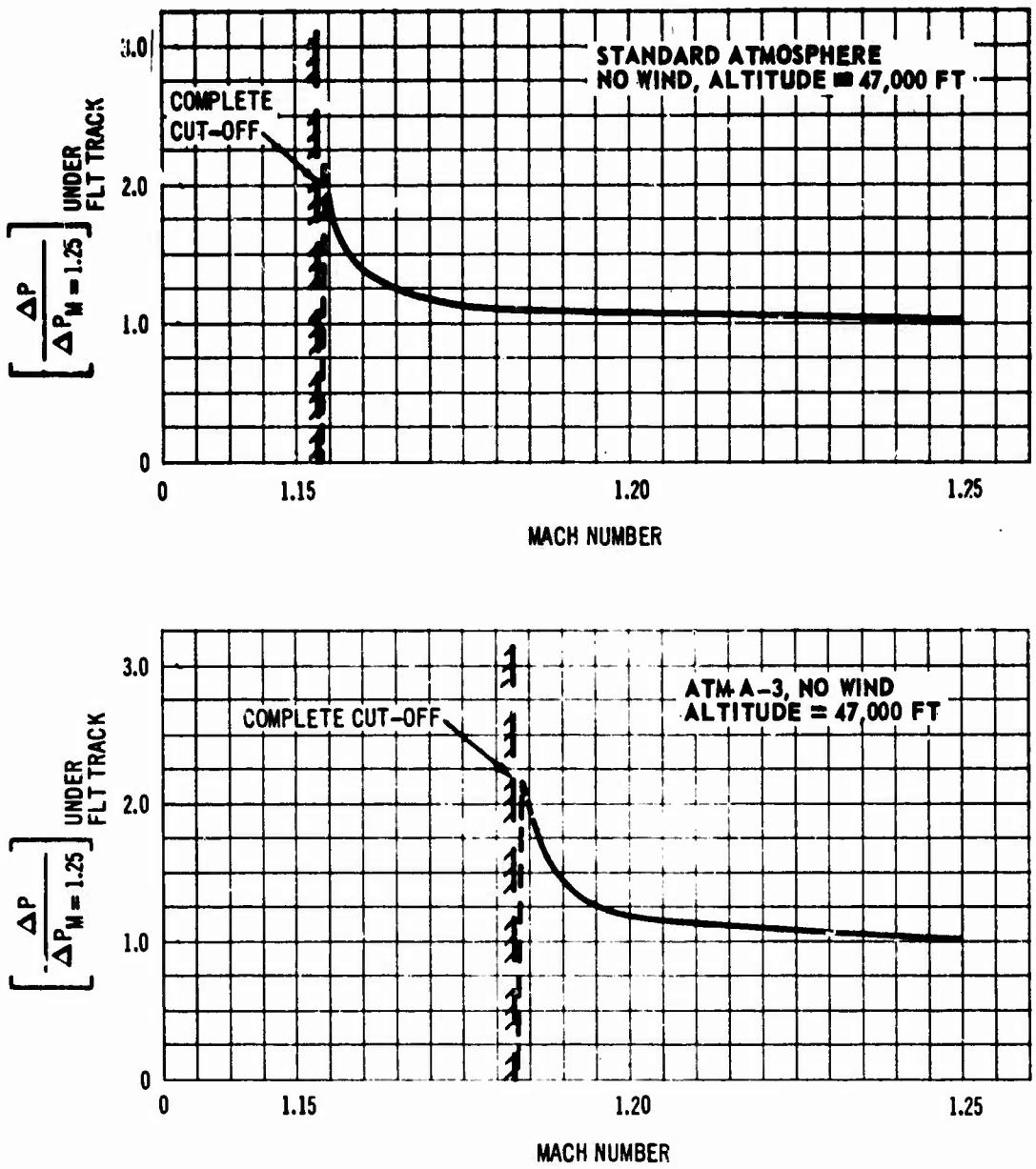

Fig. 21 Effect of Approaching M_{Focus} on Sonic Boom.

The figure shows that the boom magnitude may substantially increase as the cut-off Mach number is approached. However, two factors should be noted in considering these results. First, except for continued flight at this Mach number the focusing occurs at only one point on the ground under the flight track and thus would affect only a very small area. Second, and perhaps more important, is the interpretation of these results. At the present time, a factor is applied to all sonic boom

estimates to account for the reflection of the oblique shock wave from the ground. This factor, K_R , (Eq. (1)) is usually taken as approximately 2.0. However, at cut-off the shock front is normal to the ground and there is no reflected wave from the ground. The value of K_R is not clearly defined under these circumstances. This aspect of the problem is considered in more detail in Section III.D.1 but, to summarize here, the conclusion is that K_R must vary between approximately 2.0 for the oblique shock wave to approximately 1.0 for the normal wave at cut-off. In this respect the overpressure experienced at the ground near an atmospheric focus may be only slightly larger than that predicted for Mach numbers higher than that required for focusing, where $K_R = 2.0$. As will be shown in the following sections, the same argument would hold for wind induced focusing as this too occurs only at a cut-off where the shock front is normal to the ground.

In making routine calculations, Eqs. (8) and (9) should be checked to determine the Mach number at which cut-off or focusing may occur. If an inversion exists near the ground Eq. (9) may be ignored. When the Mach number of interest lies very close to Mach number required for focusing, (the proximity may be estimated from Fig. 21) the approximate methods outlined in Section II may not be sufficient to adequately determine the boom strength on the ground. If an estimate is required for these Mach numbers more sophisticated methods, such as those detailed in Refs. 6-8, must be applied.

(B) WIND PRODUCED ANOMALIES - Wind shears between the airplane and the ground will distort the shock front as it travels through the atmosphere. In some situations these shears may either prevent the boom from reaching the ground or significantly increase the boom lateral extent. In others they may intensify or focus the boom locally. The meteorological conditions necessary to produce these phenomena are presented in this section. These results should be used in conjunction with routine estimates to isolate those situations where unusual propagation may occur. It may be noted that with the exception of large increases in location of lateral cut-off, wind produced anomalies are generally confined to the low Mach number flight regime. At higher Mach numbers (usually above 1.3) the wind shears required to produce the unusual effects are too large to be realistic.

(1) Complete Cut-off - Investigation of the ray propagation equations, (Appendix Equations (II-1a) through (II-1f)) indicates that for an atmosphere with wind, no boom will reach the ground if the ray directly under the airplane is refracted. Experimental evidence of complete cut-off has been noted in Ref. 4 for very low Mach numbers (near 1.2). In the simplest case, this requires that the airplane speed relative to the ground be less than the speed of sound at the ground. The maximum Mach number at which cut-off would occur is given by Eq. (10) below.

$$M_{cut\text{-}off} = \frac{(a+U)_{max} - U_a}{a_a} \qquad \text{Eq. (10)}$$

where

$M_{cut\text{-}off}$ = largest airplane Mach number at which complete cut-off will occur

a = sound speed at some level between the airplane and the ground

U = tailwind speed component at the same level as selected for a. (U is negative if it is a headwind component)

U_a = tailwind component at airplane (U_a is negative if it is a headwind component)

a_a = sound speed at airplane

$(a+U)_{max}$ = largest value of sound speed and wind component speed which occurs between the airplane and the ground

The calculation of $M_{cut\text{-}off}$ is considerably simplified if the combined sound speed and wind speed for the atmospheric model being considered is plotted against altitude from the ground. This step aids in selection of the maximum value of $(a+U)$ that lies between the airplane and the ground.

Several examples of $M_{cut\text{-}off}$ have been calculated using the atmospheric models from Fig. 7 and the wind models from Fig. 11. These results are shown in Fig. 22 for both headwind and tailwind. The cut-off Mach number with no wind is shown for reference.

The figure shows that, in general, headwind components increase the cut-off Mach number above that for the no wind case, while tailwind components decrease the cut-off Mach number. However, in the case of very high speed winds, the tailwind components may increase the cut-off Mach number for altitudes above the maximum wind speed. This is illustrated in the case of the high-speed jet. It should also be noted that the altitude at which complete cut-off occurs is indicated by $M_{cut\text{-}off} = 1.0$. In the case of the high-speed jet tailwind in the Standard Atmosphere for flight at altitudes above 28,000 feet, the cut-off would occur at about or above 28,000 feet.

(2) Focusing Under the Flight Track – Under some conditions, winds may cause focusing of the sonic boom under the flight track. The mechanism is similar to that described in Section III.A.2. It has been found, upon investigation of the ray tube area expression, (Appendix Eq.(II-6)) that focusing under the flight track and complete cut-off must occur simultaneously. The boom at the ground may be intensified if the cut-off occurs at the ground. The Mach number at which focusing may occur on the ground under the flight track, in the presence of wind, is given by Eq. (11) which is developed in Appendix V.

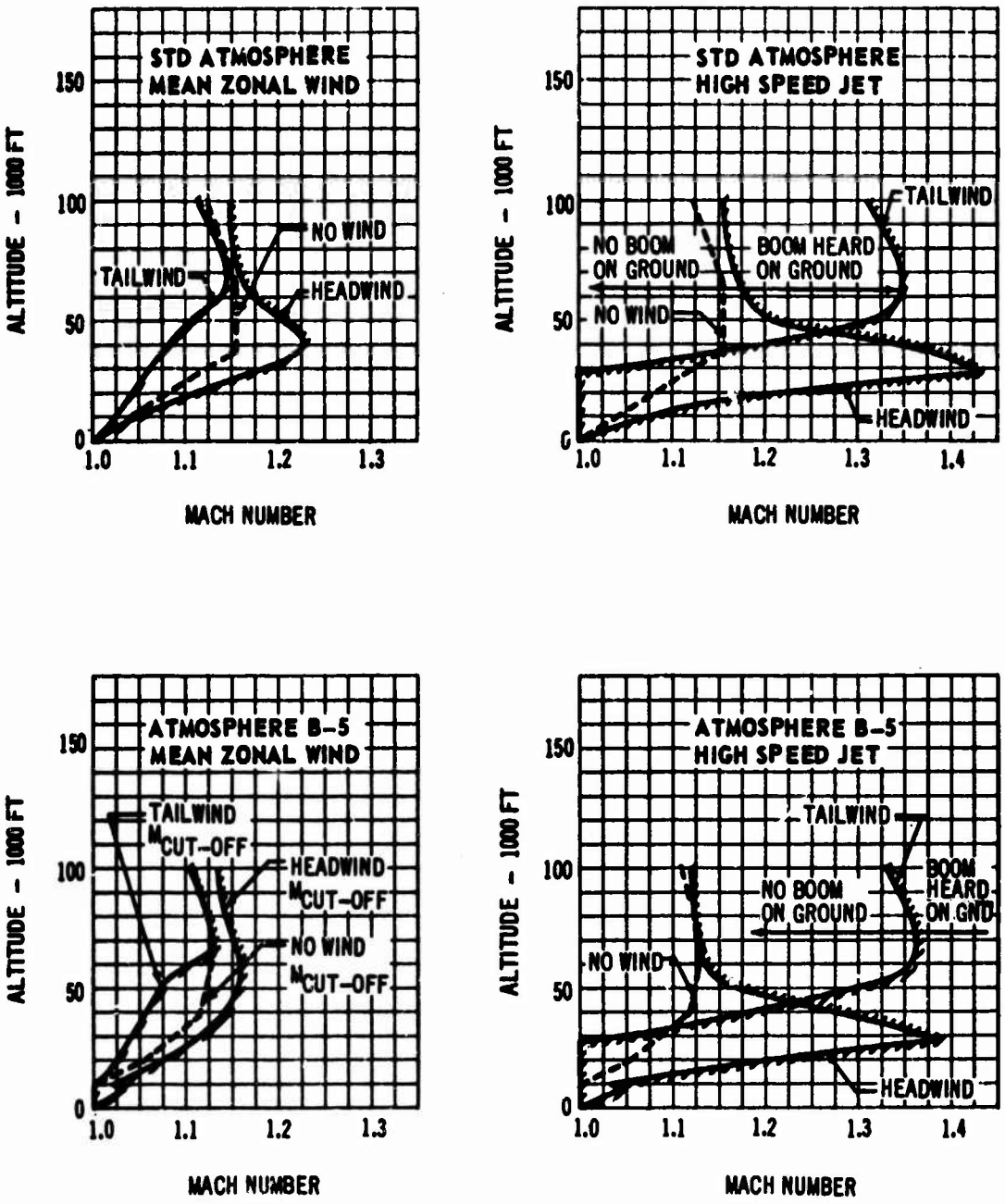

Fig. 22 Effect of Wind on Cut-Off Mach Number.

$$M_{Focus} = \frac{(a+U)_g - U_a}{a_a} \text{ if and only if } (a+U)_g = (a+U)_{max} \quad \text{Eq. (11)}$$

where

M_{Focus} = Mach number at which focusing on the ground may occur

$(a+U)_g$ = sum of sound speed and tailwind component at the ground (U is negative if it is a headwind component)

U_a = tailwind component at the airplane (U_a is negative if it is a headwind component)

a_a = sound speed at the airplane

If the quantity $(a+U)$ is not largest at the ground, cut-off and possible focusing will occur at the level where this quantity has its greatest value. This is similar to the effect of an inversion in the still atmosphere. Referring to Fig. 22, the Mach cut-off lines for the headwind and tailwind would also represent the M_{Focus} lines. An interesting example of cut-off above the ground with no focusing possible at the ground is illustrated quite vividly in the case of the Standard Atmosphere and the high-speed jet tailwind profile. For airplanes flying above 28,000 feet at Mach numbers near M_{Focus}, the cut-off would occur at 28,000 feet, thus precluding the possibility of focusing at the ground.

The effect of wind on the overpressure under the airplane was investigated by the method of Refs. 6-8, in the Standard Atmosphere for winds increasing linearly from zero at the ground to the maximum value at the airplane. The wind magnitude at the airplane was increased until cut-off and focusing at the ground were achieved. These results are shown in Fig. 23 where the overpressure with wind has been divided by that obtained without wind for the airplane at a fixed Mach number and altitude.

The figure shows that the focusing effect occurs at wind speeds very near those required to produce complete cut-off. The local intensification may not be as high as it appears at first sight because of the possible variation in ground reflection factor K_R with shock wave angle. This consideration is discussed more fully in Section III.D.1.

Another interesting consideration is that wind induced focusing can occur only at the very low Mach numbers. This may be seen if Eq. (11) is rearranged so that the wind required for cut-off and focusing at the ground may be calculated as a function of the airplane Mach number. An especially simple example may be found in the Standard Atmosphere with a wind varying linearly from zero at the ground to a maximum at the airplane and by assuming that the airplane is above 36,000 feet. The wind required for cut-off and focusing has been determined for this case and is shown plotted in Fig. 24.

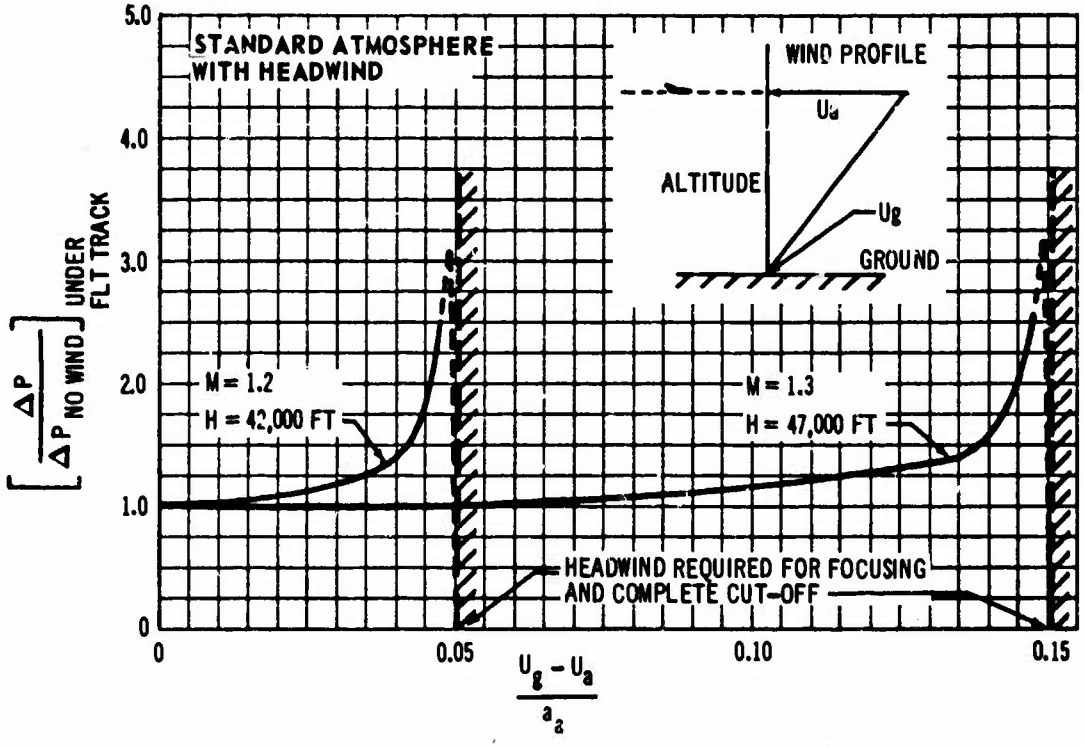

Fig. 23 Effect of Wind on Sonic Boom at the Ground at Low Mach Numbers.

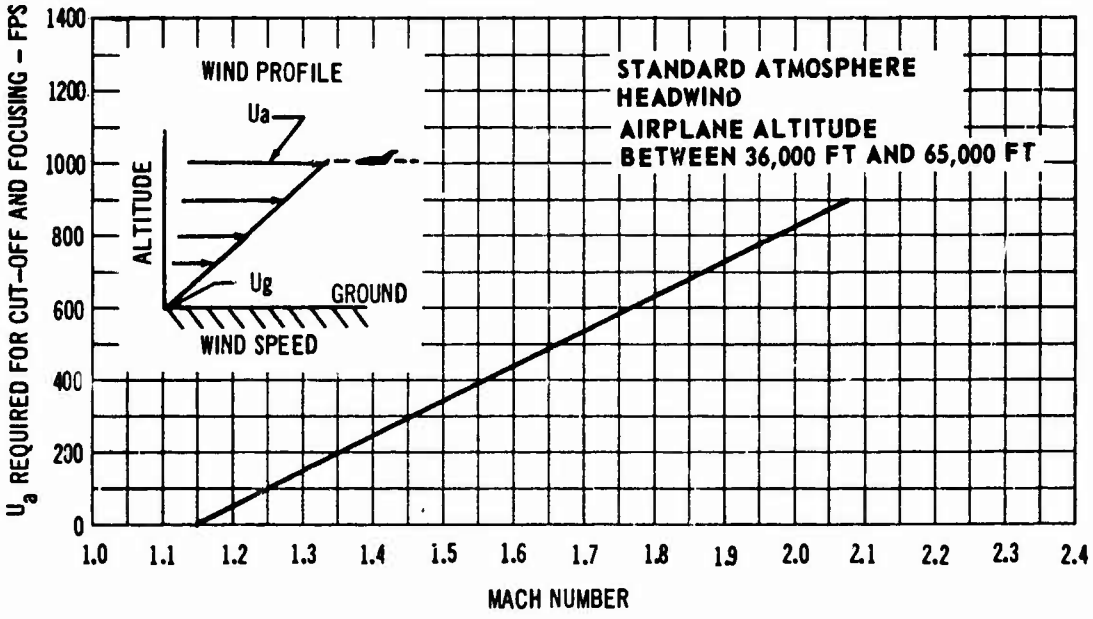

Fig. 24 Headwind Speed Required for Cut-Off and Focusing at the Ground.

The figure shows that the headwind speeds at the airplane required to produce cut-off and focusing are in excess of 200 feet per second for Mach numbers above 1.3. Wind velocities in the atmosphere rarely exceed this value at altitudes above 40,000 feet, where airplanes such as a large supersonic transport would fly at these Mach numbers. At higher Mach numbers the wind velocity required for cut-off and focusing would be larger than any which could physically exist in the atmosphere.

(3) *Focusing to the Side of the Flight Track* – As in the case of focusing under the flight track, intensification of the boom to the side of the flight track may occur simultaneously with the lateral cut-off. Investigation of the ray tube area expression in the Appendix (Eq.(II-6)) leads to an expression of the wind required to produce these phenomena. The expression for the required wind conditions is derived in Appendix VI of this report. The result has been applied to several examples which are presented in Fig. 25.

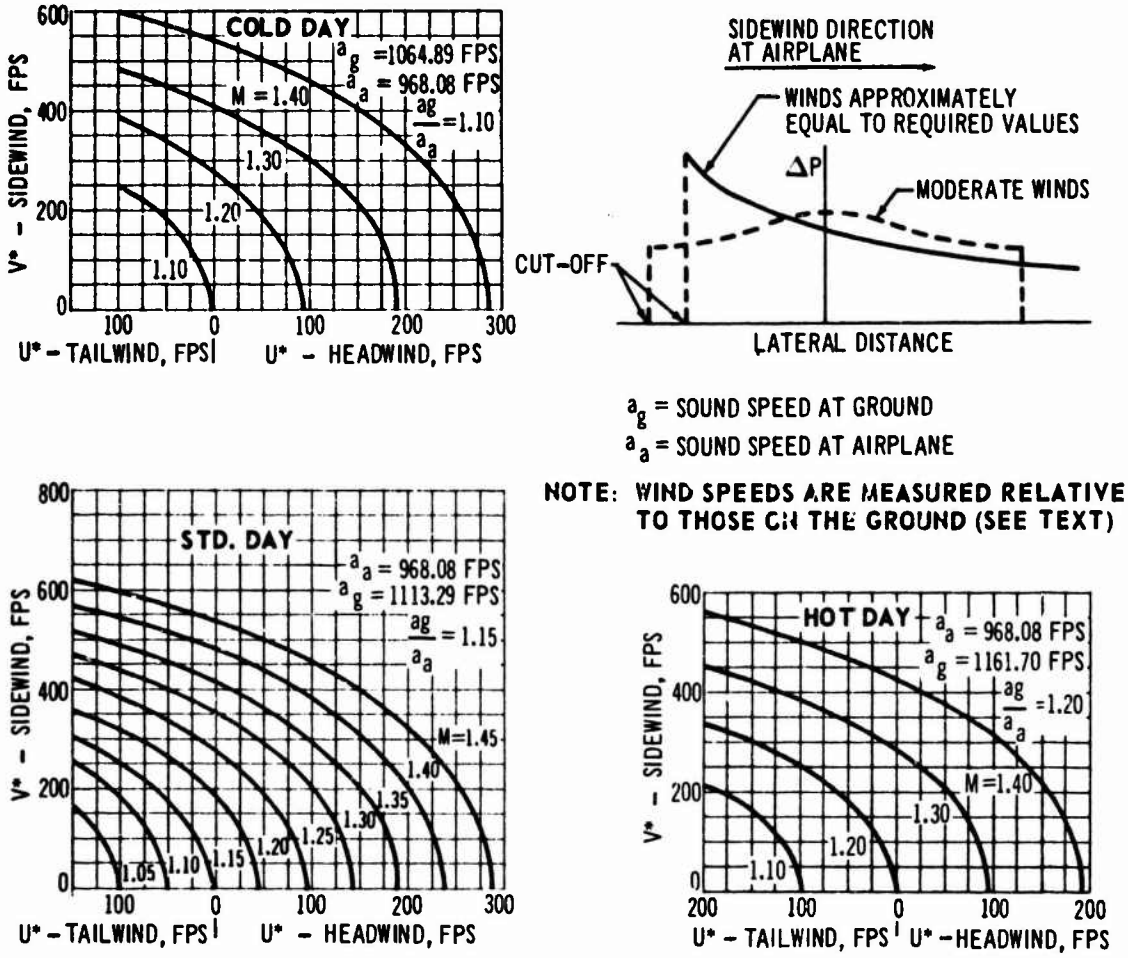

Fig. 25 Wind speeds Required to Produce Focusing Off the Flight Track.

The required wind speed components are measured relative to those on the ground. For example, the sidewind speed, V^*, would be the absolute value of the algebraic difference of the sidewind speed at the ground and that at the airplane, i.e. $|V_g - V_a|$. Wind is a vector quantity so that the direction must be accounted for by the sign of the number. The following directions were defined in developing the above curves:

- Winds in the direction of the flight path are positive (i.e. tailwinds).
- Winds in the opposite direction of the flight path are negative (i.e. headwinds).
- Winds coming from the right side normal to the flight path are positive.
- Winds coming from the left side normal to the flight path are negative.

The figure indicates the wind components required to cause off-track focusing at several Mach numbers. It is evident that this phenomenon is restricted to the very low Mach numbers because of the magnitudes of the wind speeds required at the higher Mach numbers.

To indicate the proximity to the required value of wind which may cause an unusual effect, several cases have been computed in the Standard Atmosphere. The sonic boom strength at the lateral cut-off point was computed by the method of Refs. 6-8 for various wind speeds and directions. These results were then divided by the boom strength under the flight track for no wind in order to better illustrate the variation. The effect of winds on the boom strength at the lateral cut-off point is shown in Fig. 26.

The figure shows that in some circumstances and at very low Mach numbers the overpressure to the side of the flight track may exceed that under the flight track. The same phenomenon may also be seen in Fig. 15 for the standard atmosphere with the high speed jet sidewind profile for Mach 1.2. Here again, the variation of K_R, the reflection factor, with shock angle must be considered as the focusing effect occurs simultaneously with cut-off where the shock is nearly normal to the ground. This is discussed in more detail in Section III.D.1.

A better indication of the range of wind speeds which are required to produce significant off-track focusing may be obtained by a cross-plot of the data in Fig. 26 for Mach 1.2 on the plot of Fig. 25. The winds which will produce overpressures at the lateral cut-off position equal to these normally produced under the flight track without wind were picked to form the boundary. Thus, the wind range which will produce this effect is shown as the cross hatched area in Fig. 27.

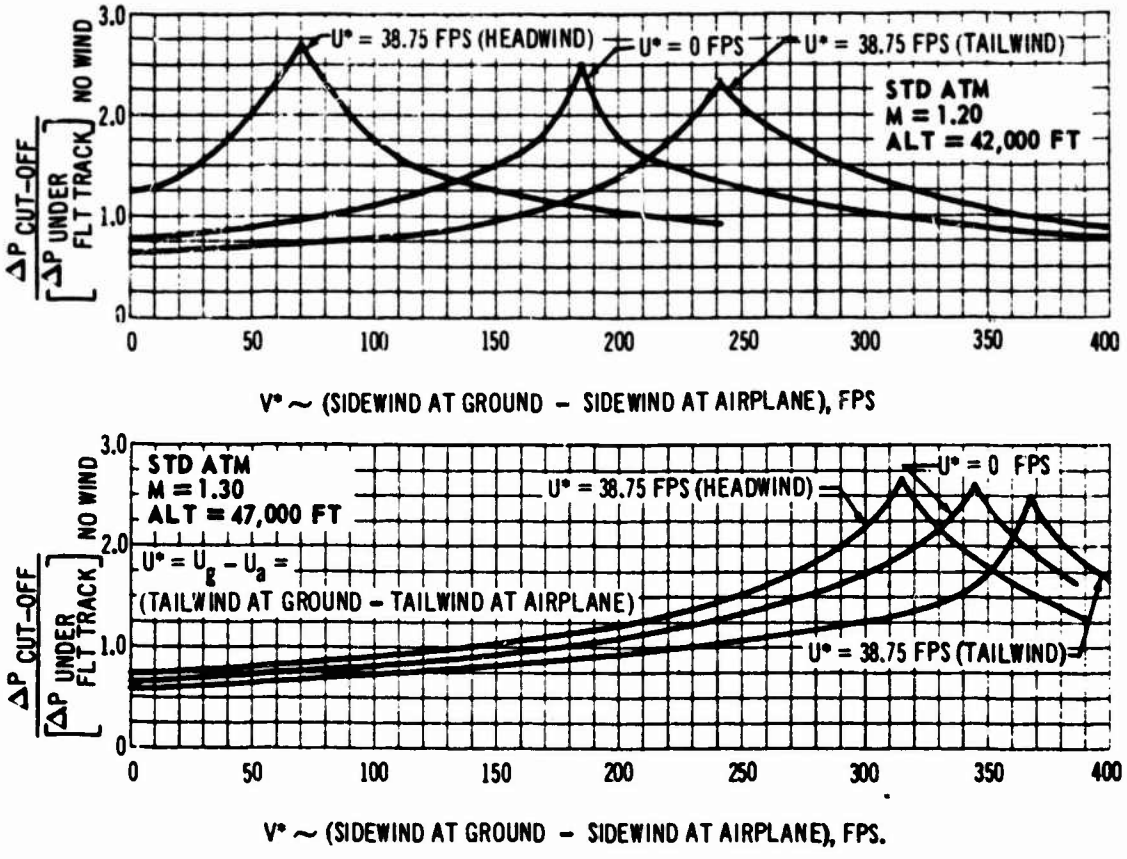

Fig. 26 Effect of Winds on Sonic Boom at Lateral Cut-Off.

For Mach numbers greater than 1.3, the relative wind speeds required to produce the off-track focusing become very large. This is illustrated when comparing the computed data for Mach 1.2 and Mach 1.3 in Fig. 15 for the high speed jet sidewind. The data at Mach 1.3 shows that the influence of the high speed winds is practically negligible. For most practical cases of transonic flight (Mach numbers near 1.0) at high altitudes (above 40,000 feet) the winds at the airplane would not be of sufficient magnitude to produce the off-track focusing effect. Thus, the primary consideration would be one of focusing under the flight track at or near the cut-off Mach number. The probability of occurrence of the focusing phenomenon either under or to the side of the flight track is considered in more detail in Section V.

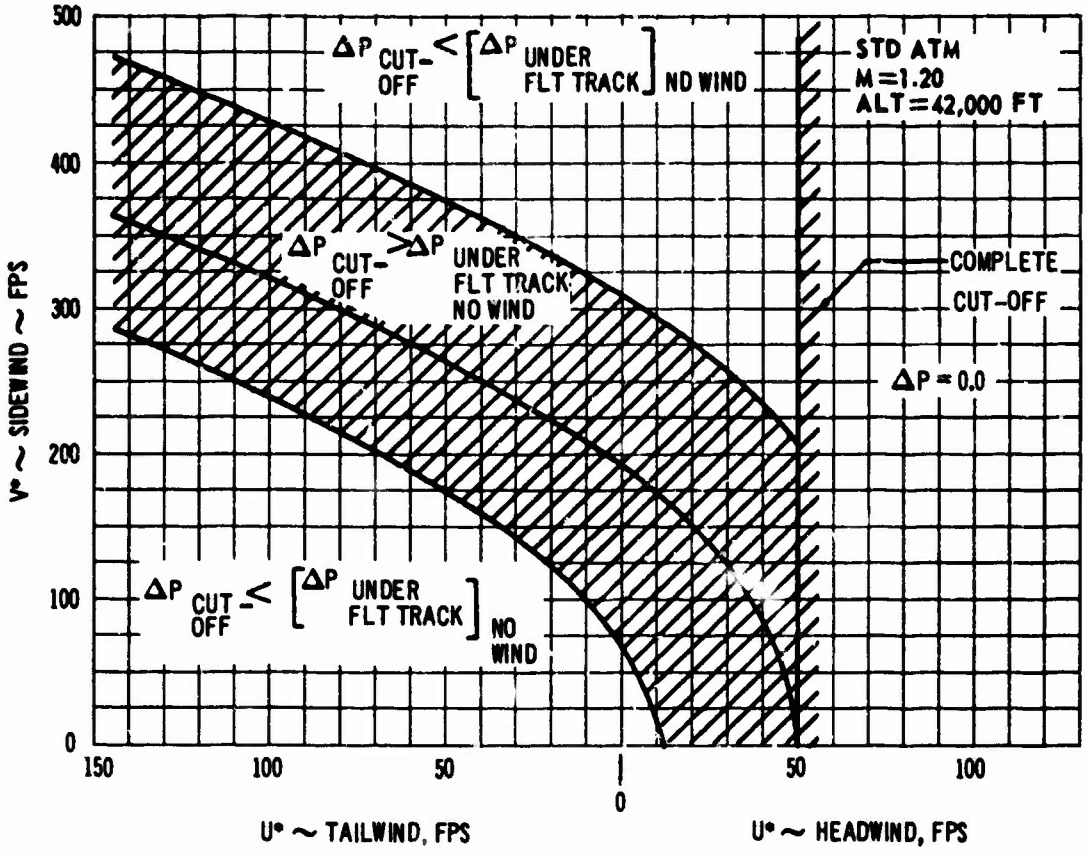

Fig. 27 Winds Required to Produce Significant Overpressure Increase at Lateral Cut-Off.

In considering routine calculations of the sonic boom the wind speed and sound speed variation between the airplane and the ground should be determined. The criterion developed in this and the preceding section should be checked in the low Mach number range to see if the possibility of focusing exists for flight at the altitudes of interest. If this possibility does exist more sophisticated methods, such as that of Refs. 6-8, must be used to determine the boom strength at the ground. Otherwise, the methods outlined in Section II should be sufficient to determine the boom strength on the ground.

(4) **Extreme Lateral Spread** - In some cases winds may increase the location of the lateral cut-off to very large distances from the flight track. This phenomenon, which has been noted here as extreme lateral

spread, may occur at all Mach numbers. An investigation of Appendix Eqs. (II-1a)through(II-1f) which describe the ray path propagation, has led to an expression for the winds required to produce the extreme spread. The relationship is given in Eq. (12) and is developed in detail in the Appendix VII.

$$A_a = \frac{U_a \pm \sqrt{M^2-1}\ V_a}{M} + a_a > \frac{U \pm \sqrt{M^2-1}\ V}{M} + a = A$$

Eq. (12)

or

$$A_a > A$$

where

U_a = Tailwind speed at airplane (negative if headwind)

V_a = Sidewind speed at airplane (positive if coming from right side of flight track

M = Airplane Mach number

a_a = Sound speed at airplane

U = Tailwind speed at height, H , above ground

V = Sidewind speed at height, H, above ground

a = Sound speed at height, H, above ground

The (+) sign on the term $\sqrt{M^2-1}\ V$ is used when investigating extreme lateral spread on the left side of the flight track and the (-) sign is used when investigating the possibility on the right side.

The equation shows that for the winds to produce extreme lateral spread the value of the quantity A at the airplane, i.e. A_a, must be greater than at any other point between the airplane and the ground. The application of Eq. (12) to a specific case will illustrate its use. The example chosen was the Standard Atmosphere with the high-speed jet profile. Airplane Mach number was chosen as 2.0, and various wind directions were selected. The right side of Eq. (12) was computed for each assumed direction and is shown plotted in Fig. 28.

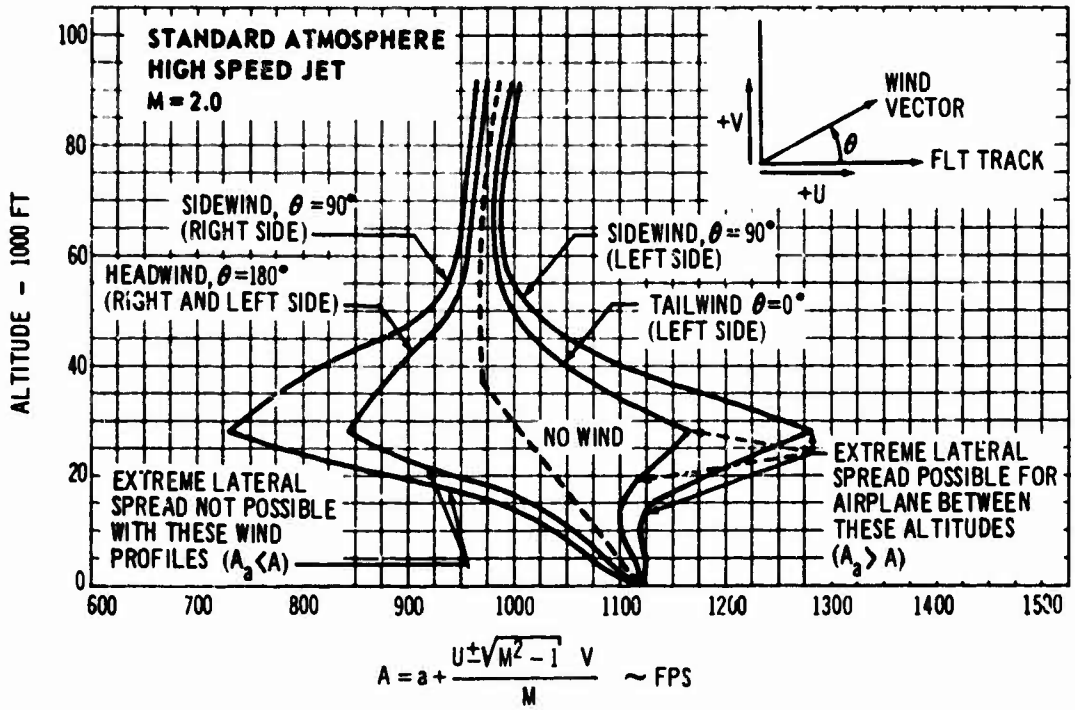

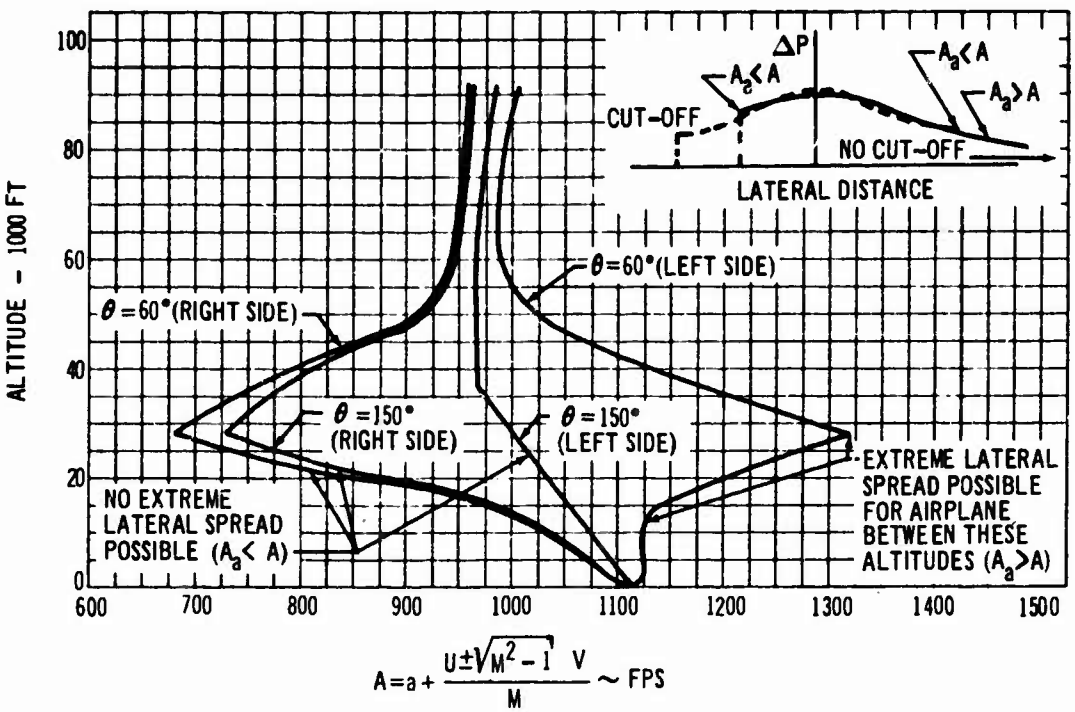

Fig. 28 Conditions Required for Extreme Lateral Spread in Standard Atmosphere.

The figure shows the altitude range and wind directions for which extreme lateral spread may occur. It should be noted that, of the wind directions selected, only the 0° (tailwind), 90° (sidewind), and 60° wind directions could cause this phenomenon, and then only if the airplane is below 28,000 feet. The former direction (tailwind) would cause the extreme spread on both the right and left sides of the flight track while the latter two directions (60° and 90°) would cause the extreme spread only on the left side. In this example, the extreme lateral spread would not occur for an airplane flying above 28,000 feet. The winds used in the example in Fig. 28 are characteristic of most wind profiles in the atmosphere. Thus, the problem of large increases of the lateral cut-off location would not exist for flight at altitudes above the level of maximum wind.

The effect of high winds on the location of lateral cut-off was investigated for a somewhat academic case, but the results were characteristic of the phenomenon. The overpressure on the ground was calculated by the method Refs. 6-8 for a wind profile which varied linearly from zero at the ground to a maximum at the airplane in the Standard Atmosphere. The magnitude of the wind at the airplane was increased until it exceeded that required to produce the extreme lateral spread. The results of this calculation are shown in Fig. 29.

The figure shows that although the wind increases the location of the lateral cut-off the overpressures in that region are quite low. For this reason routine calculations of the overpressure on the ground might ignore this effect as the overpressure beyond the normal cut-off location drops off quite rapidly with distance from the flight track. In any case, as was noted earlier, this phenomenon will probably be uncommon.

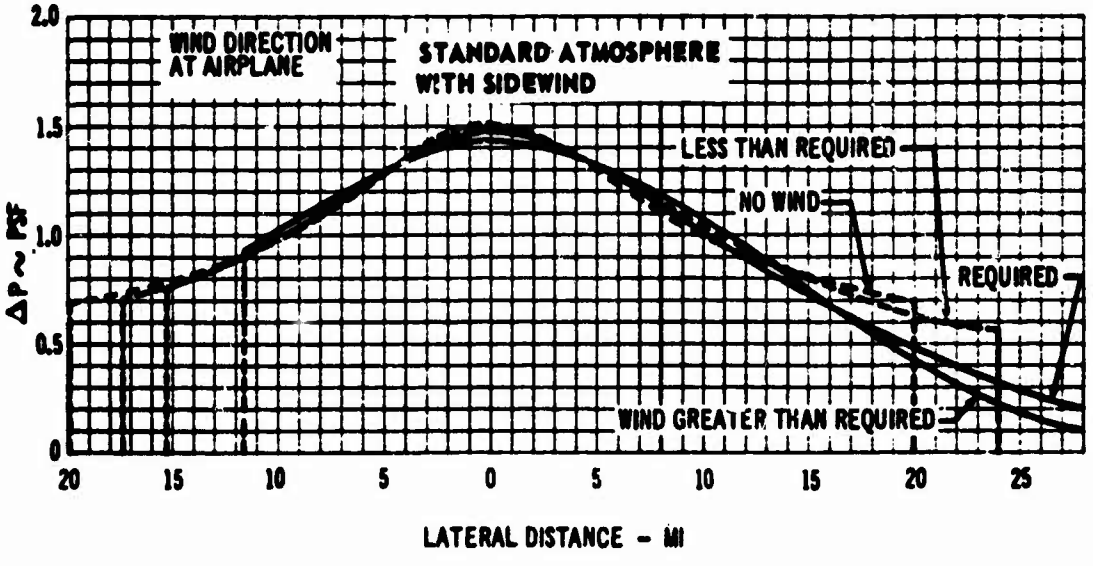

Fig. 29 Effect of Wind on Location of Lateral Cut-Off.

(C) EFFECTS OF LOW ALTITUDE TURBULENCE - The previous discussion was limited to the study of the effect of a horizontally stratified atmosphere on the propagation of the sonic boom. In this section, it will be shown that any study of the meteorological aspects of the sonic boom can be separated into effects due to the horizontally stratified atmosphere and effects due to low level turbulence. The turbulent process in the atmosphere is the result of some form of instability. This may be either a result of mechanical instability, such as produced by wind shear, or flow over obstacles, or thermal instability such as produced by solar heating of the ground. These forms of instability produce random, turbulent fluctuations in wind and temperature which can only be studied and described in statistical terms such as the correlation coefficient and spectrum analysis. Consequently, when the effects of a turbulent atmosphere on the sonic boom are being studied, it is necessary to use statistical parameters for the development of a theory of turbulent effects on the sonic boom which will be introduced in this section. The theory describes either the turbulent temperature or the turbulent wind effects on the sonic boom. The effects of combined temperature-wind turbulence are currently being studied.

(1) Atmospheric Structure - The flow patterns of the atmosphere can be visualized as being composed of oscillations varying in size from 3 to 4 thousand miles in wave length to ones which are locally on the order of a few feet. In order to ascertain the effect of the wave length of atmospheric properties on the propagation of the sonic boom, a harmonic analysis, or more rigorously a power spectrum analysis of data containing these socillations, can be made.

The power spectrum of wind shown in Fig. 30 is a typical plot of kinetic energy of the horizontal wind speed (which is obtained

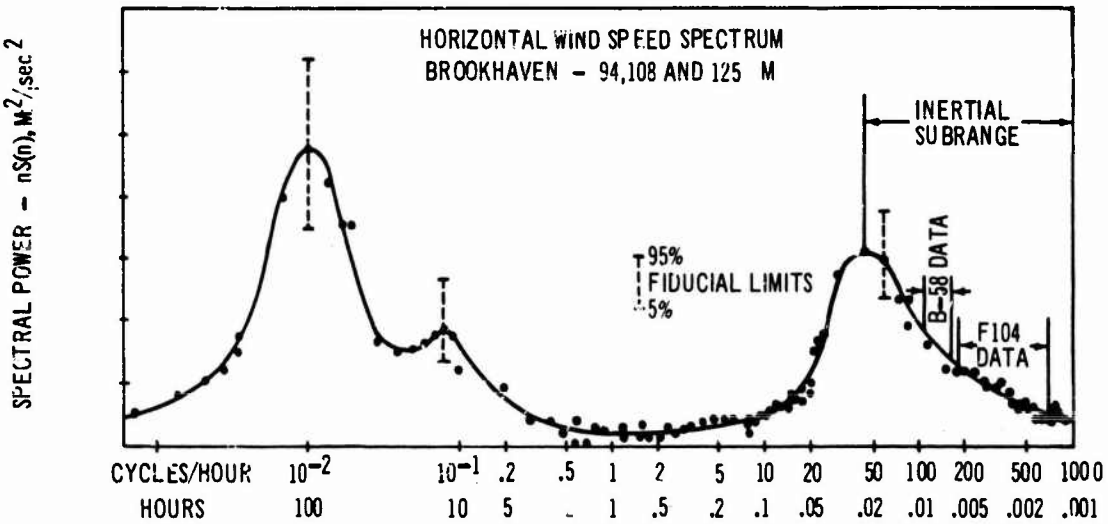

Fig. 30 Horizontal Wind-Speed Spectrum at Braakhaven National Laboratory at about 100m Height (Ref. 38).

from the spectral analysis) versus the frequency of the waves in cycles per hour. The temperature spectrum curve is very similar in form to the horizontal wind spectrum. The following results may be deduced from Fig. 30:

- There is one maximum in the wave energy spectrum near 100 hours per cycle. This represents waves due to large scale weather systems.
- A secondary maximum occurs near 12 hours per cycle which may be identified with the diurnal cycle of meteorological conditions.
- There is a broad minimum centered near a period of one hour per cycle. This flat part of the curve (the so-called spectral gap) means that there are very few eddies of a size from 1 to 20 miles in the atmosphere when, for example, the average wind speed is 10 mph.
- A third maximum is found near periods of one minute. This means that, for the same average wind speed of 10 mph, there are many turbulent oscillations with a wave length of about 900 feet imbedded in the passing atmospheric flow field.

These data show that the study of the effects of the atmosphere on the propagation of the sonic boom can be separated into two parts. One part of the study is the effect of the stratified atmosphere, in which the horizontal gradients on wind and temperature may be neglected because they are small relative to the distances (20 - 40 miles) effected by the sonic boom. As was pointed out above, eddies of this size are rare in the atmosphere. The second part of the study are the effects of turbulent temperature and wind fluctuations over small periods of time and space on the sonic boom. These fluctuations are superimposed upon the relatively slowly varying wind and temperature patterns of the large weather systems, which for purposes of studying the turbulence are treated as being nearly stationary. The magnitude and frequency of the short period variations depend upon such parameters as time to day, wind speed, cloud cover and the lapse rate of temperature with altitude.

The structure of a horizontally stratified atmosphere is obvious, but the description of a turbulent atmosphere requires the introduction of statistical concepts which may be unfamiliar. When a flow is characterized as being turbulent, it is implied that fields of irregular and random fluctuations of scalar quantities (e.g. temperature) and vector quantities (e.g. wind) occur about some mean value. The fluctuating part of the flow field can be regarded as the superposition of a large number of different sized oscillations which can be given analytical form by a three dimensional Fourier analysis of the velocity field.

To find a quantity which is easily measured and yet is a good statistical measure of the amount of energy contained within each particular eddy size of wave length, Taylor (Ref. 67) observed that the following Fourier transformation pair exists between the correlation coefficient, R_{ij} for scalar fields (or correlation tensor for vector fields) and the wave spectrum (tensor), Φ_{ij}

$$\Phi_{ij}(\vec{k}) = \frac{1}{(2\pi)^3} \int R_{ij}\, e^{-i\,\vec{k}\cdot\vec{r}}\, d\vec{r} \qquad \text{Eq. (13)}$$

and that the inverse transform of Φ_{ij} is

$$R_{ij}(\vec{r}) = \int \Phi_{ij}\, e^{i\,\vec{r}\cdot\vec{k}}\, d\vec{k} \qquad \text{Eq. (14)}$$

where $\vec{k}$ is the wave number vector which represents the turbulent eddies.

The definition of the correlation coefficient (tensor) is

$$R_{ij}(\vec{r}) = \overline{u_i(\vec{x})\, u_j(\vec{x}+\vec{r})} \qquad \text{Eq. (15)}$$

where $u_i(\vec{x})$ is a velocity component in the x_i-th coordinate direction and $u_j(\vec{x}+\vec{r})$ is a velocity component in the x_j-th coordinate direction at a distance $\vec{r}$ from $\vec{x}$ and $i,j=1,2,3$. When $i=j$ and $\vec{r}=0$, the correlation coefficient R_{ii} represents the kinetic energy per unit mass:

$$\tfrac{1}{2}\,\overline{u_i(\vec{x})\, u_i(\vec{x})} = \int \Phi_{ij}\, d\vec{k} \qquad \text{Eq. (16)}$$

while Φ_{ii} represents the energy density as a function of wave number.

The turbulent eddies decay slowly and are unchanged over the distances they travel when carried by the mean atmospheric flow during the time intervals used in correlating the measurements. This implies that for homogeneous turbulence, the Eulerian or time lag correlations may be used instead of the difficult Lagrangian or space correlation. A similar analysis might be made of the cross-spectrum between the two variables, temperature and wind, which lead to a measure of the rate at which the temperature is being advected or carried along by the turbulence. This suggests a way in which the effects of combined temperature and wind fields may be incorporated into the theory of turbulent scattering of shock waves.

Other parameters which are useful in describing turbulence are the mean wind, $\bar{u}$, and the RMS wind speed $(\bar{u}^2)^{1/2}$. From dimensional analysis (Refs. 41 and 42) it can be argued that the spectrum of the vertical eddies varies with height above the ground in such a manner that if the frequency of the eddies, ω, is divided by the mean wind $\bar{u}$ and multiplied by the height, z, a reduced frequency f is obtained which is

essentially the ratio of height to wave length, $f=\frac{z}{\lambda}$. The reduced frequency is used to normalize data to a common base. The "scale of turbulence" which is roughly 1/10 the height of the obstacles to the flow, and the variance of the longitudinal, vertical and latitudinal velocity components are also meaningful parameters which may be used to describe the turbulent variations of the properties.

(2) Variation in Turbulent Intensity - The description of how the turbulence decays progressively from large eddies to heat, led Kolmogoroff (Refs. 69 and 70) to formulate a similarity hypothesis in 1941. This hypothesis states that the influence of the large eddies on the smaller eddies as the large eddies decay to smaller ones diminishes gradually and consequently, small eddies tend to have uniform properties for all types of turbulence. Therefore, the properties of these small eddies are solely determined by the average rate of dissipation of energy per unit mass. This hypothesis leads to the form of the power spectrum in the inertial subrange (e.g. Fig. 30).

To increase the tractability of equations such as those for diffusion and acoustic propagation and to mitigate the problem of measurement of the atmospheric parameters, it is often assumed that the turbulence is homogeneous and isotropic. If the turbulence quantitatively, has the same structure in all parts of the flow, it is homogeneous. It is isotropic if its statistical properties are independent of direction. Homogeneity and isotropy are usually good approximations near the ground (in the atmosphere) when turbulence is fully developed, when the sky is clear and the winds are strong. Because of the mathematical complexity inherent in describing non-homogeneous turbulence, all investigators to date have assumed that the turbulence is isotropic and homogeneous when deriving the scattering equations.

Examination of turbulent spectra such as those assembled in Lumley and Panofsky (Ref. 41, p. 161 ff) indicates that the following significant factors about atmospheric turbulence near the ground should be borne in mind when studying the propagation of the sonic boom in low level turbulence.

- The variance of vertical wind velocity near the ground which increases with the square of the wind, is a function of the surface roughness, and is relatively independent of the lapse rate of temperature with altitude.
- The variance of the lateral component (i.e., the cross wind) is very sensitive to lapse rate, but not to surface roughness or wind speed.
- The variance of the longitudinal component of the wind (i.e., along the wind) depends upon the lapse rate of temperature, surface roughness and mean wind speed.
- Generally, the variance of the horizontal wind components is two to three times that of the vertical wind (i.e., the turbulence is non-homogeneous and non-isotropic).
- It is indicated that the eddies tend to be elongated along the mean wind direction when the winds are strong (according to Lumley and Panofsky (Refs. 41 and 42).

- Examination of the turbulent spectra presented in Ref. 41 shows the maximum value of the energy density in the spectrum of vertical velocity tends to occur near a wave length which is four times the height above the ground, while the analogous temperature spectrum maximum occurs near a wave length ten times the height above the ground. Thus, the maximum turbulent energy density tends to occur at longer wave lengths with increasing altitude.

Since the measurements, to date, of the sonic boom have taken place either over deserts or cities, it is important to note that there is little data on the homogeneity or isotropy of turbulence from that kind of region. However, the assumptions of homogeneous and isotropic turbulence should yield an adequate preliminary solution which will indicate the important parameters that influence the distortion of the sonic boom signature.

(3) Scattering of Acoustic Energy by Turbulence - The principal investigators in this field have been Perkeris (Ref. 45), Blockhintzev (Refs. 46 and 47) Lighthill (Ref. 48) and Kraichnan (Ref. 49). They have been concerned primarily with scattering of small amplitude sound waves. The problem of determining how acoustic energy is redirected (i.e. scattered) by the interaction between acoustic waves and a field of turbulence is difficult and because of the inherent complexity, the simplest case, that of homogeneous and isotropic turbulence (i.e., the intensity of the turbulence has no preferred orientation and it is uniformly distributed) has been the only case studied to date.

The initial attempt at analyzing the effects of turbulence on the sonic boom by Palmer (Ref. 81) was to extend the analysis of the variation of the amplitude due to turbulent scattering developed by Tatarski (Ref. 51), since this was the problem of greatest immediate interest.

The extension of this analysis had the advantage of having been experimentally verified (Ref. 51, 54) in the lower levels of the atmosphere for small amplitude, high frequency sound waves. Inherent disadvantages where the necessity of assuming the constancy of the structure of atmospheric turbulence with altitude, of ignoring the non-linear effects associated with large amplitude waves, and of neglecting the effects of variations in the turbulence power spectrum as a function of frequency.

This analysis consisted of treating the "N" wave as being composed of a Fourier series sum of frequencies and considering one wave from the resulting chain represented by

$$N(\omega) = \frac{2A_0}{\pi} \sum_{n=1}^{\infty} \frac{(-1)^{n+1}}{n} \sin n \omega_0 t$$

where A_0 is the amplitude of the N-wave

ω_0 is the frequency of the fundamental harmonic of the N-wave.

Tartarski (Ref. 51) has shown that the amplitude fluctuations of a sound wave that is propagating through a turbulent medium are lognormally distributed. The variance, σ^2, of the amplitude fluctuations of a monochromatic acoustic wave is then given by

$$\sigma^2 \left(\ln \frac{A}{A_0}\right) = \frac{\beta C_n^2 S^{\frac{11}{16}}}{\lambda^{\frac{7}{6}}}$$

where β is a geometrical constant, C_n is an atmospheric structure function, which depends on temperature, wind and the angle of incidence of the wave upon the turbulent region, S is the path length and λ is the wave length. The N-wave can be represented as a Fourier series, where the terms denote harmonic sine waves of varying amplitude and frequency. The total variance of the pressure amplitude of the N-wave may be found as the sum of the pressure variances of each harmonic providing that each propagates independently of all others (i.e., uncorrelated) through the turbulent regions of the atmosphere. If the harmonics do not propagate independently the lognormal form of the statistical pressure amplitude distribution is still preserved (Ref. 63) provided that the wave length of the N-wave lies within the atmospheric inertial subrange of the power energy spectrum as is shown in Fig. 30.

Since the parameters which enter into the functional form of the variance are functions of the atmospheric turbulent structure, the path length, the wave length of the N-wave, and the angle of propagation, it follows that study of the scattering of the sonic boom should classify the data according to a scheme based upon these parameters. In particular, the atmospheric turbulent structure will be related to time of day and cloud cover.

This analysis (Ref. 81) is based upon the scattering of a sinusoidal train of small amplitude waves. As a result of the tests at Oklahoma City, it became apparent that the problem of the interaction of the sonic boom with turbulence is not one of continuous interaction of a wave train with turbulence which is unaffected by boundary conditions. It is rather, one involving the near field of a large amplitude pulse scattered by a turbulent field of temperature and wind near the earth's surface. The amplitude statistics that were developed for continuous waves do not predict the angular energy distribution of the scattered energy from the direction of propagation and does not accurately depict the non-linear interactions which occur under these conditions.

The next step was to examine the theory for scattering of an acoustic pulse. Batchelor (Ref. 44) has shown that the following derivation of the field resulting from scattering of an acoustic pulse is equivalent to that developed in the differing forms of Pekeris (Ref. 45), Blockhintzev (Ref. 46 and 47), Lighthill (Ref. 48) and Kraichnan (Ref. 49). The procedure followed in formulating the theory was to derive the wave equation from the Navier-Stokes equation and the equation of continuity. A forcing function is then applied to this equation, and the solution of the resulting partial differential equation is then accomplished by using the method of perturbations and the Fourier transform. This technique gives the resultant angular distribution of scattered energy in terms of a differential cross-section which is defined as the ratio between the power scattered per unit solid angle in a given direction to the incident power intensity per unit area. The use of the Fourier transform in solving the partial differential equation, gives a solution for the angular distribution of energy which can be expressed in terms of a power spectrum of a turbulent quantity such as is described in the section on turbulence, Section III.C.2. An important concept used in the derivation is the scattering vector, $\vec{k}$, which is defined as the vector difference between the vector wave number, $\vec{K}$, representing the incident wave, and a unit vector, $\vec{\ell}$, multiplied by the absolute value of $|\vec{K}|$, which represents the scattered wave, $\vec{K}$ (i.e. $\vec{K} = |\vec{K}|\,\vec{\ell}$).

For instance, if a plane wave front such as an acoustic pulse is incident upon the scattering volume, the energy will be redirected along the vector $\vec{\ell}$. At a sufficiently large distance from the scattering volume, there will be an interaction between the incident wave and the scattered wave. The propagation of the disturbance which results from this interaction is represented by the scattering vector $\vec{k}$.

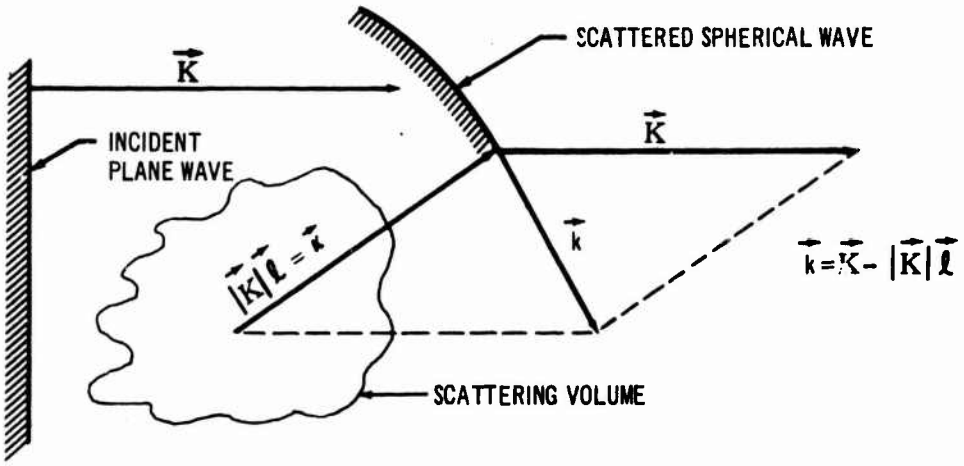

Fig. 31 Definition of Scattering Vector $\vec{k}$.

The derivation of the equations governing turbulent scattering is as follows:

The Navier-Stokes Equation:

$$\rho\left(\frac{\partial u_i}{\partial t} + u_i \frac{\partial u_i}{\partial x_j}\right) = -\frac{\partial}{\partial x_j}\left\{p + \frac{2}{3}\mu \frac{\partial u_i}{\partial x_j}\right\} - \mu\left\{\frac{\partial u_i}{\partial x_k} + \frac{\partial u_k}{\partial x_i}\right\} - \rho g \delta_{3j} \qquad \text{Eq. (17)}$$

and the equation of continuity:

$$\frac{\partial \rho}{\partial t} + \frac{\partial}{\partial x_i}(\rho u_i) = 0 \qquad \text{Eq. (18)}$$

are differentiated partially with respect to x_i and t in order to eliminate the time dependent velocity terms, where

δ_{ij} is Dirac delta = 1 when $i = j$ and is zero otherwise

ρ is the mass density

t is time

u_i is the velocity component in the x_i - th coordinate, $i = 1, 2, 3$

p is the pressure

μ is the coefficient of viscosity.

Neglect of second order terms as a result of assuming that the pressure, temperature and density, individually are the sum of a mean plus a small perturbation (this procedure is valid for small amplitude acoustic waves) and by assuming that the wave follows adiabatic processes, yields the wave equation:

$$\nabla^2 \Psi - \frac{1}{a_o^2} \frac{\partial^2 \Psi}{\partial t^2} = 0 \qquad \text{Eq. (19)}$$

where

Ψ is a parameter of the wave such as pressure or density

∇^2 is the Laplacean operator

a_o is the speed of sound

t is time

Inclusion of terms involving propagation parameters and second order quantities can be grouped in the operational calculus form:

$$\sum_n P_n(\zeta)\, D_n(\Psi) \qquad \text{Eq. (20)}$$

where

$P_n(\zeta)$ is a function describing the departures from the mean of variables describing the local properties of the medium such as temperature

D_n is a linear differential or integral operator with respect to space or time

This results in the modified wave equation,

$$\nabla^2 \Psi - \frac{I}{a_o^2} \frac{\partial^2 \Psi}{\partial t^2} = \sum_n P_n(\zeta)\, D_n(\Psi) \qquad \text{Eq. (21)}$$

When applying the method of perturbations, it is now assumed that the wave function Ψ after a single scattering is composed of the Ψ_0 incident wave Ψ_1 and a scattered wave. If it is then further assumed that the incident wave can be represented by

$$\Psi_0 = A\, e^{i(\vec{K} \cdot \vec{r} - \omega t)} \qquad \text{Eq. (22)}$$

where

A is the amplitude

$\vec{K}$ is the wave vector

$\vec{r}$ is the radius vector

ω is the angular frequency.

the second approximation to the wave function is that

$$\Psi = \Psi_0 + \Psi_1 \qquad \text{Eq. (23)}$$

Substitution of Eq. (22) and Eq. (23) in Eq. (21) yields:

$$\nabla^2 \Psi_1 - \frac{1}{a_0^2} \frac{\partial^2 \Psi_1}{\partial t^2} = A e^{i(\vec{K}\cdot\vec{r} - \omega t)} Q(\vec{r}) \qquad \text{Eq. (24)}$$

where $Q(\vec{r})$ represents the results of performing the operations indicated by Eq. 20.

The formal solution of Eq. (24) is

$$\Psi_1(\vec{r},t) = \int_V e^{i(\vec{K}\cdot\vec{r}' - \omega t) + i|\vec{K}||\vec{r} - \vec{r}'|} \frac{Q(\vec{r}')}{|\vec{r} - \vec{r}'|} d^3\vec{r}' \qquad \text{Eq. (25)}$$

where $\vec{r}'$ is a small domain near $\vec{r}$ and $Q(\vec{r}')$ is a function describing the relevant properties of the medium in $\vec{r}'$. This function represents an acoustic pulse originating at the scattering center.

The quantity

$$\frac{e^{i(\vec{K}\cdot\vec{r}' - \omega t) + i|\vec{K}||\vec{r} - \vec{r}'|}}{|\vec{r} - \vec{r}'|} \qquad \text{Eq. (26)}$$

can be expanded in an infinite series to that at large distances from the scattering element where the initial wave has not been affected by the redirection of energy, the second order terms in the series can be neglected. The scattered wave function is then

$$\Psi_1(\vec{r},t) \sim \frac{-Ae^{i(\vec{K}\cdot\vec{r} - \omega t)}}{4\pi|\vec{r}|} \int_V e^{i\vec{K}\cdot\vec{r}'} Q(\vec{r}') d^3\vec{r}' \qquad \text{Eq. (27)}$$

The quantity within the integral is the Fourier transform of the function that describes the distribution of a relevant property of the medium such as temperature fluctuations or wind within the volume which is projected along the scattering vector $\vec{K}$ by the "dot" product.

$$\Psi_1(\vec{r},t) = \frac{-A\, e^{i(\vec{K}\cdot\vec{r} - \omega t)}}{4\pi|\vec{r}|} \mathcal{F}(\vec{k}) \qquad \text{Eq. (28)}$$

Equation (28) indicates that, within the small scattering region $Q(\vec{r}')$, the only part of the complex amplitudes of the Fourier representation of the turbulence which reacts with the incident wave so that phases combined is the component along the scattering vector $\vec{k}$ (see Fig. 31). All other amplitudes will combine out of phase to cancel each other.

The directional distribution of intensity of the scattered energy can be formulated in terms of the general scattering cross-section, $\sigma(\vec{\ell})$. In physical terms, $\sigma(\vec{\ell})$ is defined as the ratio between the intensity of scattered energy per unit solid angle in the direction $\vec{\ell}$ per unit scattering volume and the intensity of the incident wave per unit area of the wave front. The intensity of any wave may be found by taking the mean of the product of the wave function Ψ and its complex conjugate Ψ^* or $\overline{\Psi\Psi}^*$. Thus, the scattering cross-section is proportional to the ratio of the intensities of the scattered wave to the incident wave, i.e.,

$$\sigma(\vec{\ell}) \propto \frac{\overline{\Psi_1\Psi_1}^*}{\overline{\Psi_0\Psi_0}^*}$$

Further, it can be shown that the spectrum of a turbulent quantity $\Phi(\vec{k})$ is given by the mean of the Fourier representation of the turbulence $\mathfrak{F}$ and its complex conjugate $\mathfrak{F}^*$, or $\overline{\mathfrak{F}\mathfrak{F}}^* = \Phi(\vec{k})$. Eq. (28) expresses the relation between the scattered wave function Ψ_1 and $\mathfrak{F}$ so that $\overline{\Psi_1\Psi_1}^*$ in terms of $\overline{\mathfrak{F}\mathfrak{F}}^*$ may be used to give the scattering cross-section,

$$\sigma(\vec{\ell}) = \frac{\pi}{2}\,\Phi(\vec{k}) \qquad \text{Eq. (29)}$$

where $\Phi(\vec{k})$ is the spectrum of the scattering quantity such as wind or temperature.

The scattering cross-section for turbulent temperature fluctuations can be found by finding the Fourier transform of the turbulent temperature field and applying Eq. (29). This gives

$$\sigma_T(\vec{\ell}) = \frac{\pi}{4}\cdot K^4 \cos^2\theta\ \Phi_T(\vec{k}) \qquad \text{Eq. (30)}$$

for the directional distribution of intensity of energy scattered by turbulent temperature field. The T subscript refers to temperature. A similar analysis for scattering by a turbulent wind field, u, gives

$$\sigma_u(\vec{\ell}) = \frac{K^2}{8a_0^2} \frac{\cos^2\theta}{\tan^2\frac{\theta}{2}} E\left(2\vec{K}\sin\frac{\theta}{2}\right) \qquad \text{Eq. (31)}$$

for the angular distribution of intensity, where E is the turbulent energy spectrum function along the incident wave vector $\vec{K}$.

When Eq. (31) is integrated over a sphere surrounding the scattering region to find the total amount of energy scattered from a weak shock wave, the integral is infinite (i.e. since $\cot\frac{\theta}{2}$ approaches infinity as θ approaches zero, an infinite amount of energy is directed forward). In order to resolve this discrepancy, Lighthill (Ref. 56) treated the scattering of a shock wave by turbulence as being due to the interaction of an acoustic pulse, represented by a Fourier sum, with a set of turbulent quadrupoles with a velocity discontinuity (εa_o) across the shock. He then assumes that the scattered energy propagates with the speed (εa_o) and develops the scattering equation

$$\sigma(\vec{\ell}) = \frac{\varepsilon^2}{64\pi r^2}\left[\frac{3}{2}\rho_o\overline{(u)^2}\right]\frac{\cos^2\theta \sin^2\theta}{(\sin^2\frac{\theta}{2} + \frac{\eta^2}{4})^{5/2}} \qquad \text{Eq. (32)}$$

where $\eta = \frac{1}{M_s} - 1$

M_s = shock Mach number.

This equation predicts a maximum of scattered energy in the direction in which the original wave is propagating after a single scattering, and that the intensity of the scattered energy will obey the inverse square law. Thus the scattered energy will remain finite. The intensity of the scattered energy depends upon the square of the wind speed fluctuations.

It has been implictly assumed in all studies of the scattering of sound by turbulence that the interaction between the acoustic energy and the turbulence is weak. However, Meecham and Ford (Ref. 59) have shown that the power spectra of the sound emitted by the turbulent surface layer have two forms depending on whether the emission is to the left or right of the peak in the inertial subrange as defined in Fig. 30.

In the inertial subrange $\Phi(\omega)$ is proportional to a function given by

$$\Phi(\omega) \sim \rho V a_o^2 M^{\frac{21}{2}} \left(\frac{\omega\ell}{a_o}\right)^{-\frac{7}{2}} \text{ in db} \qquad \text{Eq. (33)}$$

In the range of the larger eddies the relation is,

$$\Phi(\omega) \sim \rho V a_o^2 M^3 \left(\frac{\omega \ell}{a_o}\right)^4 \text{ in db} \qquad \text{Eq. (34)}$$

where $\Phi(\omega)$ is the spectral density, ρ is the density, V is the volume being considered, a_o is the speed of sound, M is the Mach number of the turbulence defined as the RMS wind speed divided by the speed of sound, ω is the angular frequency of emission and ℓ is a characteristic "length" of the turbulence. A schematic expressing this relation is shown in Fig. 32.

Since most of the turbulent acoustic power is emitted at

$$\omega = \frac{u_{RMS}}{\ell}$$

it seems reasonable to assume that the strongest interaction between the shock wave and turbulence will occur with this particular size eddy. This might imply excitation of the eddy to high energy levels and subsequent re-emission of a decaying pulse of energy or, resonant scattering. Alternatively, this interaction might introduce a perturbation on the shock wave front (Ref. 60, p. 114). This wave would then travel along the shock front transversely to the direction of propagation of the shock. This effect would be in analogy of polarization of the turbulent elements postulated by Lighthill (Ref. 56).

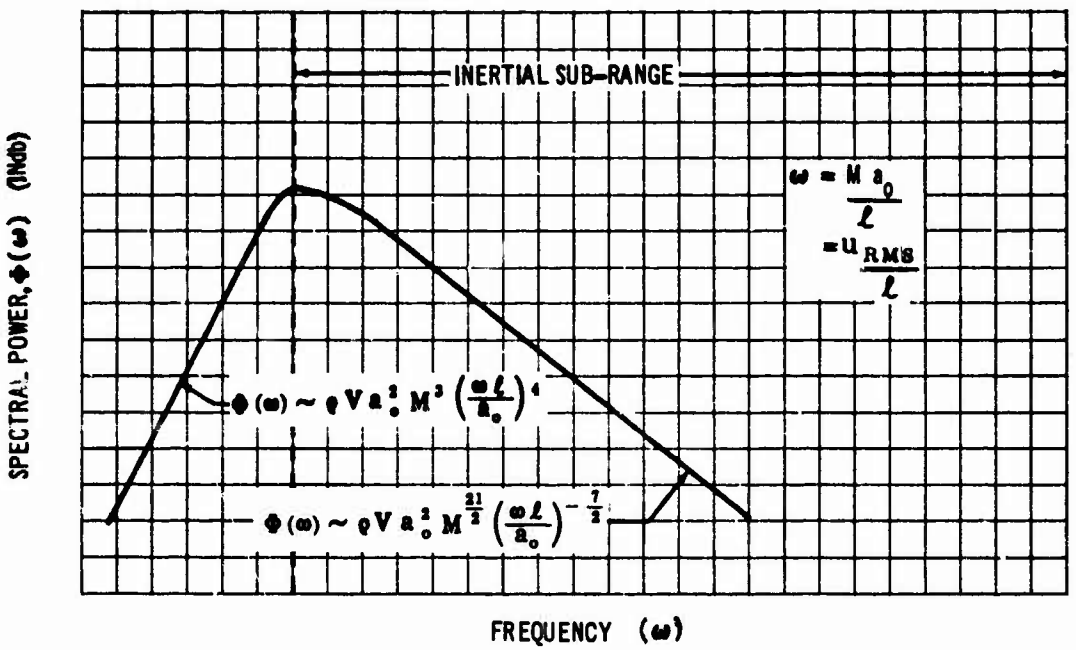

Fig. 32 Schematic of Turbulent–Acoustic Radiation.

(4) Critique of Current Acoustic Scattering Theory as Applied to Shock Waves - It is assumed in current scattering theory, either explicitly or implicitly, that the linearized wave equation holds, that the interaction between the turbulence and the acoustic energy is weak, and that the method of small perturbations is valid. Further, three dimensional geometry (implying homogeneous turbulence) is assumed which (Ref. 57) may not be applicable, particularly in view of the observed tendency of turbulent elements (Ref. 41, p. 210) to elongate along the wind. In two dimensions, Huyghens' principle does not hold, and a pulse of radiation will persist as a reverberation. In addition, it is assumed that the method of perturbations may be used (in some cases twice) and that the oscillations of the scattering elements occur in a particular mode.

The degree of complexity in studying scattering depends on the strength of the interaction of the incident wave with the scattering elements. If the distance between turbulent elements is large, it may be assumed that the scattered waves from turbulent elements do not interact with each other. If on the other hand there is a high density of scattering elements the waves interact, and any classification into weak and multiple scattered waves loses its meaning. If the scattering is weak there are two types of scattering, coherent and incoherent (Ref. 58). Coherent scattering occurs when the scattered waves are in phase in some regions and strong reinforcement occurs. Incoherent scattering occurs when all the waves are generally out of phase and destructive interference occurs. The degree of coherence depends upon the distribution of scatterers and the orientation of the scattering wave vector $\bar{k}$. If the scatterers can be treated as being orderly distributed in horizontal planes, and if the scattering vector $\bar{k}$ is normal to this horizontal plane, the maximum interaction occurs and strong beams are produced at intervals of $(m\lambda)$ where m is an integer and λ is the wave length.

It is fairly conclusive from the N-wave data obtained at Oklahoma City that the maximum of scattered energy is radiated at angles to the direction of propagation other than straight ahead as is predicted by the theory which results in Eq. (27) for high frequency fluctuations and Eq. (28) for shock wave scattering. The reason for this conclusion is derived from the statistical analysis of the Oklahoma City sonic boom test data presented in Section IV.B.4. This data shows that Test House 4, at which point the shock wave was at angle of approximately 70 degrees to the ground, had consistently more spiked N-waves of higher relative amplitude than Test House 1 where the shock wave was at an angle of about 45 degrees. If it is assumed that the intensity of the scattered wave falls off as some inverse function of distance from the scattering center (such as inverse square law for spherical waves), the observations mentioned above implies that the scattering vector $\bar{k}$, defined in Fig. 31, is more perpendicular to the ground at Test House 4 than at Test House 1. This observation does not agree with Eq. (28) which predicts a maximum scattering in the forward direction. Inspection of N-wave traces shows that the "spikes" or peaks, quite often, nearly coincide with the leading edge of the trace. This may indicate that the effect of the turbulence introduces a perturbation on the shock front which

travels transversely along the shock wave with a "group" velocity which is faster than the Mach number of the shock wave. The oscillatory nature of the traces further indicates that some degree of resonance is present. Some possible mean radiation patterns for a resonating scatterer are shown in Fig. 33.

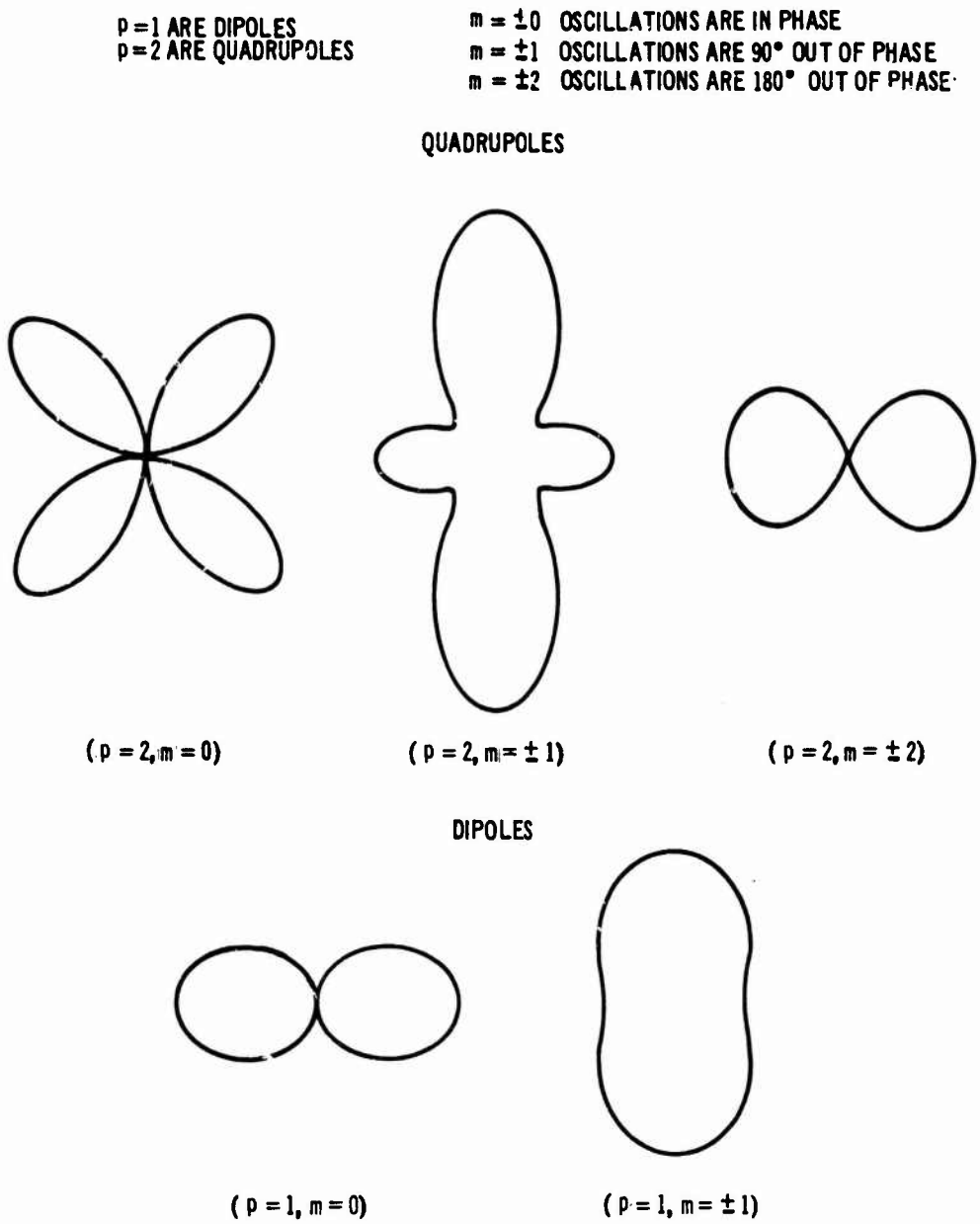

Fig. 33 Multipole Radiation Patterns.

An analytical comparison of the relative importance of the scattering effects of a turbulent velocity field, the scattering of a turbulent temperature field, and the scattering when both fields are present has not been made at this time. It is very likely that the results of the observed data which are not consistent with the theory are a result of the interaction of the shock wave with a medium in which both the temperature and wind fields are turbulent. The characteristics of the turbulent atmosphere described in Section II.C.1 indicates that further progress in quantitatively describing the effects of the earth's turbulent boundary layer on the sonic boom will depend upon theoretically extending scattering theory to incorporate combined turbulent temperature wind fields, a study of the effects of inhomogeneity and non-isotropy in the turbulence flow, and concomitant experimental measurements to serve as a guide to the theoretical development. One of the principal experimental problems is to determine the extent of the regions involved in the single scattering process together with the altitude at which it occurs. If this region is small and the altitudes low, the homogeneous, isotropic assumption will be a good approximation.

Work to date (see Appendix IX) has shown that the log-normal statistical distribution will probably describe the areal distribution of overpressures. Also, the pertinent parameters are probably the direction of propagation of the N-wave and, when taken separately, the spectrum of wind or the spectrum of temperature fluctuations. Some progress has been made in merging the effects of the two fields, but it is not sufficiently complete to be incorporated in this report.

(D) MISCELLANEOUS PHENOMENA - Various considerations have been mentioned in the previous material which could not easily be reviewed in any of those sections. The purpose of this section is to discuss these considerations in detail so that they may be used in evaluating the sonic boom produced on the ground under various circumstances.

(1) Reflection Factor Near Cut-off - In Sections III.A and III.B meteorological conditions were defined which could cause local intensification or focusing of the shock strength. It was noted in the development of these criteria that focusing, if it occurred, accompanied cut-off. At cut-off, the shock front is locally normal to the ground. This fact raises a question about the value of the reflection factor, K_R, which should be used in calculating the overpressure.

Consider first a weak oblique shock front in free air as shown in Fig. 34(a).

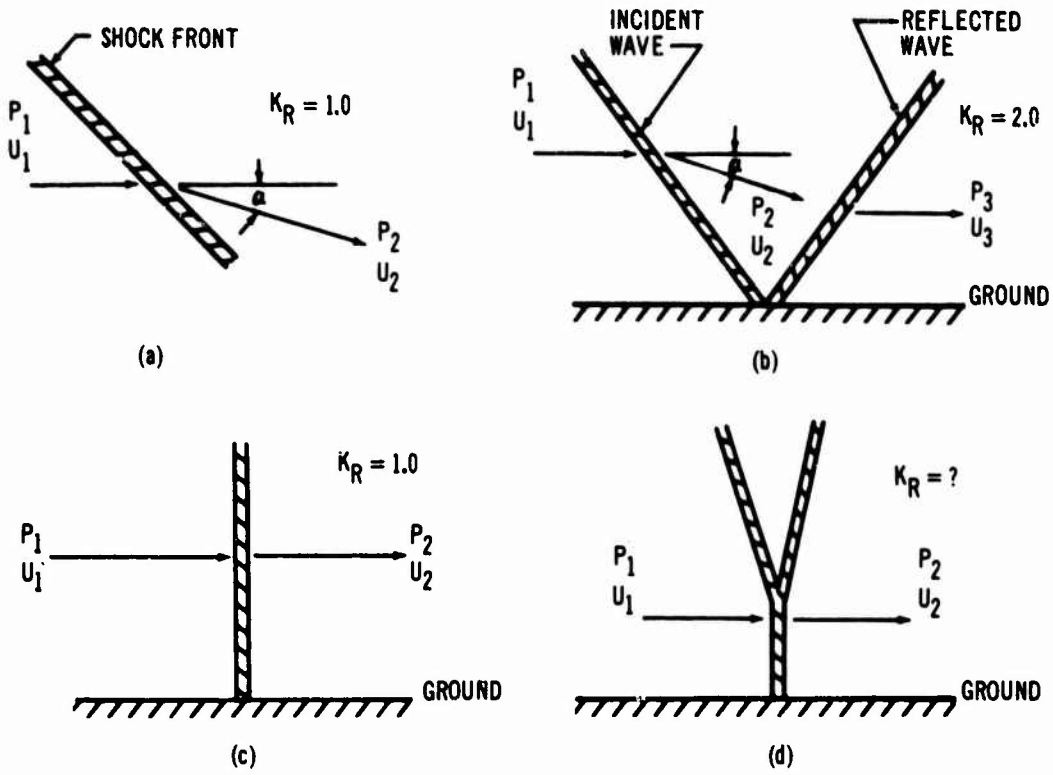

Fig. 34 Shock Front Configurations.

The pressure jump across this shock wave in free air is given by P_2-P_1 and the streamline describing the flow is turned through the angle α. The reflection factor, K_R, is defined as the total pressure jump divided by the pressure jump in free air. Thus, for the shock configuration shown in Fig. 34(a):

$$K_R = \frac{P_2 - P_1}{P_2 - P_1} = 1.0$$

If a boundary, such as the ground, is inserted then the flow must remain parallel to that boundary. This can be accomplished by the presence of a second (reflected) shock wave behind the first (incident) wave as shown in Fig. 34(b). Now, however, the total pressure jump across this configuration is P_3-P_1. If the shock waves are weak it can be shown (Ref. 71) that P_2-P_1 = P_3-P_2 so that in this case:

$$K_R = \frac{P_3 - P_1}{P_2 - P_1} = \frac{(2P_2 - P_1) - P_1}{P_2 - P_1} = 2.0$$

However, for the normal shock wave shown in Fig. 34(c), no reflected wave is required to turn the flow parallel to the ground so that the total pressure jump across this wave is just $P_2 - P_1$ i.e., the free air value. Thus, in the case of the normal shock wave:

$$K_R = \frac{P_2 - P_1}{P_2 - P_1} = 1.0$$

It is obvious that K_R must vary between 2.0 for the weak oblique shock front and 1.0 for the normal shock front. This is to say that the reflection factor is a function of the shock angle. Exactly how K_R varies is not fully understood at this time; however, some qualitative insight may be obtained from Fig. 34(c). If the incident shock angle is very near 90° and the shock wave is weak the reflected wave cannot turn the flow parallel to the ground. This situation requires that a "triple point" exist (Refs. 72 and 73), such as that shown, where the shock near the ground is normal and above it at some point the waves split into an incident and a reflected wave. This situation probably represents the transition between the oblique and normal shock fronts. Some general aspects of this problem are considered further in Refs. 74 and 82.

From this discussion it would appear that K_R should be considered a variable near cut-off. Assuming that this is the situation the variation of the overpressure near cut-off and focusing would take on the form shown in Fig. 35.

The figure shows that an instrument mounted on the ground would record some increase in the overpressure near cut-off but it would not record as high an overpressure as predicted using K_R = const. = 2.0.

It would be desirable to determine theorctically the variation of K_R with shock angle. Some of the preliminary work has been done in Refs. 72 and 74 but this work would have to be expanded to obtain a proper solution. It would also be of considerable interest to experimentally confirm the theoretical analysis, both concerning the variation of K_R and the variation of the free air overpressure predictions near cut-off and focusing. Some possible methods of accomplishing this are discussed in Section V.

(2) High Altitude Turbulence and Shower Clouds – The problem, that of deformation of the N-wave by high altitude turbulence, is essentially that of finding the scattered field at a great distance. This scattering problem is probably one in which single scattering occurs since most high altitude turbulence layers are thin (on the order of one to not much more than 3,000 feet thick). This will probably result in deformation of the N-wave to some degree, but the extent of this deformation and the effect of propagation of a deformed N-wave over great distances is unknown at this time.

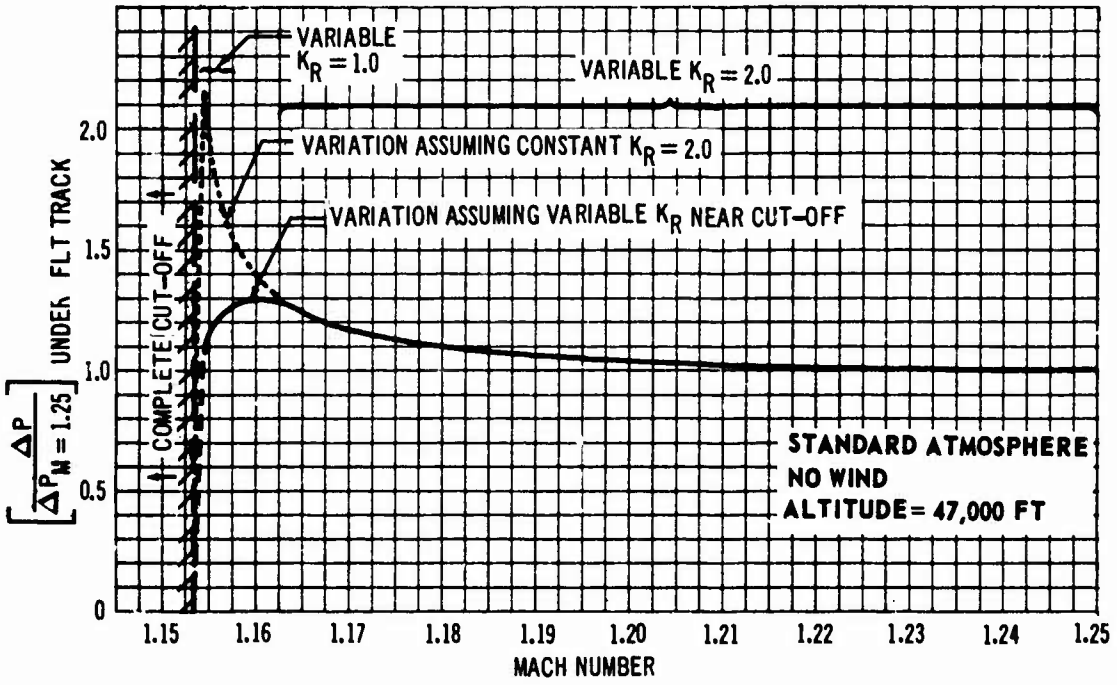

Fig. 35 Sonic Boom Near Cut-Off.

The problem of finding the effect of shower clouds on the sonic boom is much greater. Data taken during the Oklahoma City tests, such as May 29 at 0700 and 0900 CST and May 31 at 0700 CST, indicate that profound modifications of the N-wave can occur as a result of these clouds. Cumulus type clouds (such as thunderstorms) are essentially vertical in character and have a relatively limited horizontal extent. The boundaries between upward and downward air motions and between regions of precipitation and no precipitation indicate that study of shock propagation through these clouds will present a three dimensional problem in multipath propagation, edge diffraction effects as well as the problems associated with turbulent modification of the N-wave within the cloud and in the lower levels. No significant effort has yet been directed towards finding a solution to this problem.

(E) SUMMARY OF RESULTS — The meteorological conditions required to produce anomalous propagation such as focusing, complete cut-off, extreme lateral spread, and deformation of the pressure wave signature were discussed in this section. Criteria were established to predict the presence of these conditions. It was shown that realistic variations in both temperature and wind could produce focusing or complete cut-off for flight at Mach numbers below 1.3. However, the focusing would be accompanied by cut-off which would preclude the normal doubling of overpressure at the ground due to reflection of the shock wave. Extreme lateral spread and distortion of the pressure wave signature due to interactions with turbulence could occur for flight at all Mach numbers. However, the former would not occur for flight at altitudes above those where the maximum wind speeds exist regardless of the Mach number.

SECTION IV ANALYSIS OF OKLAHOMA CITY DATA

A limited amount of the flight test data measured during the sonic boom tests at Oklahoma City has been analyzed. This analysis has given some insight into the problems of evaluating the data when comparing it to the theoretical results. The purpose of this section is to present these comparisons between theory and test data. In general, excellent agreement was observed in the cases considered.

(A) INFLUENCE OF TEST AIRPLANE GEOMETRY - Each of the test airplanes was considered in detail and the shock strength parameter $[I(Y_o,\theta)]^{1/2}$ (see Eq. 1) was determined. The theory of Ref. 75 was used in developing the shock strength parameter for several angles of θ. The results for each airplane are briefly reviewed in this section.

(1) **F-104A** - Geometric descriptions for the F-104A were obtained from the Lockheed-California Company. These data were analyzed using the theory of Ref. 75. It was found that for this particular airplane more than two shock waves would be produced at some lift coefficients. Special care was required in determining the proper value of $[I(Y_o,\theta)]^{1/2}$ for the front shock wave. The results of the analysis are shown in Fig. 36 for several angles of θ. The figure shows that for a range of lift coefficients, C_L, the shock strength parameter is independent of the angle θ.

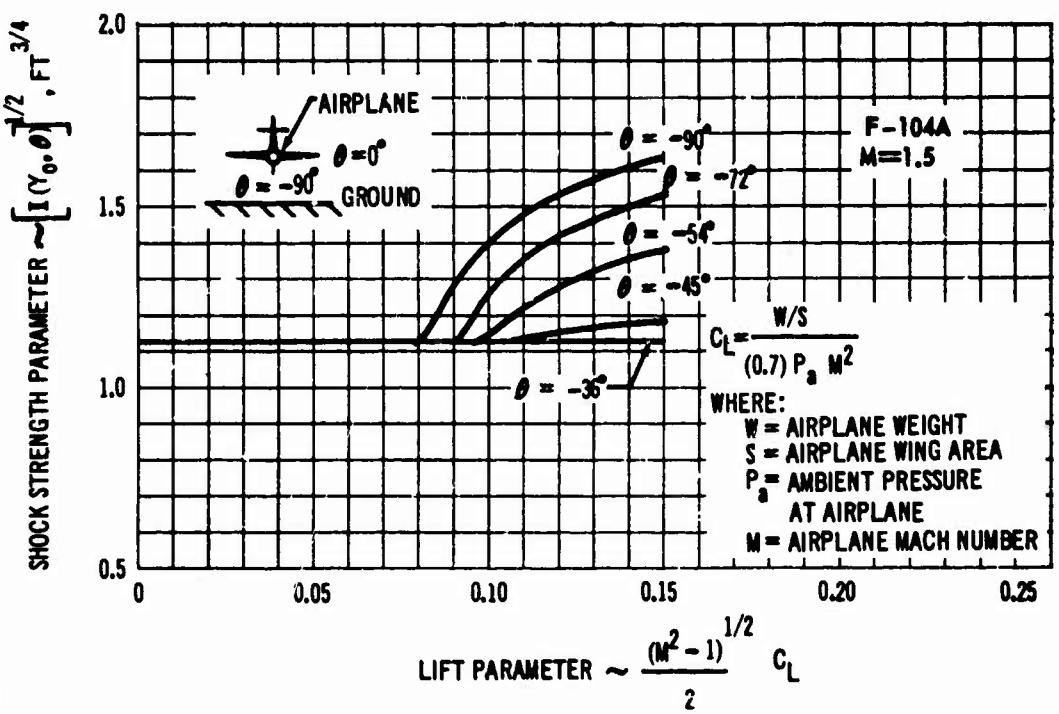

Fig. 36 Shock Strength Parameter for F-104A Airplane.

(2) B-58A - Geometric descriptions for the B-58A airplane were obtained from the Fort Worth Division of General Dynamics. These data were analyzed using the theory of Ref. 75 for several angles of θ with and without the MB pod. Results of this analysis are shown in Fig. 37.

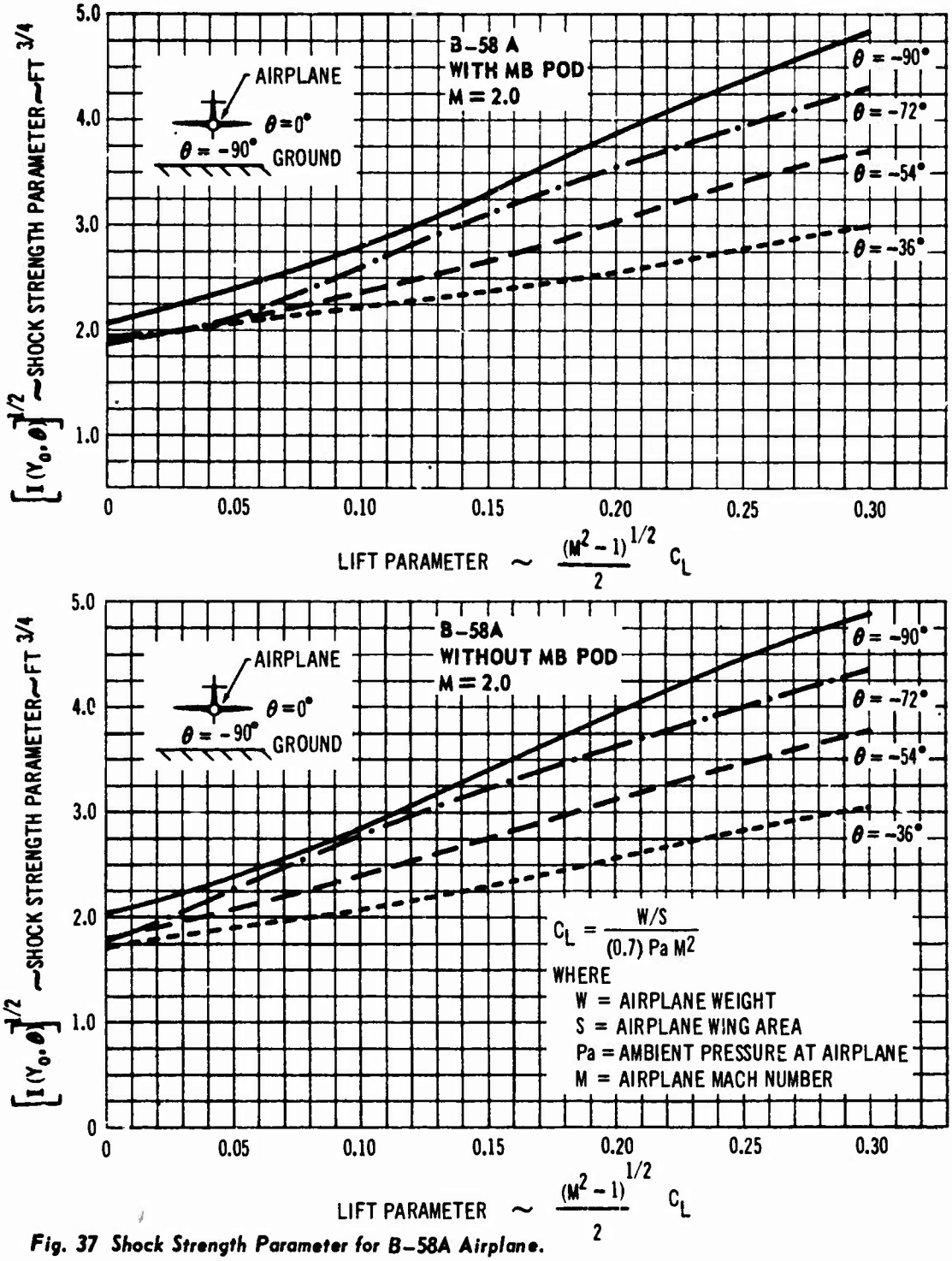

Fig. 37 Shock Strength Parameter for B-58A Airplane.

(3) F-101B - Geometric data for the F-101B were obtained from the McDonnel Aircraft Corporation. These data were analyzed using the theory of Ref. 75 for several angles of θ. Results are shown in Fig. 38.

(B) **COMPARISON OF THEORY AND TEST** - A limited number of comparisons have been made between test results and theoretical predictions using the data obtained during the Oklahoma City sonic boom test series. These comparisons have been generally broken into a study of two areas of the problem. The first concerns predictions assuming horizontally stratified atmospheric models. This has led to detailed comparisons of normal pressure wave traces with those predicted by the theory. The second concerns an investigation of deformed pressure wave signatures. These have been studied both statistically and in detail.

The test data used for these computations and comparisons consisted of pressure-time traces recorded by standard NASA instrumentation (Ref. 84), upper air winds, temperatures, and pressures measured every two hours by GMD-1A equipment, and continuous low level winds and temperatures obtained by Beckman-Whitley probes and wire sondes. The

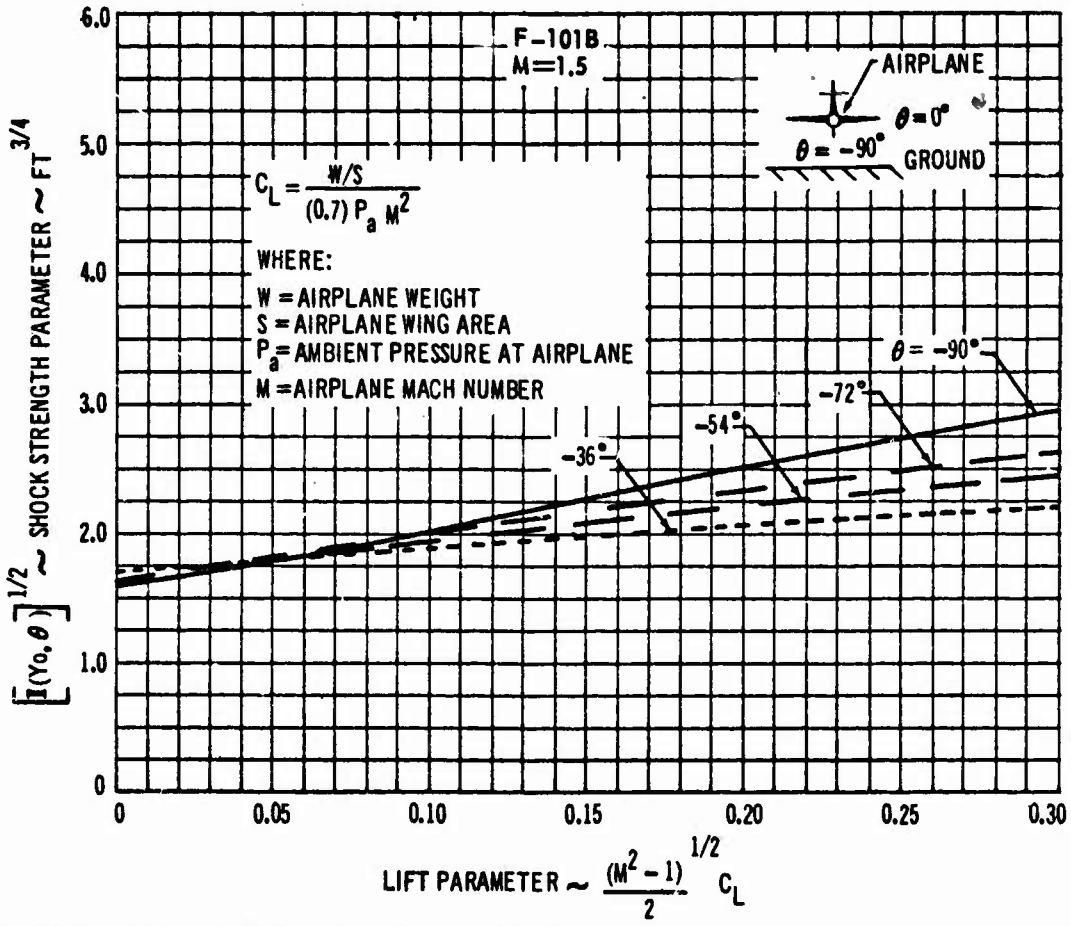

Fig. 38 Shock Strength Parameter for F-101B Airplane.

GMD-1A data were recomputed and interpolated in time (Ref. 76) to provide appropriate data for computing the sonic boom strength and signature at the ground (Ref. 8) for each test case considered. Pressure signature measurements taken in the vicinity of the low level micrometeorological instrumentation were not available, so that none of these data were reduced to provide a description of the turbulence. Such sonic boom measurements could be used in a study of the interaction between the sonic boom and low-level turbulence using the techniques of spectral analysis.

(1) Normal N-Wave Signatures - The detailed pressure wave signature was computed, for the F-104A, using the theory of Ref. 75. This signature was interesting in that an intermediate shock wave was evident between the front and rear waves. The pressures were corrected for the variable atmospheric properties between the airplane and the ground by the method of Refs. 6 through 8. A reflection factor of 2.0 at the ground was assumed. The predicted pressure wave trace was then compared to a number of undeformed measured signatures for the corresponding altitude and Mach number of the test. Some results for the F-104A are shown in Fig. 39.

In general the figure shows excellent agreement with the predicted signature. However, it is interesting to note that the slope and the peak pressure of the measured front shock wave are not in agreement with the theory. This would suggest some influence of the measuring system inertia. That is, the measured wave suggests that the system is unable to react instantaneously to the sharp pressure rise at the front shock wave. The response time lag seems to result in an observed peak overpressure which is from 7 percent to 15 percent lower than that predicted. The fact that the remainder of the measured and predicted pressure wave are quite close suggests that the assumptions used in the theory (including $K_R = 2.0$) are correct.

A number of undeformed pressure signatures produced by the F-101B have been analyzed in the same manner as described above. Some typical results are shown in Fig. 40.

These results are similar to the F-104A results in that the agreement is quite close. However, the pressure rise at the shock waves is not instantaneous as predicted by the theory. In these cases the theoretical overpressure at the bow shock wave is from 5 percent to 10 percent higher than the measured value. This, again, seems to be due to the observed rise rate at the front shock. In all other respects the theory seems to have adequately predicted the pressure signature observed on the ground.

A very limited number of undeformed B-58A pressure wave signatures were available for analysis. These were analyzed in the manner described above and the results are shown in Fig. 41.

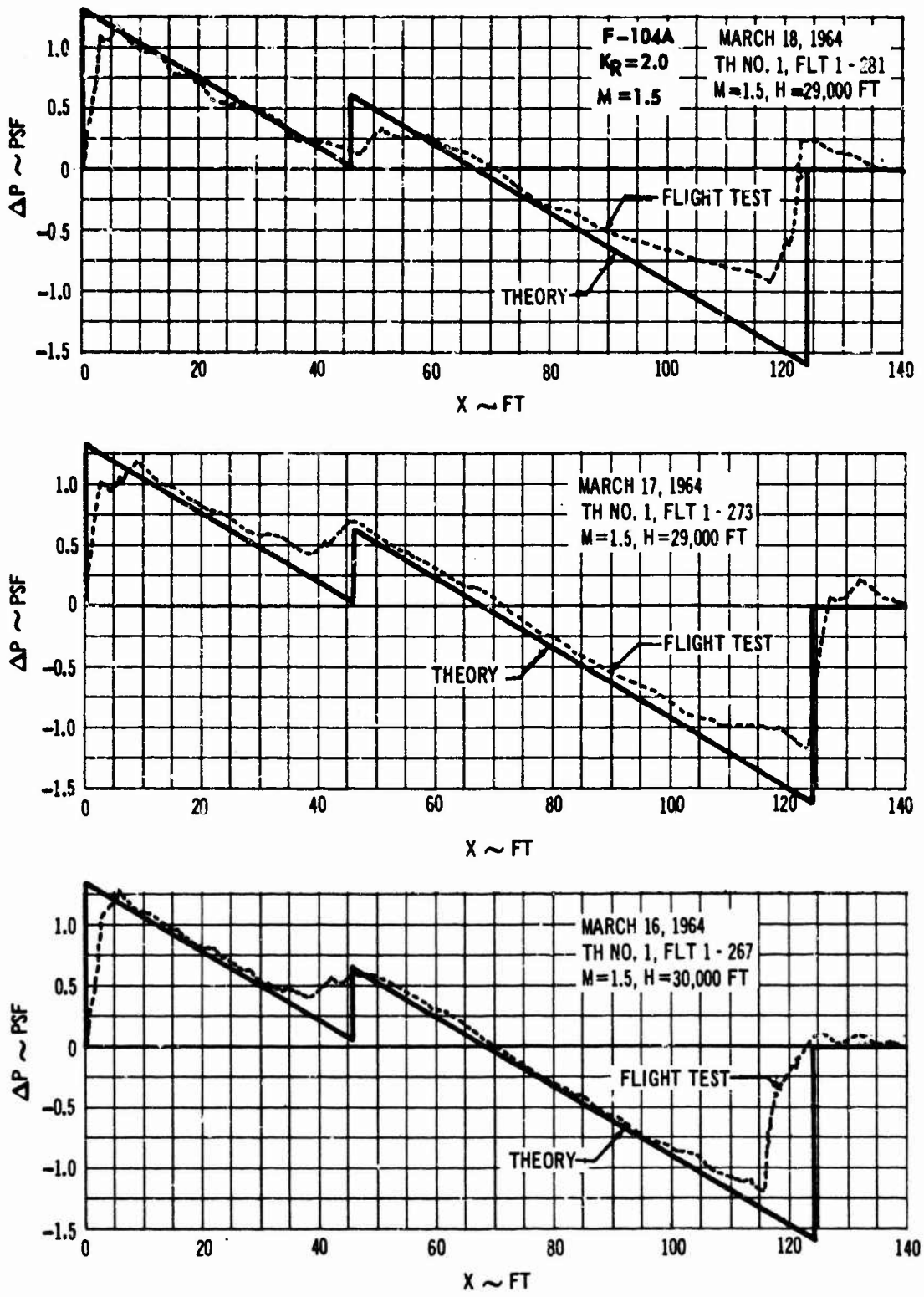

Fig. 39 Comparison of F-104A Theoretical and Measured Pressure Wave Signatures.

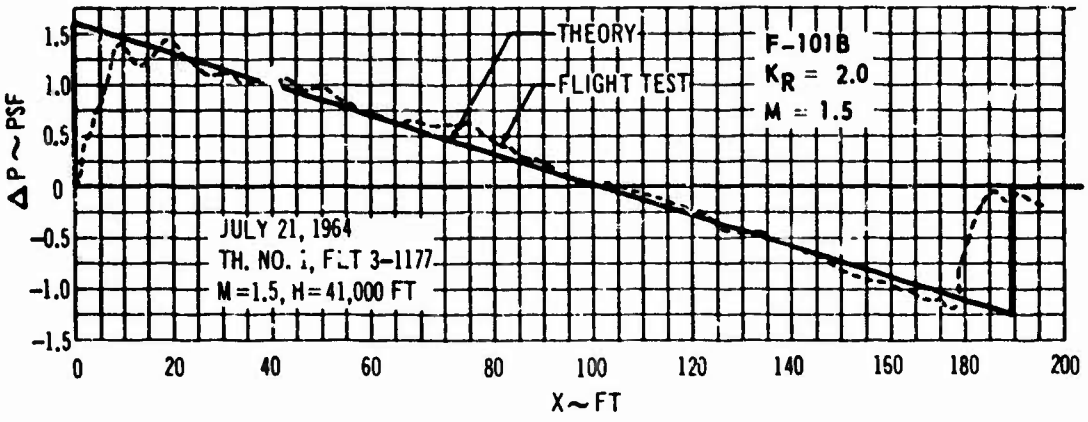

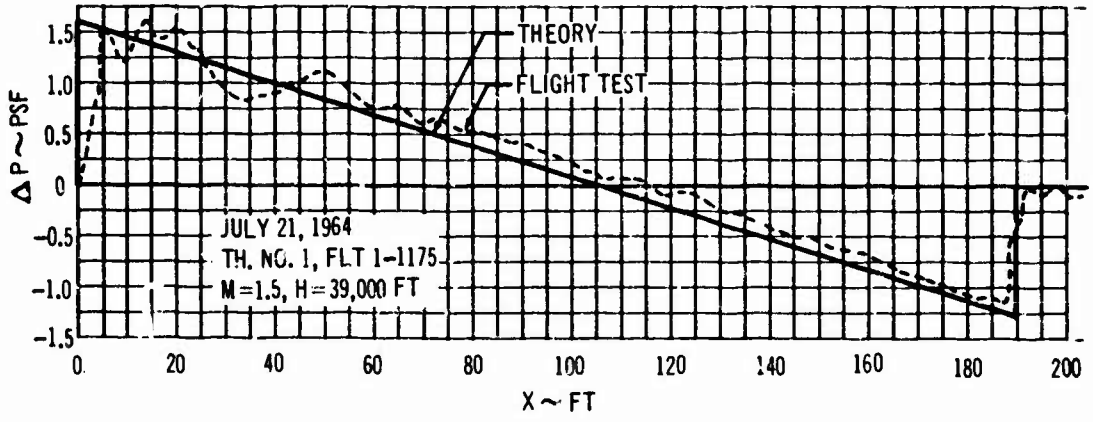

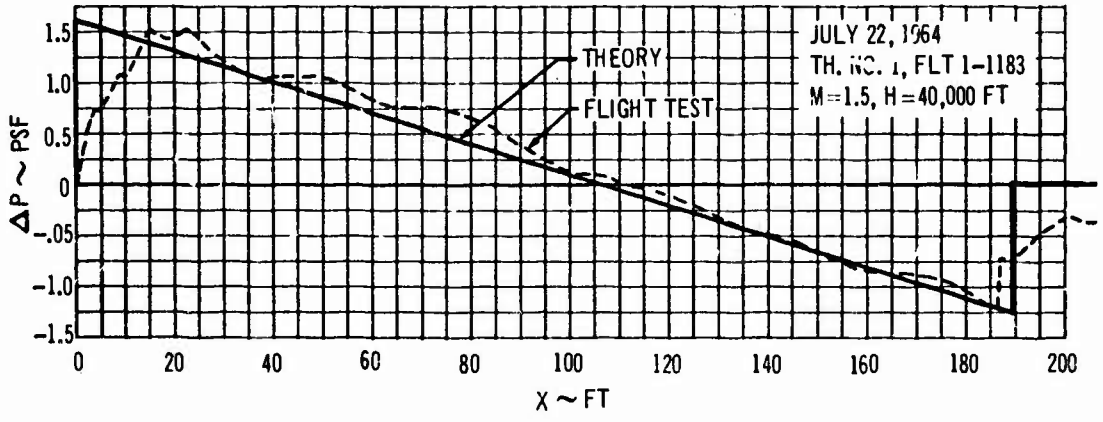

Fig. 40 Comparison of F-101B Theoretical and Measured Pressure Wave Signatures.

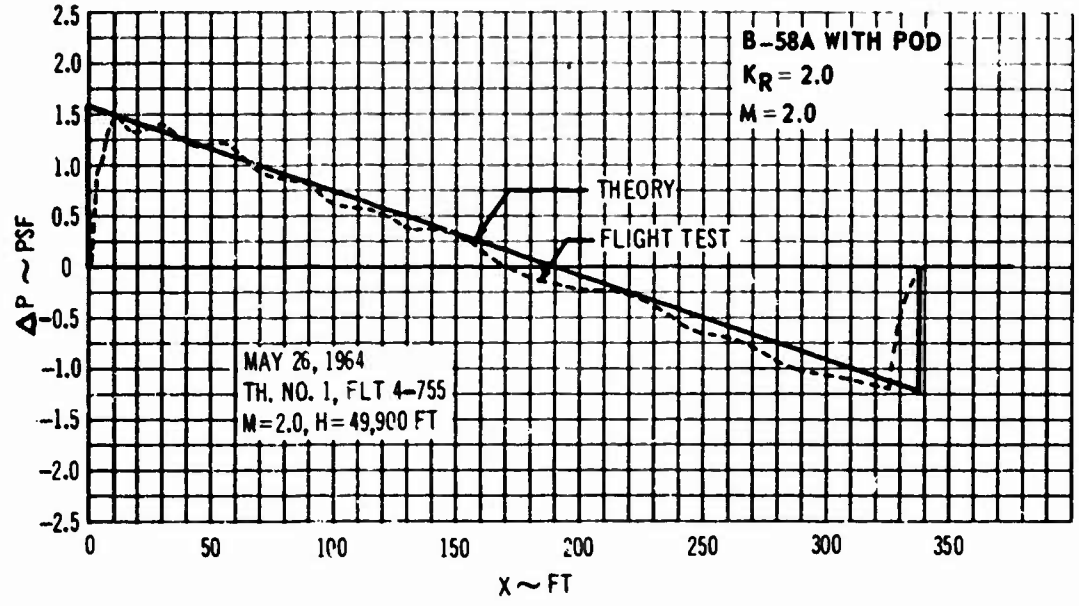

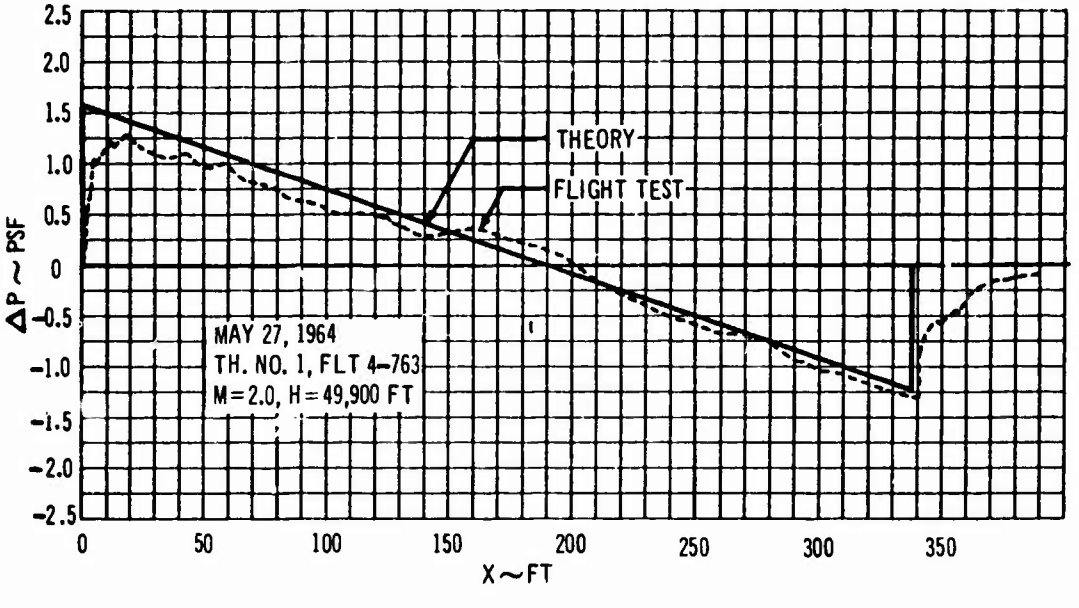

Fig. 41 Comparison of B-58A Theoretical and Measured Pressure Wave Signatures

The figure shows that the agreement of the observed pressure trace with the theory is very close. Sufficient data were not available, however, to estimate the differences between the theoretical and measured front shock overpressure which results the slow rise of recorded signature.

These comparisons indicate that when considering only the agreement between the predicted and observed overpressure of the front shock wave for undeformed signatures, a reflection factor of 2.0 may yield results which are higher than the observed value. This may be compounded by the fact that measured data repeatability for the front shock overpressure may vary by as much as ±12 percent. These considerations have led to the conclusion that when comparing experiment and theory the whole pressure signature should be analyzed. Comparisons of front shock overpressure alone could easily lead to erroneous conclusions concerning the validity of the theory.

(2) Distorted N-Wave Signatures – Comparisons between predicted and measured F-104A, F-101B, and B-58A pressure signatures were developed assuming horizontally stratified atmospheric models, $K_R = 2.0$, and using the theory of Ref. 75. Comparisons of measured spiked waves and measured rounded waves for the F-104A and F-101B are shown in Fig. 42 and Fig. 43 respectively. A similar comparison of a spiked wave produced by the B-58A is shown in Fig. 44. (No rounded waves were obtained in the limited data observed for this airplane during the Oklahoma City tests.)

Again, these figures seem to illustrate some effect of instrument response in that the pressure rise of the front shock is not instantaneous, as predicted by theory. This is probably caused by the inability of the measuring system to respond instantaneously to the pressure rise across the front shock. It is interesting to note that in the case of the spiked waves the pressure trace is generally similar to the predicted normal signatures with the exception of the impulses attached to each shock wave. The forward portion of the rounded wave is similar to the predicted wave but the peak is severely flattened. It would appear that, at one time, both signatures were of the type predicted by theory. Somewhere in the atmosphere between the airplane and the instrument they seem to have been distorted by the addition or subtraction of a pressure pulse at each shock wave. A feature of the distorted waves is that the portion of the signature away from the shocks agrees reasonably well with the theoretical (and observed) undistorted signatures.

In general, the maximum overpressure of the measured spiked front wave exceeds that predicted by theory while the overpressure of the rounded front wave is less than that predicted by theory. Because of this type of distortion of the measured pressure wave signatures, extreme care should be exercised when comparing only front shock wave overpressure data with the predicted theoretical values. If this sort of comparison is to be made, each wave should be classified as to its form, i.e. spiked, rounded, normal, or a combination of these. The most significant comparisons which could be made are of the type shown in

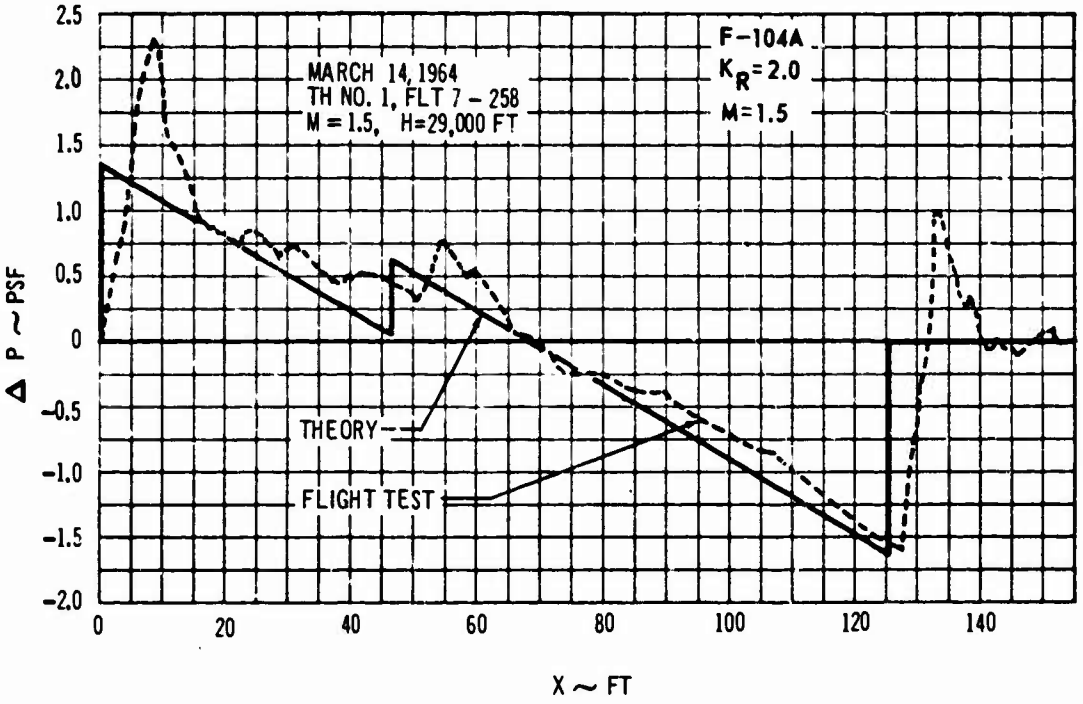

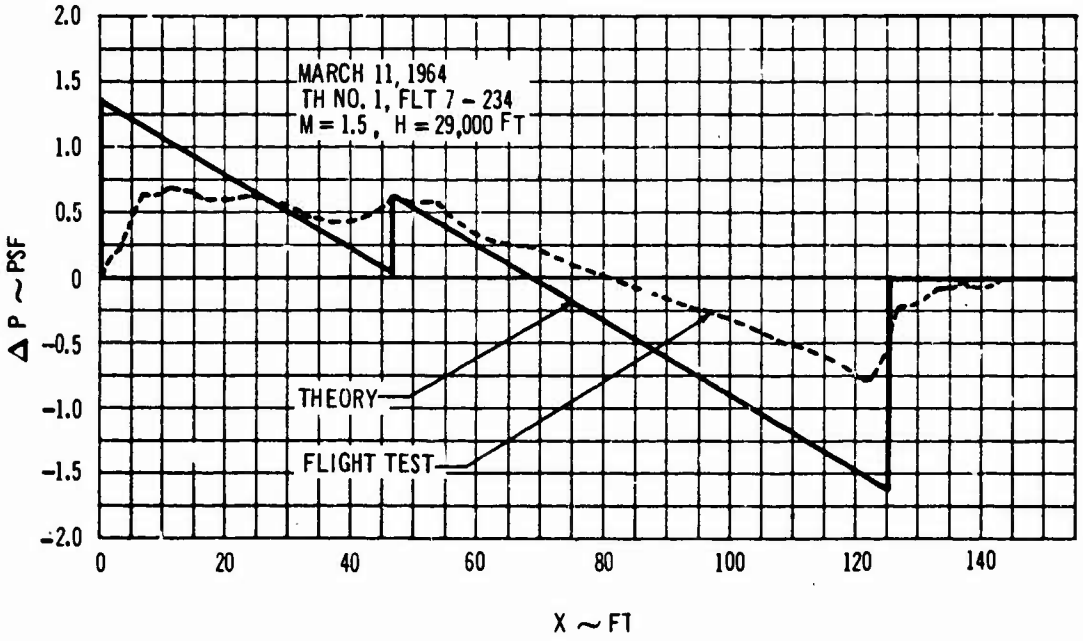

Fig. 42 Comparison of Theory with Deformed F-104A Pressure Wave Signatures.

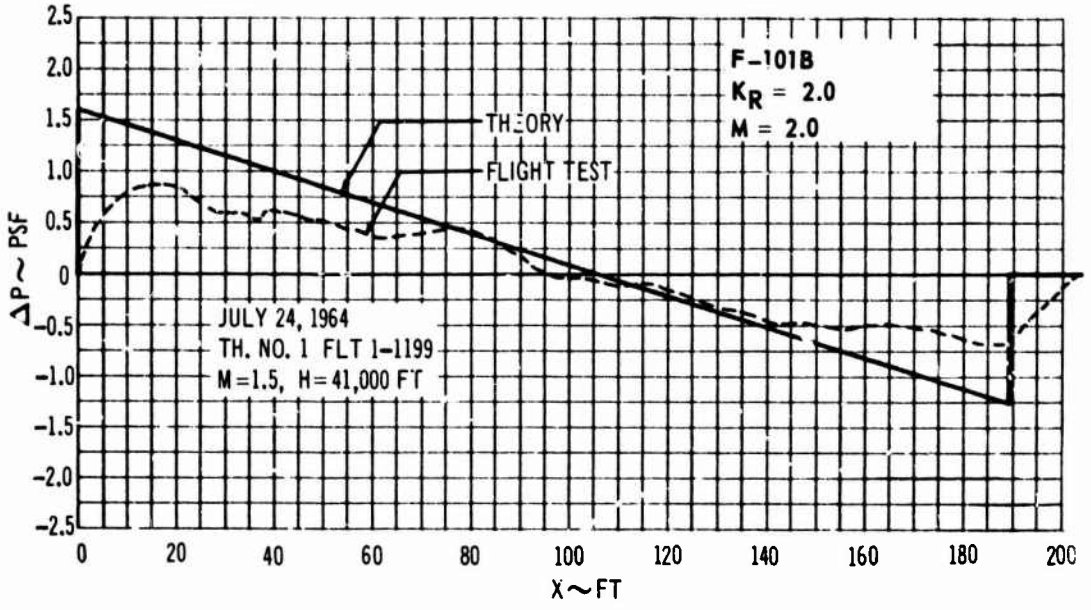

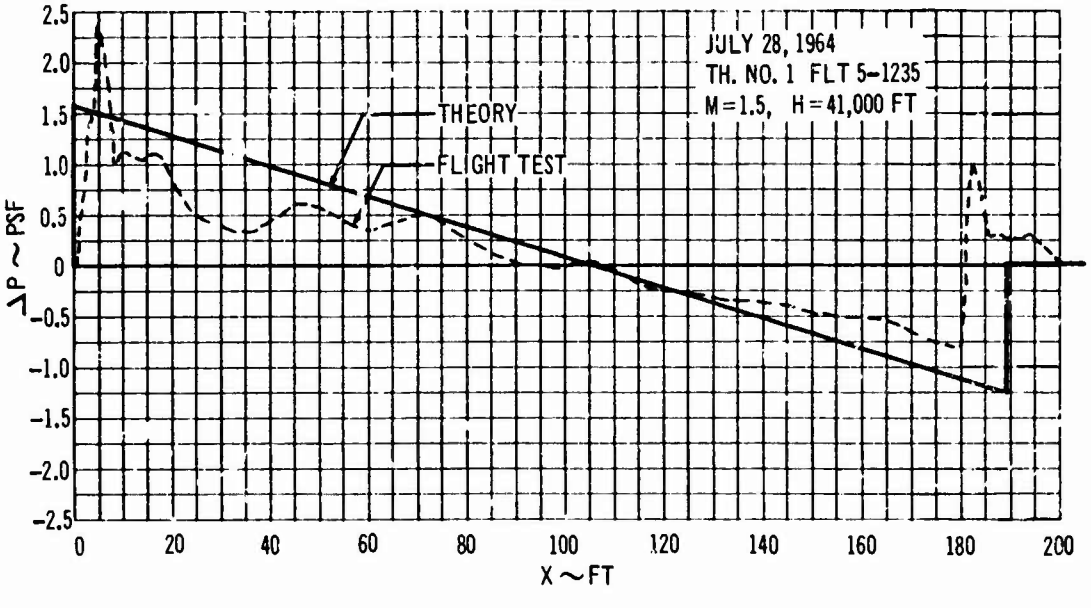

Fig. 43 Comparison of Theory with Deformed F–101B Pressure Wave Signatures.

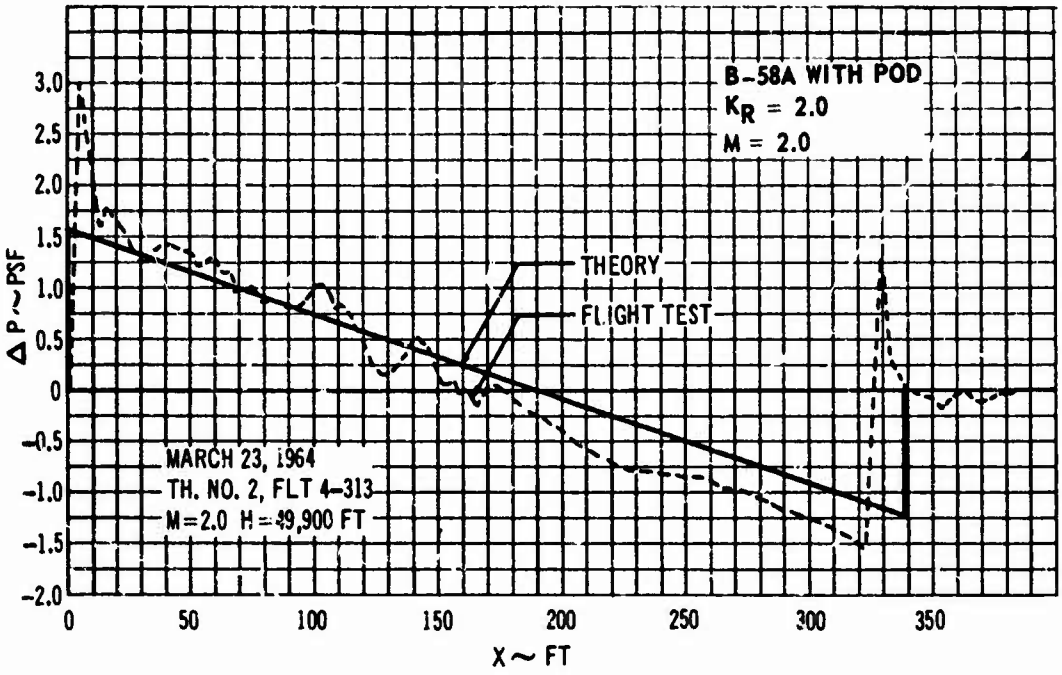

Fig. 44 Comparison of Theory with Spiked B-58A Pressure Wave Signature.

Figs. 39 through 44. Effort of this sort would yield a much better understanding and proper interpretation of the data.

The data in Fig. 45 shows how atmospheric turbulence may affect the shape of the sonic boom N-wave signature over short distances along the ground. The measurements were taken at 0730 hours, in a flat, open area near Lake Hefner (northwest of Oklahoma City). The overpressure signatures were produced by an F-104A aircraft, flying at Mach 1.7, at an altitude of 28,000 ft. The weather conditions at the ground during the time of flight were: clea sky, visibility greater than 15 miles, barometric pressure 28.14 inches mercury, temperature 65 degrees Fahrenheit, relative humidity 43 percent, and surface wind from 210° at 42.6 ft/sec. The radio sonde data at 0700 hours indicate a stable temperature lapse rate, but the strong wind and the 65°F temperature at 0730 suggests that a strong turbulent layer about 500 feet deep had developed. The sun was 12 degrees above the horizon, which implies that the ground heating and consequently the vertical wind velocities were negligible. As a result of these considerations, the low level turbulence can be assumed to be two-dimensionally isotropic and homogeneous in the horizontal plane.

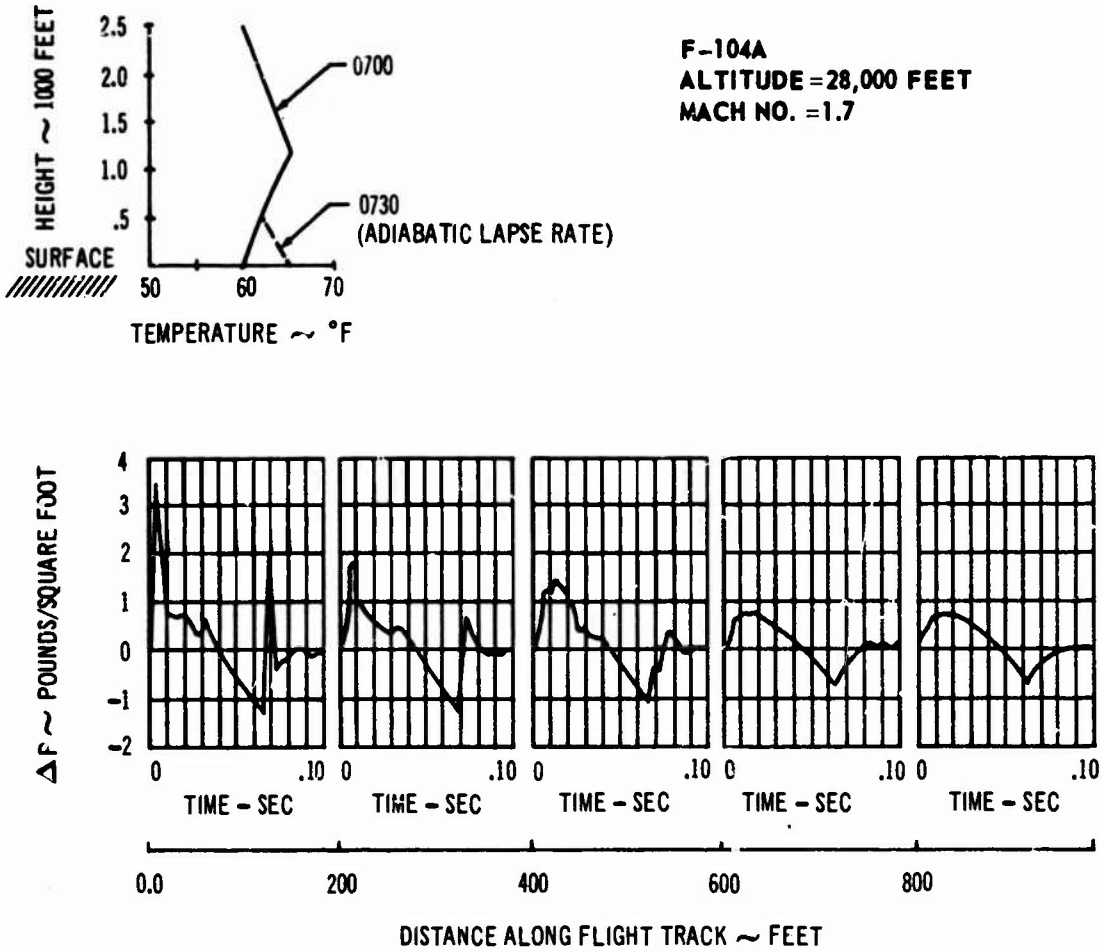

Fig. 45 Pressure Wave Signature Variation

(3) Lateral Distribution of Sonic Boom – Lateral distribution of the front shock wave strength was investigated for several flights during the Oklahoma City tests. Theoretical predictions were obtained using the method of Refs. 6 through 8. Data for each flight were obtained from several sources. The airplane shock strength parameter was obtained from Fig. 36 for the F-104A airplane. Meteorological data throughout the day were obtained from rawinsonde measurements of the Air Force Mobile Weather Squadron (Tinker AFB). A digital computer program (Ref. 76) was designed to compute the appropriate data for the time of each flight from the rawinsonde measurements. This program was used to define the horizontally stratified model atmospheres for each flight. A number of comparisons of the type shown in Fig. 39 were used to define the ratio between the measured and theoretical bow shock wave overpressure. This was done to allow proper evaluation of the measurements in the light of the instrument system response. From these comparisons an instrumentation response factor of 0.9 was selected for evaluation of the F-104A front shock wave overpressures only.

Theoretical prediction of the lateral distribution of the front shock wave overpressures was calculated for several flights with the above assumptions and appropriate calculated data. The measured data was classified into several groups of signature types which included spiked waves (noted by an S), rounded waves (R), normal waves (N), and combinations of these such as normal waves with slight spikes (NS), normal waves with slight rounding of the peaks (NR), and rounded waves with spikes (RS). These data were compared to the theoretical predictions for the undeformed signature. A typical set of these comparisons is shown in Fig. 46 for the flights of April 19, 1964.

These data show that with the exception of the first flight (0700) all the normal wave traces agree to within about ±10 percent of the predicted value. This variation is within the experienced bow wave overpressure measurement error. It may also be noted that, in general, the spiked front wave overpressures are higher than that predicted for the normal wave, while the rounded front shock overpressures are less than predicted. This illustrates that when the theory is correctly evaluated agreement with measured data is quite close.

(4) Statistical Analysis of N-Wave Amplitudes – During the passage of the sonic boom through the lower turbulent levels of the atmosphere its interaction with this turbulence produces marked effects on its shape and amplitudes. There is evidence that turbulent scattering is actively effecting the sonic boom signature. This evidence may be deducted from almost any measured N-wave by the following reasoning: If there is turbulent scattering of the shock wave, the changes of the turbulent structure of the atmosphere between the instant of passage between the bow shock wave and the aft shock wave are very small and the front and aft shock waves should be effected in the same way. The following experiment can be used to test this deduction. First, make a tracing of the distorted N-wave signature. Then, place this tracing below the original trace so that the axis corresponding to time is parallel to the original N-wave signature (as in Fig. 47). Next, translate the trace (to the left in this example) so that the point at which the aft shock wave begins and the front shock wave begins coincide vertically. Next, perform an algebraic-graphical subtraction in which values below the "zero" ΔP line are treated as negative. This procedure, illustrated in Fig. 47, should restore the original form of the N-wave. Such is indeed the case for this signature and for a number of others that this experiment has been tried upon. It appears, therefore, that turbulence is scattering the energy of the sonic boom.

An adequate description of turbulence can only be made in statistical terms. For this reason treatment of data from sonic boom tests in which the atmosphere was turbulent will require some sort of statistical treatment.

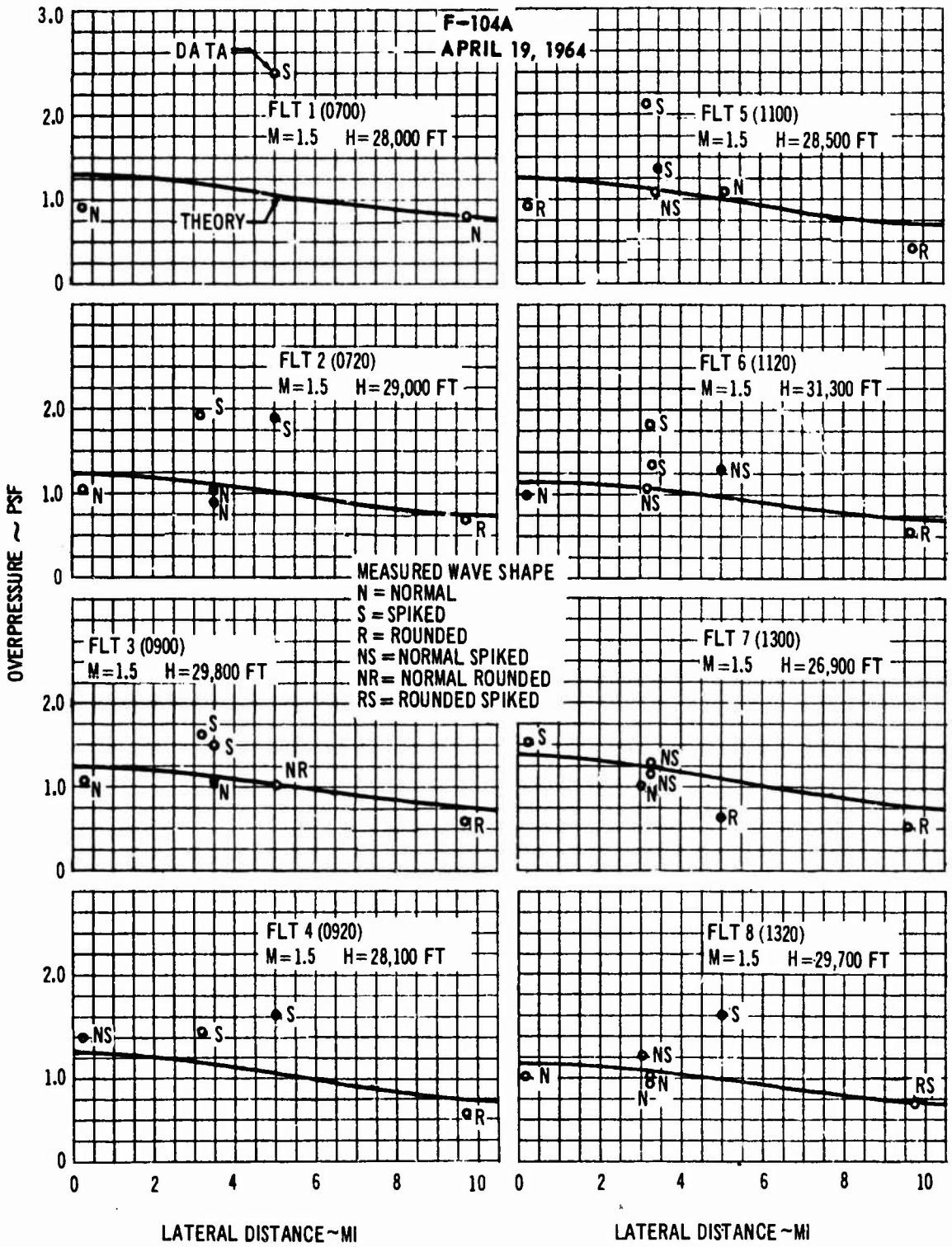

Fig. 46 Comparison of Lateral Distribution of Shock Front Overpressures.

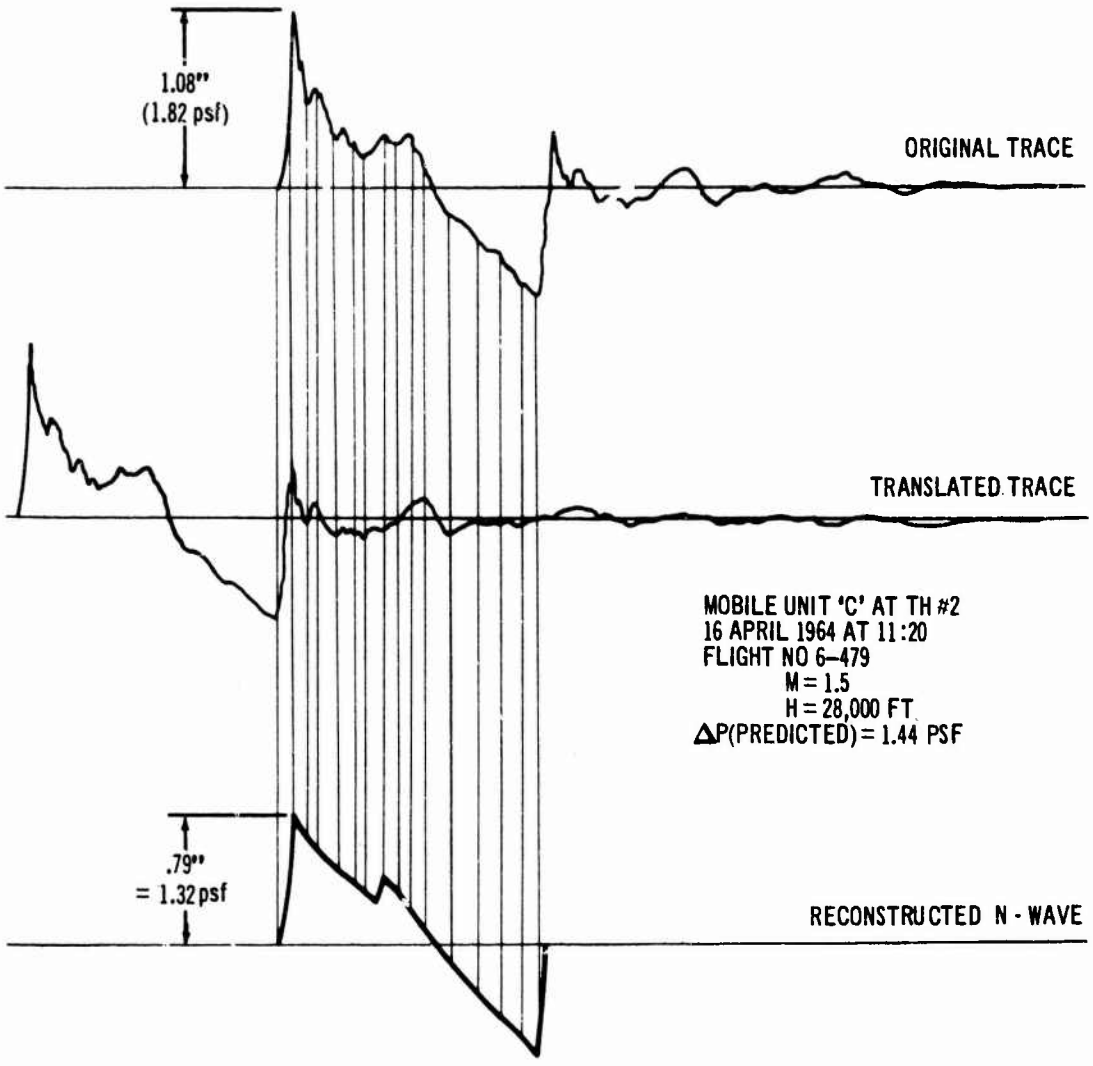

Fig. 47 Reconstruction of Wave Signature by Graphical Method.

Usually, the first attempt to treat data involves the use of the normal statistical distribution. The normal curve, which was first developed by deMoivre in 1753 has been studied extensively by many mathematicians. Its properties such as the standard deviation, which is a measure of the dispersion of the data, the skewness which is a measure of the asymmetry of the data and the kurtosis, which is a measure of the peakness of the data, are well understood. It is important to either show that the data is normally distributed or find an appropriate transformation to convert the observations to a normal distribution. Otherwise, the mathematical tools such as those mentioned above provide a poor description of the data and a loss in the understanding of relative importance of the meaningful physical parameters. This in turn leads to poor or invalid results when the statistics are used for value judgements.

The normal distribution has a number of disadvantages when it is applied to the statistical study of a set of measured sonic boom overpressures. First, it is an infinite distribution and, if used for estimating the upper and lower limits of overpressure, will predict negative "peak positive overpressures" as well as infinite peak overpressures if the confidence limits are set high enough. A negative "peak positive overpressure" is obviously physically unreal, even a zero peak positive overpressure would require either locally complete reflection or refraction. The infinite peak overpressure is similarly physically unrealistic.

Since the action of turbulence is to locally redirect (i.e. scatter) the energy from the N-wave according to some angular pattern, a consequence of this effect, when the centers of scattering action are randomly distributed in space above a two dimensional sampling array, is that data will be logarithmically distributed. This is shown for the case of scattering by a turbulent temperature field in Appendix IX. It therefore appears that the data should be handled by a transformation that has the following properties:

- It should have an upper and lower bound.
- It should be of a logarithmic form.

The four parameter lognormal distribution has these desired characteristics. A complete treatment of the lognormal distribution may be found in Refs. 63, 64, 65, and 66. The general properties of a lognormal distribution may be considered in terms of the number of parameters involved. A parameter here means the number of quantities that are necessary to describe the distribution. The minimum number of parameters is two; they are the mean, μ and the variance, σ^2 (the square of the standard deviation). It is to be emphasized that the variate cannot assume zero values, since the transformation $Y = \log X$ is not defined for $X = 0$.

If there are physical reasons to believe that a lower or upper bound exists, then the three parameter log-normal distribution in which the transformation, $Y = \log (X \pm \gamma)$, is the appropriate one. This results in either a threshold or an upper bound of the distribution γ. The three parameters are then the mean, the variance, and either the upper and lower bound as appropriate. Further, if there are physical reasons (such as with the sonic boom) to believe that there is some upper bound and a lower bound that the values of the parameter may assume, then the appropriate substitution is $Y = \log \frac{(X - \gamma)}{(\theta - X)}$ and we have the four parameter log-normal distribution in which the parameters are the mean, the variance, the lower bound, θ, and the upper bound, γ.

The higher order log-normal distributions are difficult to study analytically, particularly when the upper and/or lower bounds are not known. Fortunately, however, a special type of graph paper, i.e. logarithmic probability paper (K & E 468043) can be used with great ease.

The procedure for using it is as follows: First, the observations are arranged in order of increasing value. Second, the percentage of observations less than, or equal to, a given value is computed. This value is then plotted on the abscissa against the value of the variate on the logarithmic ordinate. The mean and the standard deviation now can be easily determined and the upper and lower bounds estimated.

This method of statistical analysis is illustrated in Fig. 48 for a specific set of data. First, the data was ordered and the corresponding percentages were found. The data were plotted on lognormal probability paper according to the procedures described above. It is apparent from these data that a simple straight line of the two parameter lognormal distribution will not adequately represent the data. It appears that there may be either three discrete sets of data intermixed or that there are some sampling fluctuations. However, since there are physical reasons to believe that upper and lower bounds exist, any curve through the data must be asymptotic to these values. If statistical homogeneity is assumed, then a smooth "S" curve similar to the inverse tangent curve (Ref. 64) symmetric about the 50 percentile value should represent the data. This is characteristic of the four parameter type lognormal distribution. The curve illustrated in the Figure represents a fit of this type curve with an upper bound approximately 1.8 psf and a lower bound near 0.3 psf. The median value is 0.7 psf while a one σ standard deviation about the median is (+0.5, -0.3) psf.

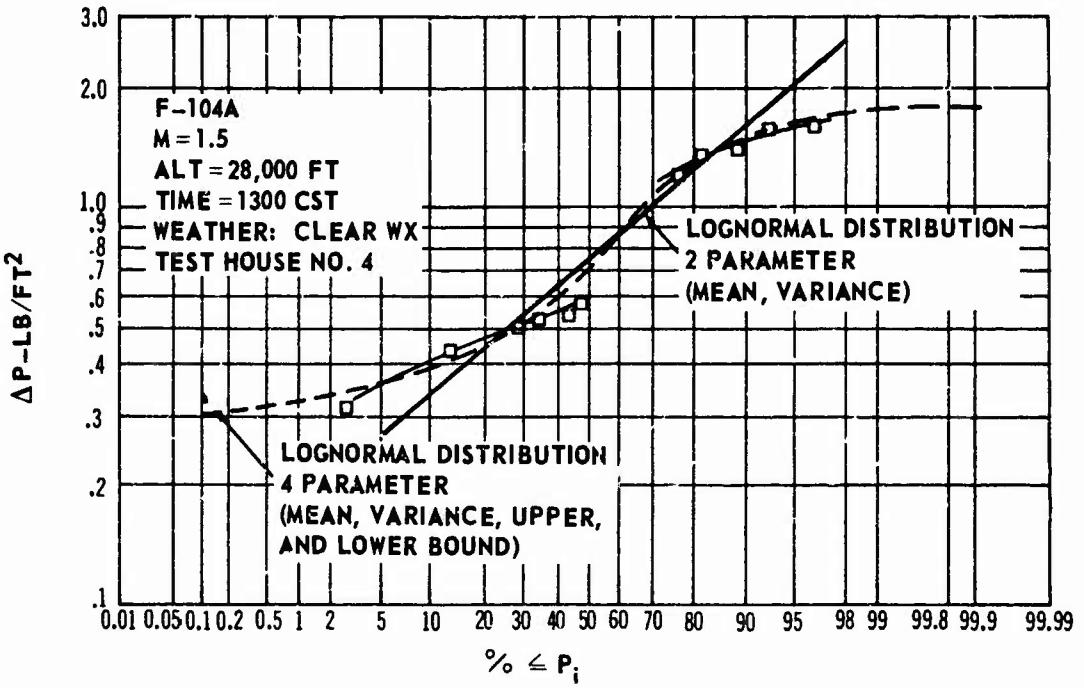

Fig. 48 Statistical Distribution of Overpressure Data.

The variability of data obtained from a series of sonic boom measurements is a function of a number of parameters. Among these are variations due to changes in the large scale atmospheric flow, variation due to changes in the type of aircraft used, changes in Mach numbers, changes in altitude, and differences in intensity of the low level turbulent flow.

To eliminate as many variables as possible, data for the F-104A aircraft, at an altitude of 28,000 feet, flying at Mach 1.5, was chosen for this initial study. Further, since it is apparent that clouds will present a turbulent field of different character than turbulence near the ground, only those booms at times with less than 3/10 clouds were considered. The wind records for Oklahoma City were examined, and in no case was the surface wind less than 10 knots for these observations. This implies that the atmosphere was always somewhat turbulent near the ground. The data was grouped at times of 0700, 0900, 1100, and 1300 Central Standard Time, in order to classify the data as nearly as possible, according to turbulent intensity. This is plotted in Figs. 49, 50, 51, and 52.

Several things are apparent from these figures.

- The variability is greatest in the afternoon as would be expected.
- The variability is a function of the horizontal distance of the observation from the flight path. Even at 0700, Test House 4 at 10 miles from the flight path exhibits large variability.
- Some of the data seems to almost indicate that there were three discrete sample populations, one at high overpressures, one near normal, and at low overpressure. This is particularly evident at Test House 4.
- There appears to be an upper bound near a value of two times the mean of the observed overpressure and a lower bound near 0.3, the mean of the observed overpressure.

It is probable that the angle at which the sonic boom is propagating is important. This is due to the fact that the turbulent power is greatest in the horizontal plane (Ref. 41, p. 161ff).

(C) SUMMARY OF RESULTS - The theory used in this report was compared with some of the test data obtained during the Oklahoma City sonic boom tests. It was found that when observed undeformed pressure signatures were compared to those predicted by the theory the agreement was quite good. The pressure rise, trace length, and slope of the expansion region between the shocks agreed closely with the predicted wave. However, the pressure rise at the shock waves of the measured trace was not instantaneous as predicted by the theory. This results in some disagreement between the theory and test when only the front shock overpressures are compared. Some of the deformed pressure waves were analyzed statistically. It was found, from this analysis, that the important scattering parameters are the angle of the path of propagation of the shock wave, and the time of day as related to the turbulent intensity near the ground.

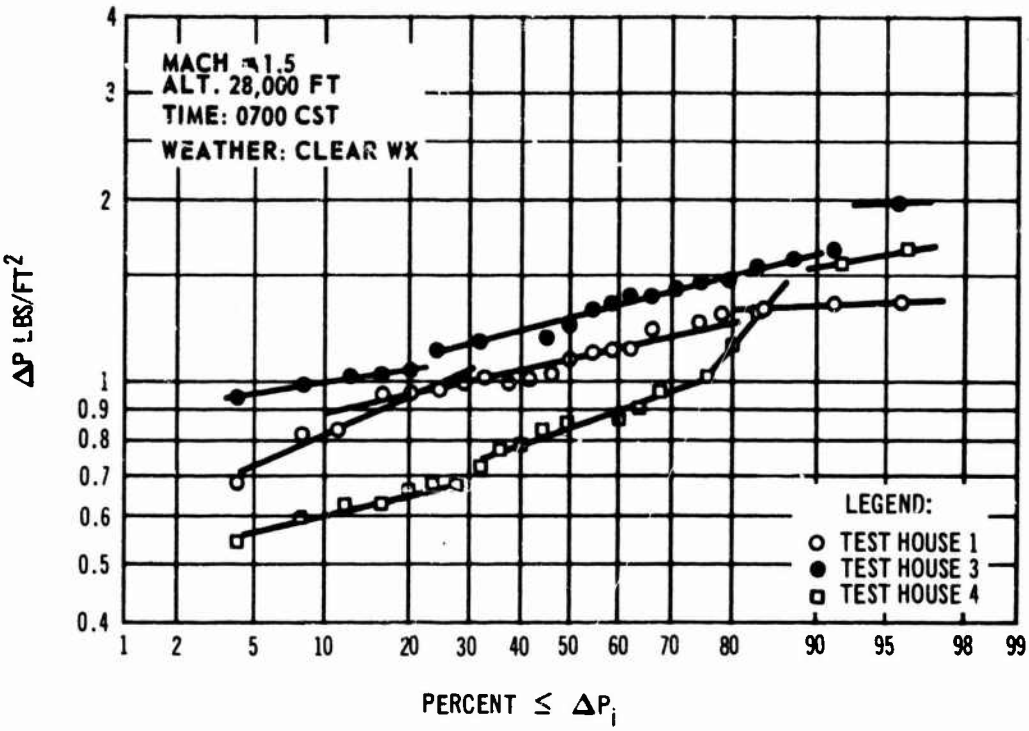

Fig. 49 Overpressure Distributions at Test Houses 1, 3, 4 at 0700 CST.

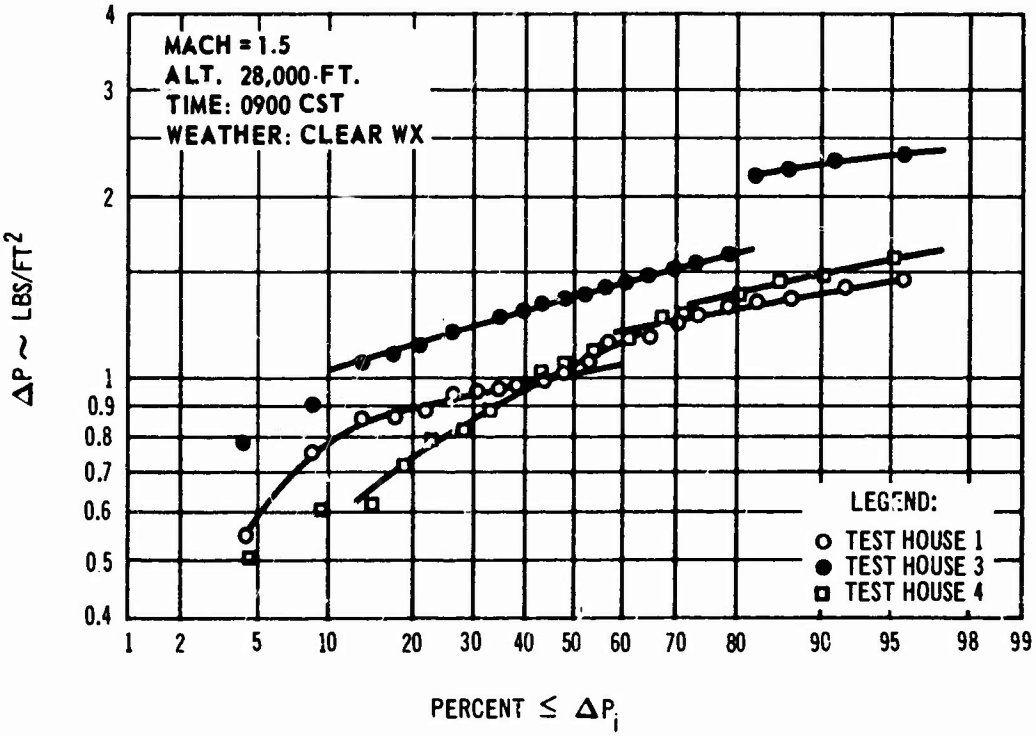

Fig. 50 Overpressure Distributions at Test Houses 1, 3, 4 at 0900 CST.

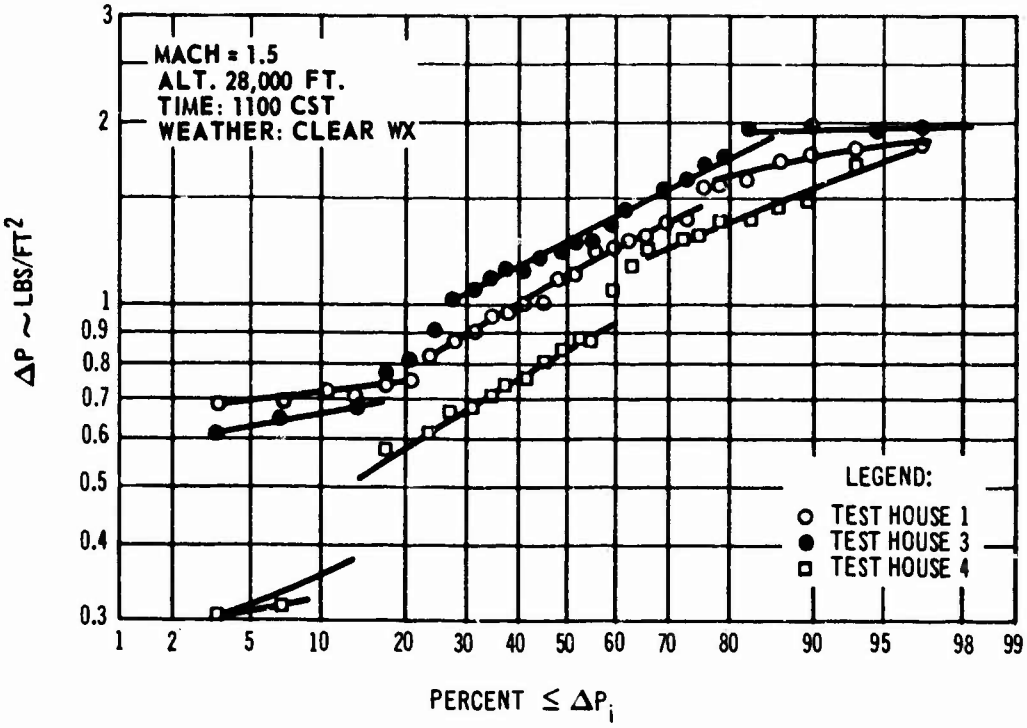

Fig. 51 Overpressure Distributions at Test Houses 1, 3, 4 at 1100 CST.

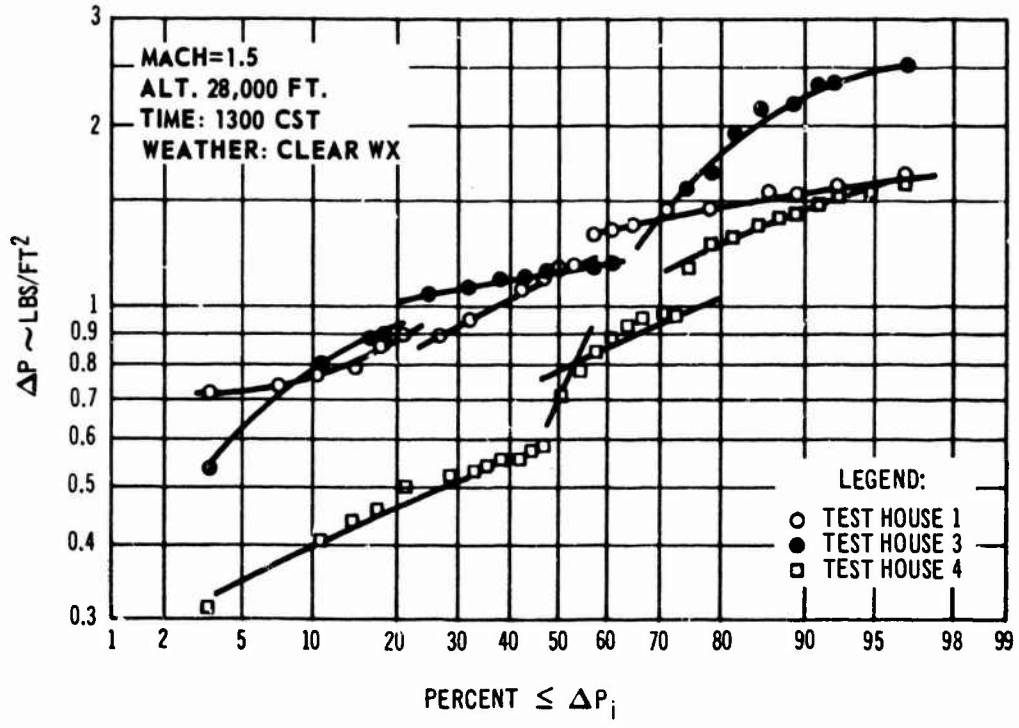

Fig. 52 Overpressure Distributions at Test Houses 1, 3, 4 at 1300 CST.

SECTION V FREQUENCY OF OCCURRENCE OF UNUSUAL PROPAGATION CONDITIONS

Any discussion of the frequency of occurrence of anomalies in the sonic boom overpressure and distribution must include an assumption about the flight profile of the airplane. In the following discussion a typical supersonic transport is assumed which first exceeds Mach 1.0 at altitudes near 40,000 feet above the ground. No supersonic flight is planned for altitudes below this. A survey of wind speed as a function of altitude for the mid-latitudes has indicated that 99.9 percent of the time the maximum wind speeds occur at altitudes very near or below 40,000 feet.

The cut-off and possible focusing phenomena were shown in Section III to occur at low Mach numbers for physically possible wind speeds. For temperature profiles with an inversion near the ground, cut-off and possible focusing will occur above the ground. Thus, this phenomena may occur when no inversion exist near the ground (i.e., approximately 50 percent of the time). From this discussion, it would appear that cut-off and possible focusing under or to the side of the flight track would occur at least once on the ground during the low Mach number portion of the flight when no temperature inversions exist near the ground (i.e., approximately 50 percent of the total available time). Whether or not this phenomena constitutes a significant increase in the boom strength on the ground is still not resolved because of the question of the variation of the reflection factor near cut-off.

Extreme lateral spread is possible only in the presence of very strong winds with maximum speeds above 150 feet per second. However, as these maximum speeds exist below 40,000 feet 99.9 percent of the time, flight above this altitude would not produce this phenomena. It would appear that because of the high altitudes selected for supersonic portions of the flight the sonic boom will not extend to extreme lateral distances to the side of the flight track.

Considering the flight profiles contemplated for the supersonic transport, it becomes apparent that only the boom produced during the first and last few minutes of supersonic flight may be significantly influenced by the meteorological conditions between the airplane and the ground. The boom produced during the remainder of the flight would be relatively unaffected by the meteorological conditions between the airplane and the ground.

SECTION VI EVALUATION OF THE ACCURACY OF THE THEORY

The correction factor presently used to account for the influence of the variable properties of the atmosphere, $\sqrt{PaPg}$, seems to be somewhat less than predicted by the present theory. Comparisons with Oklahoma City sonic boom data indicate that the accuracy of the theory and method of Refs. 6-8 is quite good in accounting for the influence of the meteorological conditions. However, this data is very limited in scope because the test airplane altitudes were relatively low where the differences between the more sophisticated approach and $\sqrt{PaPg}$ are small. A limited amount of high altitude flight test data is available and has been analyzed. These data (Ref. 80) were compared in Fig. 53 with the theoretical predictions using the present theory. Here again, the theory is in close agreement with the test data. However, more comparisons of this sort would be very desirable.

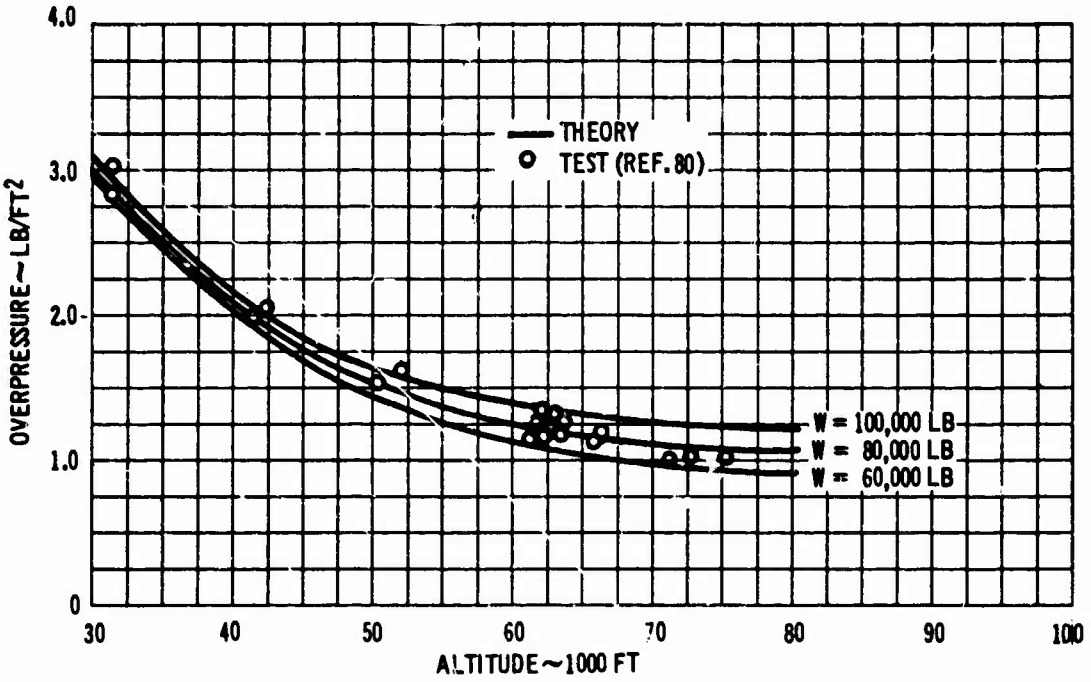

Fig. 53 Comparison of Test and Theory for High Altitude Flight.

It was shown in Section II that rather large variations in the properties of a stratified stmosphere cause small changes (±5 percent) in the sonic boom strength generated by airplanes flying at Mach numbers above 1.3. These same variations produced larger changes (approximately ±20 percent) for flight at Mach numbers below 1.3. In terms of the meteorological observations, these atmospheric variations encompass a range in the mean absolute temperature (which is used to determine the pressure altitude) over the altitudes of interest of 6.6 percent. Errors of this magnitude in any single observation are very rare. Further, when it is realized that any single observation is compared with nearby observations during the analysis of the atmospheric flow field the probability of such a large error going undetected is almost zero. A similar comparison holds for the effect of errors in the measurement of wind. Thus, it would be expected that small errors in the daily observations (say 1 percent) would cause small changes (±5 percent at the maximum) in the theoretical predictions even for the low Mach number range of flight. Based on the results in Section II, then, it would appear that data from present day upper air sounding are sufficiently accurate to be used in planning flights for the supersonic transport.

SECTION VII CONCLUSIONS

The effects of varying meteorological conditions on the intensity and spread of the sonic boom have been investigated. This has been accomplished by constructing several stratified atmospheric models and comparing sonic boom calculations in these atmosphere with results in the U. S. Standard Atmosphere, 1962.

It has been found that the influence of wind and temperature variation from standard conditions is primarily a function of Mach number, while the influence of pressure variation is independent of Mach number. It was also determined that for flight at Mach numbers above 1.3 the largest influence of varying the meteorological conditions from those in the Standard Atmosphere is a change in the sonic boom overpressure of about ±5 percent. Flight at Mach numbers below 1.3 may result in more significant variations.

The meteorological conditions required to produce focusing, complete cutoff, extreme lateral spread, and deformation of the pressure-wave signature have been investigated and methods for predicting the occurence of these conditions have been established. It has been found that realistic variations in temperature and winds could produce focusing or complete cutoff for flight at Mach numbers below 1.3. Focusing would occur simultaneously with cutoff where the shock waves are normal to the ground, and the normal doubling of the overpressure due to oblique shock wave reflections would not occur in this region. Extreme lateral spread and deformation of the pressure wave due to interactions with turbulence may occur at all Mach numbers. The former would not occur, however, for flight at altitudes above those where the maximum winds exist, regardless of the Mach number.

The flight path contemplated for a typical commercial supersonic transport includes extremely rapid transition through Mach numbers near 1.0 at altitudes near or above 40,000 feet above the ground. The time spent in accelerating through Mach 1.3 during the initial phases of supersonic flight and in decelerating through Mach 1.3 during the latter phases of supersonic flight amounts to only a few minutes. In this respect, then, it becomes apparent that for the supersonic transport only the boom produced during the first and last few minutes of supersonic flight may be significantly influenced by the meteorological conditions between the airplane and the ground. Furthermore, because the supersonic flight altitudes are generally above those where the maximum wind speeds exist, the probability of the occurrence of extreme lateral spread would be very small.

A number of comparisons have been made with flight test data obtained during the Oklahoma City flight test series. Predicted and measured pressure-wave signatures have been compared for each test airplane. It was generally found that the pressure rise, length, and slope of the expansion region between the shocks of the measured wave agreed closely with the predicted wave. The pressure rise of the observed

shock waves is not instantaneous as predicted by the theory. This has led to some disagreement between theory and test data when only front shock overpressures are considered. The presence of turbulence near the ground results in the deformation of the incoming pressure-wave signature and some of these deformed signatures have been analyzed. A statistical analysis of these data has indicated that the important scattering parameters are the angle of the path of the shock wave and the time of day as related to the turbulent intensity near the ground.

The effect of viscosity on the sonic boom has not been included in these studies. Viscosity does not significantly influence very low frequency waves which would constitute the fundamental harmonics of the sonic boom N-wave (see Refs. 85 and 86). Thus, this would be of minor importance when investigating the propagation of sonic boom through the atmosphere.

SECTION VIII RECOMMENDATIONS FOR CONTINUED THEORETICAL AND EXPERIMENTAL WORK

A number of aspects of the sonic boom problem still remain unresolved. Although a substantial amount of effort has already been expended in obtaining an understanding of the problem, further theoretical and experimental work aimed at improvement and extension of the present theory would be desirable. The purpose of this section is to discuss some of the unresolved areas and to outline possible theoretical and experimental approaches which might be taken in seeking solutions.

(A) THEORETICAL - The theory developed to date seems to be sufficient for estimating the shock wave overpressures and pressure signatures received on the ground for an airplane in steady level flight through a nonuniform nearly stratified atmosphere. Comparisons with available experiment such as those presented in Section IV have led to this conclusion. However, the theoretical development should be extended to include the effects of general aircraft maneuver and the turbulence effect near the ground. Some preliminary work has been done in both these areas. The latter was outlined in Section III.C. Further work should be directed toward seeking a solution of the pressure wave history near and beyond cut-off, and toward an understanding of the effect of interactions of the pressure wave with regions of high altitude turbulence such as exist in towering cumulus clouds. Guidelines for these theoretical investigations are outlined in the following material.

(1) Extension to General Maneuvers - The prediction of sonic boom overpressures on the ground for an airplane engaged in general maneuvers in a nonuniform atmosphere is a quite complicated task. The ray tube area concept, used in Refs. 6 through 8, lends itself to considerations of this sort. The expression for the ray tube area (for instance that presented in Appendix II) may be modified by the inclusion of terms which describe the distortion of the ray paths due to the maneuver. Some preliminary work has been done in Ref. 77 toward the development of the required terms.

In addition to developing these terms, one of the major problems involved in making sonic boom estimates for a maneuvering airplane is the obtaining of a description of the shock front intersection with the ground, and the location of the points at which this front may cusp (or fold over on itself) to form a focused so called "super" boom. The transformations between the ray intersections with the ground and the shock front location are extremely complicated because of flight path and velocity variation, and because of variation in the atmospheric properties. At the present time, it is felt that the shock front can be located by trial and error (Ref. 6). Furthermore, the ray tube area concept cannot account for the situation when two rays generated by the airplane at largely different times reach the ground at the same point and time (shock front crossover). This situation could occur when the airplane is engaged in a short radius circular turn (Fig. 7, Ref. 78).

Both the cusp and the shock front crossover are regions which should receive special attention when investigating the shock strength distribution on the ground. The work which has been referenced above would prove useful in any future theoretical development.

(2) Shock History At and Beyond Cut-off – The region near the cut-off of the boom is not fully understood. In aerodynamic terms it consists of a region of mixed flow where in an area slightly before cut-off the flow is supersonic and in an area beyond cut-off the flow is subsonic. In physical terms this means that a shock wave cannot exist beyond cut-off. However, some sort of pressure distribution will be propagated through the air. The type of disturbance is properly illustrated in Fig. 5.

A number of approaches may be used in seeking a solution to the shock wave history in this region. One of these might be to extend the Whitham theory of Ref. 2 to account for variable speed of sound in the supersonic region. This would allow the description of the pressure perturbations generated by the airplane to be described up to the cut-off. The subsonic description might be obtained by the classical methods outlined by Prandtl (Ref. 79). The two solutions could then be investigated in the region of the cut-off to describe the transition of the pressure distribution from the supersonic shock wave to the subsonic pressure wave. The variation of the reflection factor, K_R, should also be investigated in the same region.

(3) Extension of Analysis of Turbulent Effects – The theory of scattering of acoustic and shock waves inherently postulates a weak interaction between the acoustic or shock waves and the turbulent field. This allows the assumption, that the wave length of the acoustic energy is much less than the wave lengths of the turbulence to be made and results in considerable simplification in the theory. At the wave lengths associated with the sonic booms produced to date, this approximation is of extremely dubious validity and will become even more so for larger aircraft.

Two possible alternative explanations may be offered to explain the spikes observed in the N-wave traces such as those from Oklahoma City. First, they may be the result of coherent scattering in which the phases of the waves combine at certain points so as to give reinforcement. Coherent scattering can occur when the interaction is weak. Alternatively, the spikes may be due to strong, resonant interaction between the shock waves and turbulent eddies. This type of interaction is extremely nonlinear and the terms usually neglected in the partial differential equations must be retained. In addition, if there is strong interaction between the N-waves and the turbulence, the separation of the cross-sections into one due to temperature and one due to wind is incorrect. Consequently, effects of a random temperature field and a random wind field must be considered simultaneously. The resolution of the problem of the mode of interaction between the sonic boom and turbulence can only be made by appeal to experiment, since the only "a priori" reason for preferring one scattering mode to the other, is the requirement that the eddies have an ordered, spatial distribution for coherent

scattering. However, an exact physical description of turbulence is lacking at the present time and this requirement for an ordered distribution cannot be either used or rejected.

Appeal to such experiments as the closely spaced microphone arrays used during some of the Oklahoma City sonic boom tests tentatively indicate that coherent scattering does not occur. For instance, if the records from Mobile 1, Flight 2 on 2 April 1964 are considered, spikes should occur at intervals at least every 196 feet (the wave length of the fundamental harmonic of the "free air" N-wave), or very close to every microphone for the 200 foot spacing of this array. This rises from the requirement considered in Section III.C for a resonant peak at intervals of $(m\lambda)$ where m is an integer and λ is the wave length of the fundamental N-wave harmonic. This is not the case. Rather, a regular progression from a peak value of overpressure to a minimum is observed over a distance of 800 feet. Coherent scattering can thus be tentatively ruled out in this case. The further observation can be made that the cross-section (i.e. the area affected by the eddy) must be at least 570 feet in radius; possibly as much as 1140 feet. For these sizes it is implied that there is some degree of resonance.

For this reason it is suggested that the analysis of the interaction of the sonic boom be extended as follows:

- Extend the mathematical analysis to include the study of strong scattering. Green's functions, the Fourier transform (or possibly the 3-dimensional LaPlace transform) and of spherical harmonics can be profitably applied to this study, since a more general type of solution can be generated by this technique. Currently, initial steps have been made in this analysis, but are not sufficiently complete to include in this report.
- Analysis of a representative sample of the Oklahoma City micrometeorological data to determine the spectral densities of temperature and wind.
- Consideration of the nonhomogenous turbulent-scattering problem in which reverberations can occur.

Providing an analytical solution of this problem can be achieved, reasonably exact statements about the spatial distribution and the maximum values of the overpressure as well as the wave-length of the spikes, can be expected for the case of single scattering.

Multiple scattering is a very difficult problem and progress will be slow in this case.

The problem of propagation through convective clouds should be studied to some extent since anomalous propagation almost surely occurs. The internal structure of convective clouds is sufficiently well known that a preliminary study can be made, neglecting turbulence.

(B) EXPERIMENTAL - Additional experimental confirmation of the theories presented in this report would be desirable, especially near cut-off. Controlled experimental data would also be helpful in understanding

more about the effect of turbulence on the pressure signature. A test program is briefly outlined in the following material which might yield useful data in both of these areas.

(1) **Measurement of Shock Strength At and Beyond Cut-off, Steady Flight** - It was noted in Section III that local intensification of the boom may occur only simultaneously with cut-off. It was further observed that the reflection factor, K_R, might also vary in the same region. A series of field tests could possibly verify both of these postulates.

The theory and method developed in Refs. 6 through 8 indicate that the free air overpressure (i.e. accounting for no reflection) may increase rapidly in a very small region near cut-off. This is illustrated in Fig. 54 for the free air overpressure under the flight track of an airplane in steady flight in a headwind.

The figure shows that the theoretical intensification of the free air overpressure takes place over a very short distance. If an airplane were flown over an instrumented tower at nearly the cut-off Mach number for the conditions of the flight the variation of shock with distance might be measured. These measurements could be compared with theoretical predictions for the same meteorological and flight conditions.

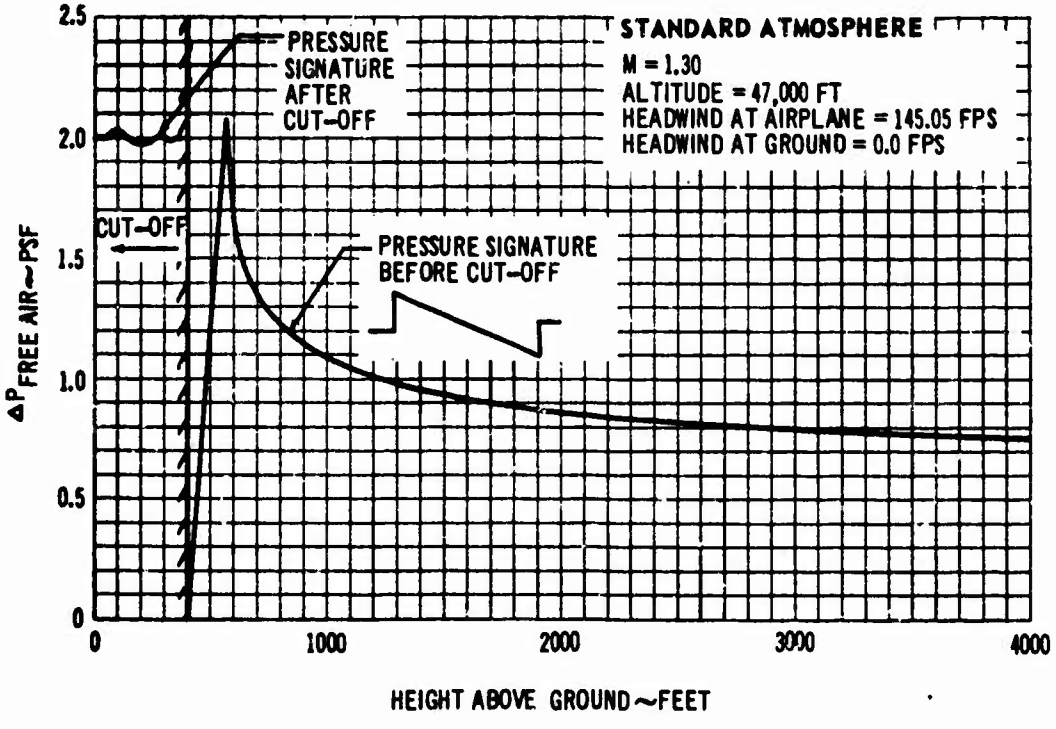

Fig. 54 Shock Strength History Near Cut-Off Under Flight Track.

The tower height should be in excess of 1000 feet and should contain a dense array of microphones at regular intervals along its height. It should also be equipped to continuously measure wind velocity and temperature at regular intervals along its height. The surrounding terrain should be relatively flat and the area near the ground should be such that relatively quiescent conditions exist at some time during the day or night. This would be to avoid possible interactions with turbulence near the ground which may make data interpretation difficult. Facilities should be available to obtain good forecasts and measurements of the wind and temperatures between the airplane and the ground so that each flight may be programmed to obtain cut-off under the flight track near the ground. Facilities should also be available for tracking the airplane flight path and coordinating it with the tower instrumentation. The flight path should be directly over the tower and directed generally into the wind. One possible location for these tests might be the BREN tower located at the AEC Nevada test site.

In addition to the free air microphones a set of microphones might be mounted on reflecting boards at the same regular intervals to obtain the variation of K_R near the cut-off. This could be accomplished by comparing the two simultaneous sets of measurements.

The same type of facility may also be useful in obtaining measurements of the turbulent scattering phenomena at various levels above the ground. Flights could be made over the tower during the time of day when there is the greatest probability of turbulent activity in the area near the ground. Details of this portion of the test program are outlined in Section V.B.2.

(2) Measurements of Pressure Wave Distortion by Low Altitude Turbulence – Present indications are that the single scattering interaction of the sonic boom with turbulence is most important from an overpressure standpoint. It is probably limited to the lower 1000 to 3000 feet of the atmosphere. If the turbulence extends to greater depths, the probability of multiple scattering increases. A further indication is that the distribution of the spike amplitudes in single scattering is trigonometrically distributed. It would be very desirable to determine the effect of turbulence at various levels above the ground. The preferred setup for this purpose would be a fixed installation such as a high tower with microphones both on the tower and on the ground around it, no further than the "free" air wave length of the sonic boom apart and arranged to obtain the overpressures over an area on the order of eight wave lengths on a side. The tests should include tests at various angles of incidence of the N-wave, and under varying wind speeds and vertical temperature lapse rates. It must be pointed out that a series of runs will be necessary, since the eddies are randomly distributed.

The BREN tower at the AEC Nevada Test Site is 1527 feet high, is instrumented meteorologically and is remotely located from inhabited areas. It would seem to be an excellent facility for experiments of this kind.

APPENDIX I VARIATION OF K_A WITH HEIGHT OF GROUND ABOVE MEAN SEA LEVEL (MSL)

The location of the ground above mean sea level will have an effect on the atmospheric correction factor, K_A (see Eq. (2)). The curves in Figs. I-1, I-2, and I-3 were prepared to facilitate prediction of this effect for areas of the country which lie significantly above 0 feet mean sea level.

These curves were developed assuming U. S. Standard Atmosphere, 1962 conditions from 0 feet mean sea level in each case. Thus, the temperature and pressure at the ground in each figure were taken as the standard values at 2000, 4000, and 6000 feet above mean sea level respectively.

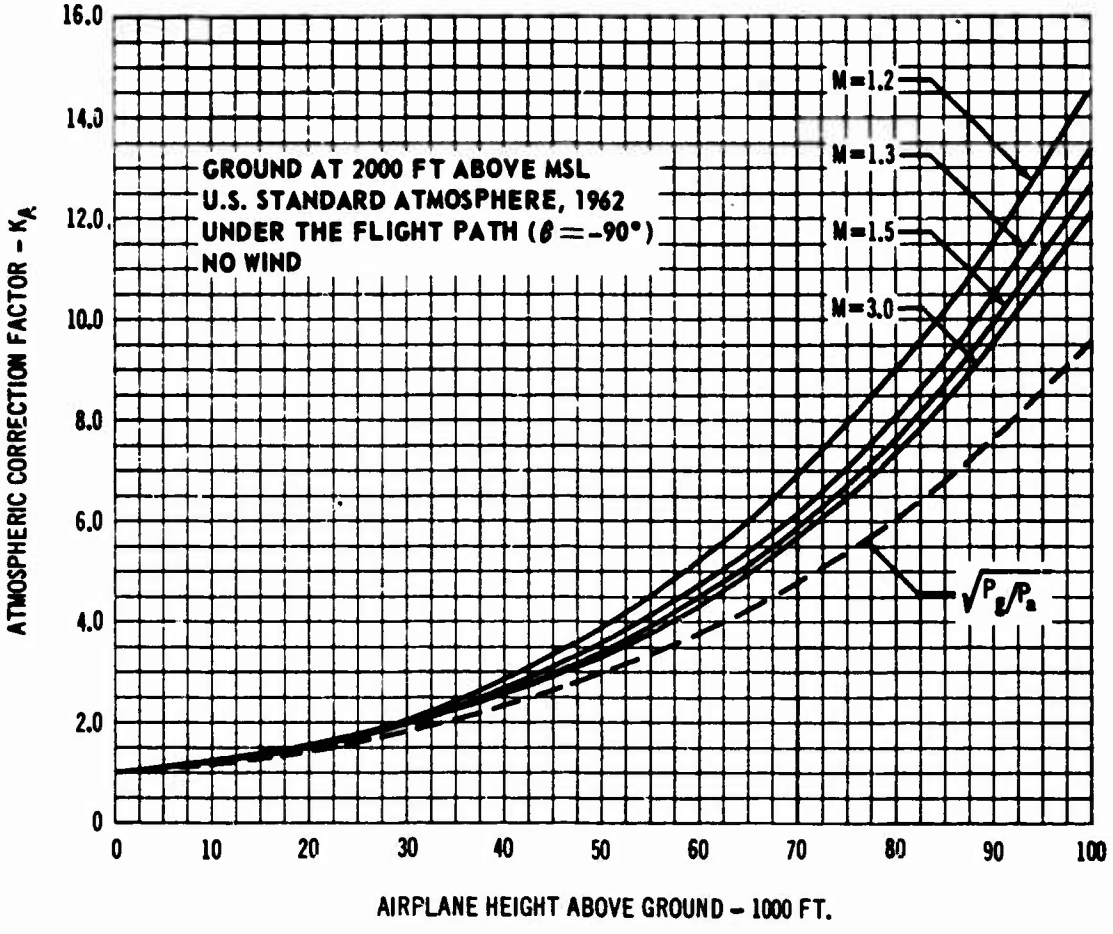

Fig. I-1 Atmospheric Correction Factor for the Ground at 2000 feet above MSL.

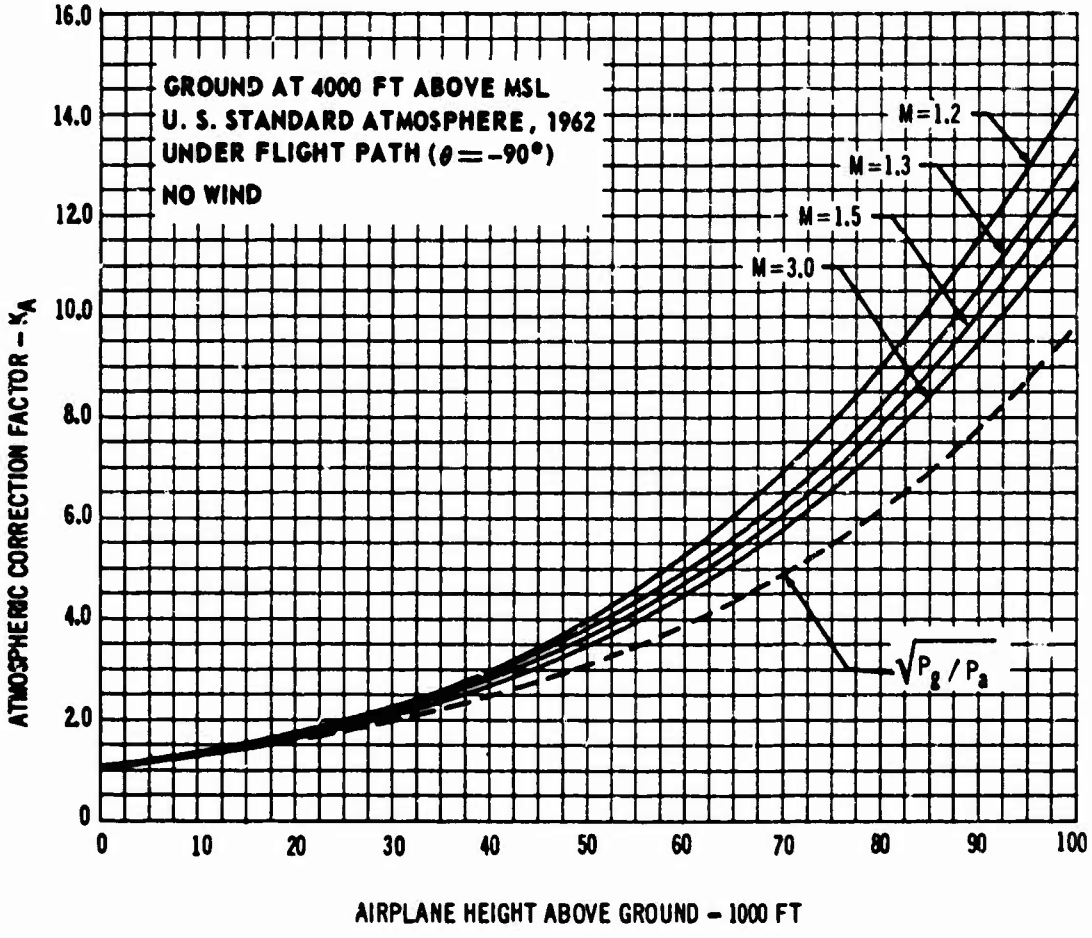

Fig. I-2 Atmospheric Correction Factor for the Ground at 4000 feet above MSL.

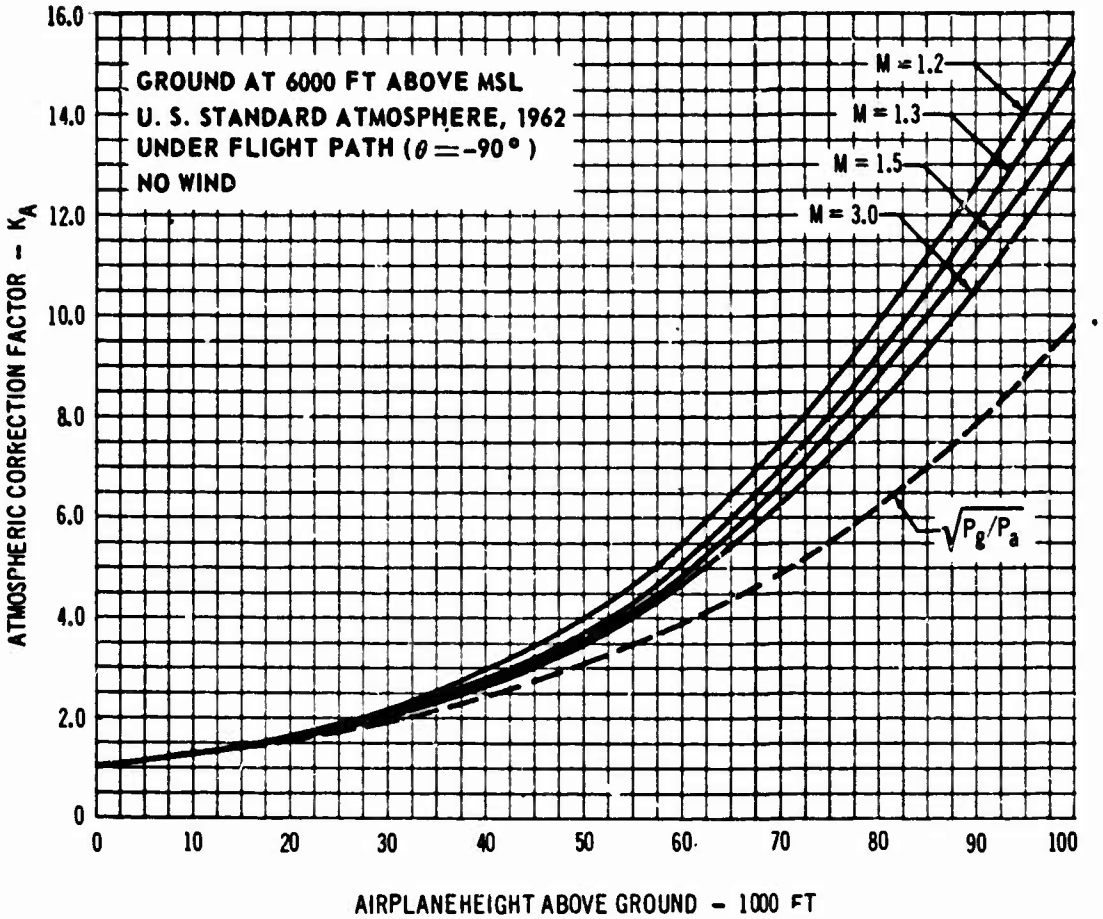

Fig. I-3 Atmospheric Correction Factor for the Ground at 6000 feet above MSL.

APPENDIX II A REVIEW OF THE THEORY FOR SHOCK WAVE PROPAGATION THROUGH A NONUNIFORM MEDIA –

The purpose of this section is to summarize the results of the work of Refs. 6 through 8. Specific details concerning the development of this theory may be obtained from Ref. 6. Basically, the results describe second order perturbations in particle velocity, pressure, and density behind a weak shock wave in terms of the first order undisturbed quantities. The assumptions are: (1) that the third order perturbations are small compared to the second order perturbations so that they may be ignored, and (2) that the shock wave propagates with the velocity $\bar{a}$ which is a function of its strength, i.e.

$$\bar{a} = a\left[1 + \frac{\gamma+1}{2\gamma}\,\frac{\Delta P}{P}\right]^{1/2}$$

Furthermore, it is assumed that the rays which describe the path of propagation of the shock wave and the ray tubes, which are formed by bundles of the rays, propagate independently.

Before summarizing the results, some nomenclature will be established. The coordinate system shown in Fig. II-1 will be used in this and the following sections, III through VII.

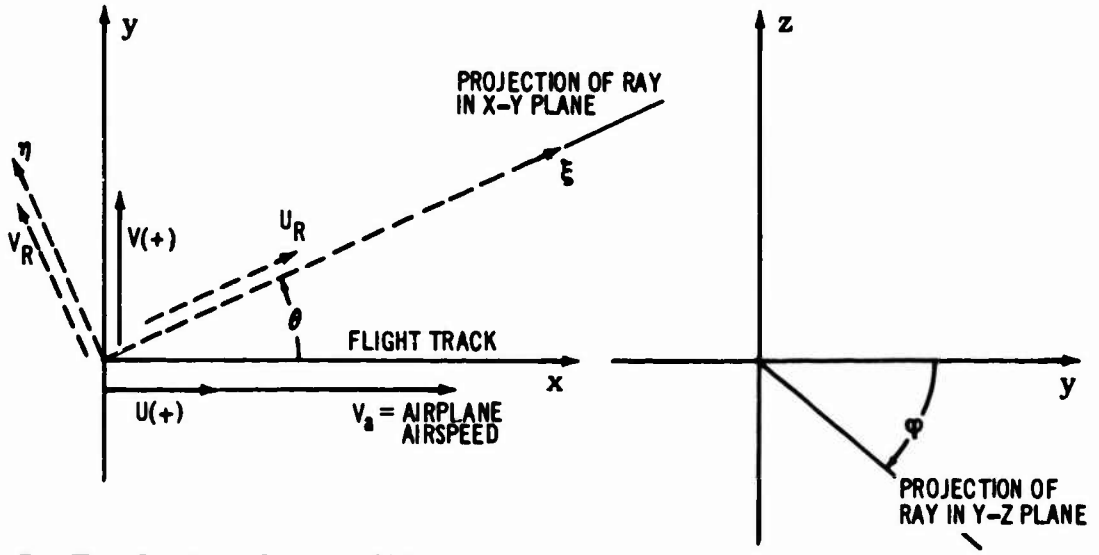

Fig. II-1 Coordinate System and Wind Axes.

The subscript "R" notes quantities in the (ξ , η) coorinate system rotated through the angle θ to coincide with the initial ray direction. Starred quantities note winds relative to those at the airplane so that $U^* = U(z) - U(z=0)$. The subscripts "a" and "g" refer to the value of the quantity at the airplane and the ground respectively. No subscript indicates the value of the quantity at any point between the airplane and the ground.

The following is a review of the equations used to compute the shock wave strength in nonhomogeneous media. Distances are measured from the airplane and the coordinate system is taken to move with the airplane (and hence with the winds at the airplane altitude).

The equations of the rays in the ξ , η , z system are given by:

$$\frac{d\xi}{dz} = \frac{\ell_R \ \bar{a} + U_R^*}{n_R \ \bar{a}} \qquad \text{Eq. (II-1a)}$$

$$\frac{d\eta}{dz} = \frac{V_R^*}{n_R \bar{a}} \qquad \text{Eq. (II-1b)}$$

$$\frac{dt}{dz} = \frac{1}{n_R \bar{a}} \qquad \text{Eq. (II-1c)}$$

$$\frac{dS}{dz} = -\left[\left(\frac{d\xi}{dz}\right)^2 + \left(\frac{d\eta}{dz}\right)^2 + 1\right]^{1/2} \qquad \text{Eq. (II-1d)}$$

$$\ell_R = \frac{\bar{a}}{V_a \cos\theta - U_R^*} \qquad \text{Eq. (II-1e)}$$

$$n_R = -(1 - \ell_R^2)^{1/2} \qquad \text{Eq. (II-1f)}$$

Transformations between the x, y, z and the ξ , η , z systems are given by:

$$x = \xi \cos\theta - \eta \sin\theta \qquad \text{Eq. (II-2a)}$$

$$y = \xi \sin\theta + \eta \cos\theta \qquad \text{Eq. (II-2b)}$$

$$U_R^* = U^* \cos\theta + V^* \sin\theta \qquad \text{Eq. (II-2c)}$$

$$V_P' = -U^* \sin\theta + V^* \cos\theta \qquad \text{Eq. (II-2d)}$$

$$\cos\theta = \frac{1}{\left[1+(M^2-1)\cos^2\varphi\right]^{1/2}} \qquad \text{Eq. (II-2e)}$$

$$\sin\theta = \frac{(M^2-1)^{1/2}\cos\varphi}{\left[1+(M^2-1)\cos^2\varphi\right]^{1/2}} \qquad \text{Eq. (II-2f)}$$

Transformations between a fixed ground system X, Y, Z and the x, y, z system are:

$$X = x + U(O)\,t \qquad \text{Eq. (II-3a)}$$

$$Y = y + V(O)\,t \qquad \text{Eq. (II-3b)}$$

$$Z = z \qquad \text{Eq. (II-3c)}$$

where

$$U(O) = U(z=O), \text{ etc.}$$

Some necessary auxiliary relations are as follows:

$$U^* = U(z) - U(O) \qquad \text{Eq. (II-4a)}$$

$$V^* = V(z) - V(O) \qquad \text{Eq. (II-4b)}$$

$$M = \frac{Va}{a(O)} \qquad \text{Eq. (II-4c)}$$

$$\bar{a}(z) = a(z)\left[1 + \frac{\gamma + 1}{2\gamma}\frac{\Delta P}{\bar{P}(z)}\right]^{1/2} \qquad \text{Eq. (II-4d)}$$

$$w^*(z) = \frac{U_R^*\frac{d\xi}{dz} + V_R^*\frac{d\eta}{dz}}{\frac{ds}{dz}} \qquad \text{Eq. (II-4e)}$$

where $a(z)$ is the ambient sound speed in the atmosphere, and $P(z)$ is the ambient pressure in the atmosphere.

The shock wave may be located on the ground in the X, Y, Z, system through the following transformations for steady level flight:

$$X_{shock} = x + U(O)t_o - V_a(t - t_o) \qquad \text{Eq. (II-5a)}$$

$$Y_{shock} = y + V(O)t_o \qquad \text{Eq. (II-5b)}$$

where $t_o = t$ for the $\varphi = -90°$ ray to reach the ground.

The ray tube area is given by:

$$A(z) = S\left\{\left[\left(\frac{U_R^*}{V_a} - \cos\theta\right)n_R\right]^2 + \left[\frac{V_R^*}{V_a} - \sin\theta\right]^2\right\}^{1/2} \qquad \text{Eq. (II-6)}$$

where

$$V_a = M\,a(0)$$

$$S = \int_o^z \frac{dz}{n_R}$$

The shock strength $\frac{\Delta P}{P(z')}$, is given by:

$$\frac{\Delta P}{P(z')} = \frac{\dfrac{2^{3/4}\,M^{3/4}}{(M^2-1)^{1/4}}\;\dfrac{\gamma}{(\gamma+1)^{1/2}}\;D(O)\left[I(Y_o,\theta)\right]^{1/2}}{a(z')B(z')\left\{\displaystyle\int_o^{z'}\frac{\frac{dS}{dz}\cdot dz}{(w^*+a)^2\;B(z)}\right\}^{1/2}} \qquad \text{Eq. (II-7)}$$

where

$$B(z) = \left[\frac{A(z)\;P(z)}{a(z)}\right]^{1/2} Q(z)$$

$$Q(z) = \exp\left\{\int_o^{|z|}\frac{\frac{dw^*}{d\zeta} - \frac{(\gamma-1)}{2}\,w^*\left(\frac{1}{P}\,\frac{dP}{d\zeta} - \frac{2}{a}\,\frac{da}{d\zeta}\right)}{(w^*+a)}\,d\zeta\right\}$$

$$D(0) = \left\{\frac{\left[n_R^2\;(0)\cos^2\theta + \sin^2\theta\right]^{1/2}\;P(o)}{a(0)}\right\}^{1/4}$$

$P(0) = P(z=0)$, etc.

Numerical solutions may be obtained by an iteration procedure where in the first iteration the assumption $\bar{a}(z) = a(z)$ may be used. The second iteration may use $\bar{a}(z)$ computed using the first value of $\frac{\Delta P}{P(z)}$ and so cn. It has been found that in regions away from cut-off and focusing the iteration converges quite rapidly.

The above equations are developed in Ref. 6 (see also Refs. 7 and 8). The equation for the ray tube area, given here, (Eq. (II-6), is an improved, more accurate version of the equation in Ref. 6 and is developed in the Appendix of Ref. 7.

APPENDIX III DEVELOPMENT OF AMBIENT PRESSURE EFFECT ON BOOM STRENGTH –

The equation for the sonic boom overpressure on the ground under the flight track for no wind may be obtained by specializing Eq. (II-7). The result is:

$$\frac{\Delta P}{P_g} = \frac{2^{3/4} M^{3/4}}{(M^2-1)^{1/4}} \frac{\gamma}{(\gamma+1)^{1/2}} \left(\frac{P_a}{M a_a}\right)^{1/4} \left[I(y_o,-90)\right]^{1/2} \Bigg/ a_g \left(\frac{A_g P_g}{a_g}\right)^{1/2} \left\{ \int_0^{z_g} \frac{\frac{ds}{dz} \cdot dz}{a^2 \left(\frac{\Delta P}{a}\right)^{1/2}} \right\}^{1/2}$$

where

ΔP = Sonic boom overpressure

P_g = Ambient pressure at ground

P_a = Ambient pressure at airplane

M = Airplane mach number

γ = Ratio of specific heats

$I(Y_o,-90°)$ = Airplane shock strength parameter

a_g = Sound speed at ground

a_a = Sound speed at airplane

A = Ray tube area

z = Distance measured down from airplane

S = Distance measured along ray path

The ray path and ray tube area are primarily functions of the temperature variation in the atmosphere. The effect of variations in ambient pressure can be obtained by allowing only the pressure-height curve to vary, and by dividing the above equation using the standard

pressure-height curve by that using a nonstandard curve. Because the temperature-height curve is assumed to remain constant, the result is:

$$\left(\frac{\Delta P}{\Delta P_{\substack{\text{std.}\\ \text{press.}}}}\right)_{\substack{\text{under}\\ \text{flt. track}}} = \frac{\dfrac{P_g P_s^{1/4}}{P_g^{1/2}}}{\dfrac{(P_g)_{\text{std.}}(P_s)_{\text{std}}^{1/4}}{(P_g)_{\text{std.}}^{1/2}}} \quad \frac{\left\{\displaystyle\int_o^{z_g} \frac{\frac{ds}{dz}\,dz}{a^2\left(\frac{\Delta P}{a}\right)^{1/2}}\right\}_{\text{std.}}^{1/2}}{\left\{\displaystyle\int_o^{z_g} \frac{\frac{ds}{dz}\,dz}{a^2\left(\frac{\Delta P}{a}\right)^{1/2}}\right\}^{1/2}}$$

As variations from the standard pressure-height curve in the real atmosphere are generally small it may be assumed that the integrals will remain approximately equal. Thus the relationship becomes:

$$\left(\frac{\Delta P}{\Delta P_{\substack{\text{std.}\\ \text{press.}}}}\right)_{\substack{\text{under}\\ \text{flt. track}}} = \left[\frac{P_g}{(P_g)_{\text{std.}}}\right]^{1/2}\left[\frac{P_s}{(P_s)_{\text{std.}}}\right]^{1/4} \qquad \text{Eq. (4)}$$

This relationship was compared with computer program output in Section II.B.2 to check the validity of the assumptions. It was seen that the assumptions are acceptable.

APPENDIX IV DEVELOPMENT OF GENERAL EQUATION FOR LATERAL CUT-OFF LOCATION -

Consider a general temperature profile such as that shown in Fig IV-1, in which the temperature between any two significant levels is assumed to vary linearly.

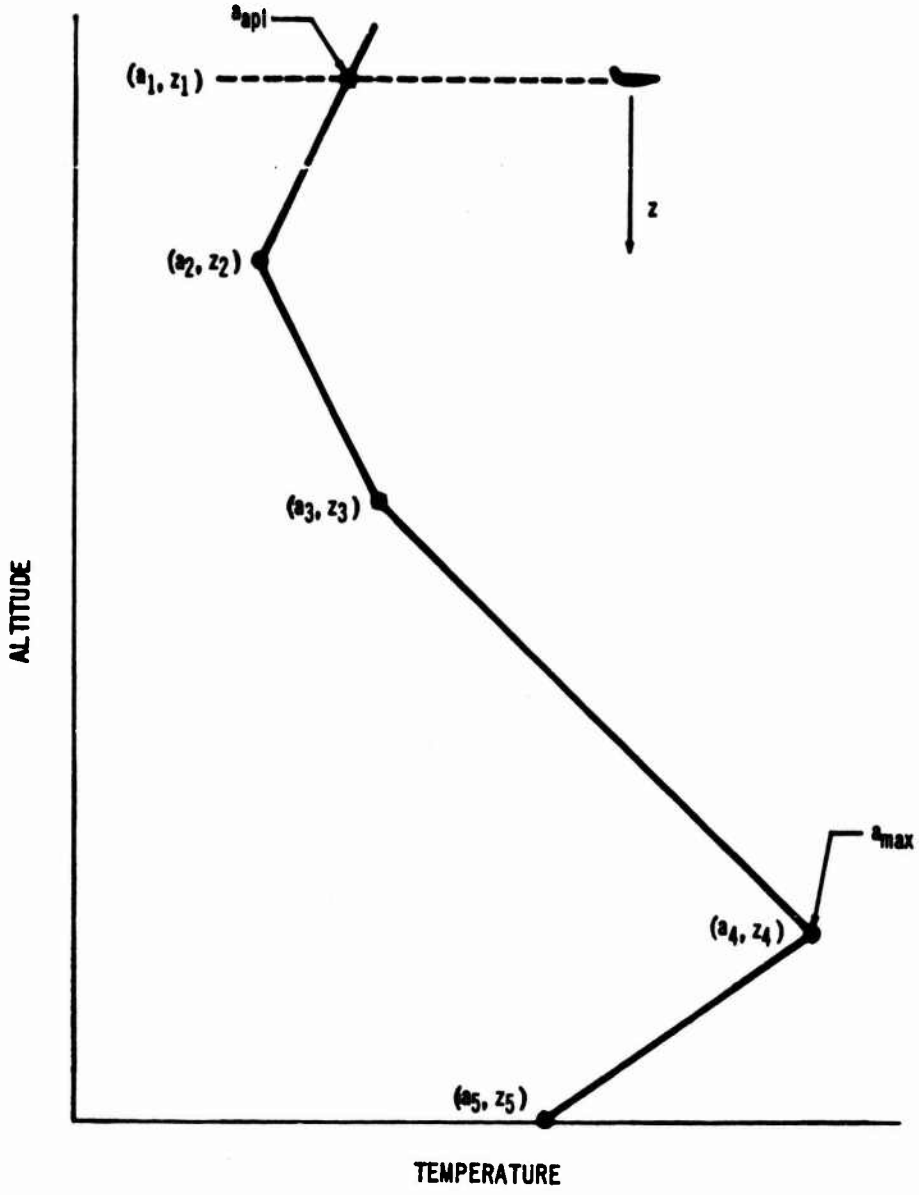

Fig. IV-1 General Temperature Profile.

For any portion of this profile a ray path is described by Eqs. (II-1a) and (II-1b). Assuming no wind the first of these becomes:

$$\frac{d\xi}{dz} = \frac{\ell_R}{n_R} = \left(\frac{1}{n_R^2} - 1\right)^{1/2}$$

Further the lateral (y) displacement of the ray for no wind (Eq. (II-2b)) is:

$$y = \xi \sin\theta$$

$$= \sin\theta \int \left[\frac{1}{n_R^2} - 1\right]^{1/2} dz$$

Employing the definition of n_R from Eq. (II-1f), assuming that $\bar{a} = a$, and putting V_a in terms of Mach number, $M = V_a/a_{apl}$ the above becomes:

$$y = \sin\theta \int \frac{\frac{a}{a_{apl}}}{\sqrt{(M\cos\theta)^2 - \left(\frac{a}{a_{apl}}\right)^2}} \, dz$$

Integration of this equation can be facilitated if the variable of integration, z, is put in terms of a/a_{apl}. Assuming that the sound speed, a, also varies linearly between two points (valid as long as the lapse rates are of the magnitude normally encountered) the relation between a and z may be written as:

$$a = a_n + \alpha_n (z - z_n)$$

where

a_n = Sound speed at level z_n

α_n = Sound speed lapse rate between levels z_n and z_{n+1}

$$= \frac{a_{n+1} - a_n}{z_{n+1} - z_n}$$

Using the above expression

$$dz = \frac{a_{apl}}{\alpha_n} \, d\left(\frac{a}{a_{apl}}\right)$$

so that

$$y = \frac{a_{apl}}{\alpha_n} \sin\theta \int_{a_n}^{a_{n+1}} \frac{\left(\frac{a}{a_{apl}}\right)}{\sqrt{(M\cos\theta)^2 - \left(\frac{a}{a_{apl}}\right)^2}} \, d\left(\frac{a}{a_{apl}}\right)$$

The lateral location of any ray is given by the summation of the above integrals for each significant level between the airplane and the ground. The integration and summation yields:

$$y = a_{apl} \sin\theta \sum_{n=1}^{n=j-1} \frac{\left[(M\cos\theta)^2 - \left(\frac{a_n}{a_{apl}}\right)^2\right]^{1/2} - \left[(M\cos\theta)^2 - \left(\frac{a_{n+1}}{a_{apl}}\right)^2\right]^{1/2}}{\alpha_n}$$

where "j" represents the values at the last significant level (in most cases the ground). The last ray to reach the ground (or last significant level) is the one for which the direction cosine, ℓ_R , is equal to 1.0 at the level where $a = a_{max}$. Using Eq. (II-1e) the angle θ of the last ray is given by (assuming $\bar{a} = a$, and no wind):

$$\ell_R = 1.0 = \frac{\frac{a_{max}}{a_{apl}}}{M\cos\theta}$$

or

$$M\cos\theta = \frac{a_{max}}{a_{apl}}$$

and

$$\sin\theta = \left[1 - \left(\frac{1}{M} \, \frac{a_{max}}{a_{apl}}\right)^2\right]^{1/2}$$

Using these expressions and the definition for α_n, the lateral location of the last ray to reach the last significant level is given by:

$$y_{max} = \left[1 - \left(\frac{1}{M}\,\frac{a_{max}}{a_{apl}}\right)^2\right]^{1/2} \sum_{n=1}^{n=j-1} \frac{\left[a_{max}^2 - a_n^2\right]^{1/2} - \left[a_{max}^2 - a_{n+1}^2\right]^{1/2}}{a_{n+1} - a_n} \left(z_{n+1} - z_n\right)$$

Eq.(6)

In some cases the temperature between two levels does not change, as in the stratosphere of the standard atmosphere. Assuming that this occurs between levels z_m and z_{m+1} (i.e. $a_m = a_{m+1}$) the term involving $(z_{m+1} - z_m)$ would become indeterminate. The simplest method of obtaining the form of this term is by taking the limit using L'Hospital's rule as $a_m \rightarrow a_{m+1}$. Thus, this term becomes:

$$\lim_{a_m \rightarrow a_{m+1}} = \lim_{a_m \rightarrow a_{m+1}} \frac{\left[a_{max}^2 - a_m^2\right]^{1/2} - \left[a_{max}^2 - a_{m+1}\right]^{1/2}}{a_{m+1} - a_m} \left(z_{m+1} - z_m\right)$$

$$= \lim_{a_m \rightarrow a_{m+1}} \frac{-a_m \left[a_{max}^2 - a_m^2\right]^{1/2}}{-1} \left(z_{m+1} - z_m\right)$$

$$= \frac{a_{m+1}}{\left(a_{max}^2 - a_{m+1}^2\right)} \left(z_{m+1} - z_m\right)$$

Eq.(7)

To illustrate the application of this relationship, Eqs. (6) and (7) have been applied to the U.S. Standard Atmosphere, 1962 (Ref. 1) where a_{max} would occur at the ground, i.e., $a_{max} = a_g$. Thus, for an airplane flying between 36,000 feet and the ground:

$$y_{max} = \pm\left[1 - \left(\frac{1}{M}\,\frac{a_g}{a_a}\right)^2\right]^{1/2} \frac{\left[a_g^2 - a_a^2\right]^{1/2}}{a_g - a_a} \left(z_g\right)$$

For an airplane flying between 36,000 and 65,000 feet:

$$y_{max} = \pm\left[1 - \left(\frac{1}{M}\,\frac{a_g}{a_a}\right)^2\right]^{1/2} \left\{ \frac{a_{36,000}}{\left[a_g^2 - a_{36,000}^2\right]^{1/2}} \left(z_{36,000}\right) + \frac{\left[a_g^2 - a_{36,000}^2\right]^{1/2}}{a_g - a_{36,000}} (36,000) \right\}$$

And for an airplane flying above 65,000 feet.

$$y_{max} = \pm\left[1 - \left(\frac{1}{M}\,\frac{a_g}{a_a}\right)^2\right]^{1/2} \left\{ \frac{\left[a_g^2 - a_a^2\right]^{1/2} - \left[a_g^2 - a_{65,000}^2\right]^{1/2}}{a_{65,000} - a_a} \left(z_{65,000}\right) \right.$$

$$\left. + \frac{a_{36,000}}{\left[a_g^2 - a_{36,000}^2\right]^{1/2}} (29,000) + \frac{\left[a_g^2 - a_{36,000}^2\right]^{1/2}}{a_g - a_{36,000}} (36,000) \right\}$$

APPENDIX V DEVELOPMENT OF FOCUSING CRITERIA UNDER FLIGHT TRACK

The ray tube area expression, Eq.(II-6), is repeated below:

$$A = S\left\{\left[\left(\frac{U_R^*}{V_a} - \cos\theta\right)n_R\right]^2 + \left[\frac{V_R^*}{V_a} - \sin\theta\right]^2\right\}^{1/2} \qquad \text{Eq. (II-6)}$$

The shock strength will increase if this quantity vanishes as it appears in the denominator of the expression for the overpressure Eq. (II-7). The ray tube area can tend toward zero only if the expression inside the brackets tends toward zero as S is the length of the ray. Setting $A = 0$, specializing this for no wind, and investigating the ray under the airplane ($\theta = 0$) this becomes:

$$n_R = 0$$

The quantity n_R Eq. (II-1f) is the direction cosine of the normal to the shock front with the z axis and is given in general by:

$$n_R = -\left[1 - \left(\frac{a}{V_a \cos\theta - U_R^*}\right)^2\right]^{1/2}$$

assuming that the shock front propagates at nearly the local speed of sound. When this quantity is zero the shock front is normal to the ground. Thus for no wind and $\theta = 0°$, A can tend toward zero if $V_a = a$. Putting this in terms of the Mach number and specializing it further by assuming that the maximum speed of sound occurs on the ground (i.e., $n_R = 0$ only at the ground)

$$M_{Focus} = \frac{a_g}{a_a} \qquad \text{Eq.(9)}$$

From this discussion it can be seen that focusing occurs simultaneously with cut-off ($n_R = 0$).

For the case with wind and $\theta = 0$ it is evident that:

$$\left[\left(\frac{U_R^*}{V_a} - 1\right)n_R\right]^2 + \left(\frac{V_R^*}{V_a}\right)^2 = 0$$

for focusing to occur. It can be seen that this is impossible unless V_R^* is also equal to zero. Making this additional assumption the above expression becomes:

$$\left(\frac{U_R^*}{V_a} - 1\right)n_R = 0$$

This leaves two choices. Either $U_R^* = V_a$, which is physically unlikely, or $n_R = 0$. Using the second choice and putting V_a in terms of the Mach number.

$$M = \frac{a}{a_a} + \frac{U_R^*}{a_a} = \frac{(a+U) - U_a}{a_a}$$

Assuming that cut-off occurs at the ground this becomes

$$M_{Focus} = \frac{(a+U)_R - U_a}{a_a} \qquad \text{Eq. (11)}$$

It is apparent that the maximum value of $(a + U)$ must occur at the ground for $n_R = 0$ at the ground. Here too, cut-off and focusing occur simultaneously.

APPENDIX VI DEVELOPMENT OF LATERAL FOCUSING CRITERIA

Considering the entire ray tube area expression Eq. (II-6) it is apparent that it can go to zero if, and only if, both portions of the term in the brackets go to zero simultaneously. This requires that:

$$\left(\frac{U_R^*}{V_a} - \cos\theta\right) n_R = 0$$

$$\frac{V_R^*}{V_a} - \sin\theta = 0$$

at the same location. Here again two possibilities are open. These are that $\frac{U_R^*}{V_a} - \cos\theta = 0$ when $\frac{V_R^*}{V_a} - \sin\theta = 0$, or $n_R = 0$ when $\frac{V_R^*}{V_a} - \sin\theta = 0$.

It can be shown that the first of these leads to

$$\sqrt{U^{*2} + V^{*2}} = V_a$$

which is physically unlikely. Investigating the second a simultaneous solution must be sought for:

$$1 - \left(\frac{\frac{a}{a_a}}{M\cos\theta - \frac{U_R^*}{a_a}}\right) = 0$$

$$\frac{\frac{V_R^*}{a_a}}{M} - \sin\theta = 0$$

A solution for the value of V^* required in terms of the Mach number, U^*, and sound speeds can be obtained if the following transformations are used:

$$U_R^* = U^*\cos\theta + V^*\sin\theta \qquad \text{Eq. (II-2c)}$$

$$V_R = -U^*\sin\theta + V^*\cos\theta \qquad \text{Eq. (II-2d)}$$

$$\cos\theta = \frac{1}{\left[1+(M^2-1)\cos^2\varphi\right]^{1/2}} \qquad \text{Eq. (II-2e)}$$

$$\sin\theta = \frac{(M^2-1)^{1/2}\cos\varphi}{\left[1+(M^2-1)\cos^2\varphi\right]^{1/2}} \qquad \text{Eq. (II-2f)}$$

After substituting these in the above expressions, equating them, and after some algebraic manipulation it can be shown that:

$$\frac{V_g^*}{a_a} = \left\{\frac{\left\{2\left[M^2-\left(\frac{U_g^*}{a_a}\right)^2\right] + \left(\frac{a_g}{a_a}\right)^2\right\} - \left(\frac{a_g}{a_a}\right)\sqrt{8M\left[M+\frac{U_g^*}{a_a}\right]+\left(\frac{a_g}{a_a}\right)^2}}{2}\right\}^{1/2} \qquad \text{Eq. (VI-1)}$$

This relationship was used in developing the curves in Fig. 25. Here again it is evident from the derivation that focusing and lateral cut-off (in this case) occur simultaneously.

APPENDIX VII DEVELOPMENT OF EXTREME LATERAL SPREAD CRITERIA

The sonic boom distribution can extend over large lateral distances if the ray which leaves the airplane in the x - y plane (Fig. II-4) reaches the ground. The conditions required to produce this effect can be obtained from an investigation of the expression for ℓ_R, Eq. (II-1e). For any ray to reach the ground $\ell_R < 0$ throughout the path of propagation.
Thus:

$$\ell_R = \left[1 - n_R^2\right]^{1/2} = \frac{\frac{a}{a_a}}{M\cos\theta - \frac{U_R^*}{a_a}} < 0$$

The two rays which leave the airplane in the x - y plane are the $\Psi = 0°$ and $\Psi = 180°$ rays. Using the relationships between θ and Ψ, Eqs.(II-2e) and (II-2f) for $\Psi = 0°$ and 180°:

$$\cos\theta = \frac{1}{M}$$

$$\sin\theta = \pm\frac{(M^2-1)^{1/2}}{M}$$

Thus, the ray in the x - y plane will reach the ground if

$$\frac{\frac{a}{a_a}}{1 - \frac{U_R^*}{a_a}} < 0$$

Rearranging this, the wind required to produce this effect is given by:

$$U_R^* < a_a - a$$

The quantity U_R^* can be written as

$$U_R^* = U^*\cos\theta + V^*\sin\theta \qquad \text{Eq. (II-2c)}$$

which for the $\Psi = 0°$ or $180°$ ray becomes:

$$U_R^* = \frac{U^* \pm (M^2-1)^{1/2}\, V^*}{M}$$

$$= \frac{U \pm (M^2-1)^{1/2}\, V}{M} - \frac{U_a \pm (M^2-1)^{1/2}\, V_a}{M}$$

Using this in the above inequality and rearranging slightly

$$a_a + \frac{U_a \pm (M^2-1)^{1/2}\, V_a}{M} > a + \frac{U \pm (M^2-1)^{1/2}\, V}{M}$$

or

$$A_a > A \qquad \text{Eq. (12)}$$

This expression shows that for the ray in the x-y plane to reach the ground the value of the expression for A at the airplane (A_a) must be greater than at any point between it and the ground.

APPENDIX VIII REVIEW OF ROUTINE CALCULATION OF SONIC BOOM IN STANDARD AND NON-STANDARD ATMOSPHERES.

In order to aid in obtaining rapid estimates of the sonic boom produced in a real atmosphere the information of Sections II.A.4, and II.B.7 is repeated here. These methods must be used with extreme care for making estimates at Mach numbers less than about 1.3. The criterion developed in Section III should be checked for flight at these low Mach numbers to determine if anamalous propagation may occur. The conditions which can cause complete cut-off are given in Sections III.A.1 and III.B.1. The conditions which can cause focusing at the ground are given in Sections III.A.2, III.B.2, and III.B.3, while the conditions which can cause extreme lateral spread are given in Section III.B.4.

A. CALCULATIONS IN STANDARD ATMOSPHERE - Once the airplane geometry inputs, $I(Y_o, \theta)$, (see Eq. (1)) have been established for each altitude and Mach number of interest, routine calculations of sonic boom strength, lateral distribution, and lateral extent for steady level flight in the U.S. Standard Atmosphere, 1962 may be obtained in the following manner:

(a) Compute $\Delta P_{\text{under flt. track}}$ from Eq. (2) and Fig. 2 for each Mach number and altitude.

(b) Compute lateral distribution of the boom strength from Eq. (3) for each Mach number and altitude.

(c) Obtain the location of lateral cut-off from the curves in Fig. 4 for each Mach number and altitude, and terminate the lateral distribution of boom strength at this point.

B. CALCULATIONS IN NON-STANDARD ATMOSPHERE The method for calculating sonic boom distribution on the ground was outlined above, for the U.S. Standard Atmosphere, 1962, with no wind. A similar procedure would be used in making routine estimates for a general atmosphere with wind. The following method should be used with extreme care for Mach numbers between 1.0 and 1.3, especially in cases when wind shears are to be considered. Criteria for meteorological conditions which can cause anomalies in the overpressure and distribution of the sonic boom are developed in Section III. These should be checked when making calculations in the above Mach number range.

Once the airplane geometry influence, $I(Y_o, \theta)$, (see Eq. (1)) has been determined for each Mach number and altitude of interest the calculation of sonic boom strength and distribution may proceed as follows:

(a) Calculate $\Delta P_{\text{under flt. track}}$ from Eq. (5) and Fig. 2 (or Appendix Figs. I-1, I-2, or I-3) for ground located above 0 ft. MSL for each altitude and Mach number.

- The variation of the temperature correction factor, K_T, may be estimated from Fig. 8, with the value at Mach 1.2 estimated from Fig. 9.
- The variation of the correction for wind shears with Mach number may be estimated from Fig. 12 with the value at Mach 1.3 taken from Fig. 13.

(b) Compute the lateral distribution of sonic boom strength from Eq. (3) for each altitude and Mach number. (Caution must be exercised when estimating the lateral distribution for low Mach numbers and high winds, Fig. 15).

(c) Obtain the location of lateral cut-off from Eq. (6) and Eq. (7) for each Mach number and altitude, and terminate the lateral distribution at that point. (Effect of moderate winds on the lateral cut-off location may be estimated from Fig. 19.)

The above procedure is illustrated schematically in Fig. VIII-1.

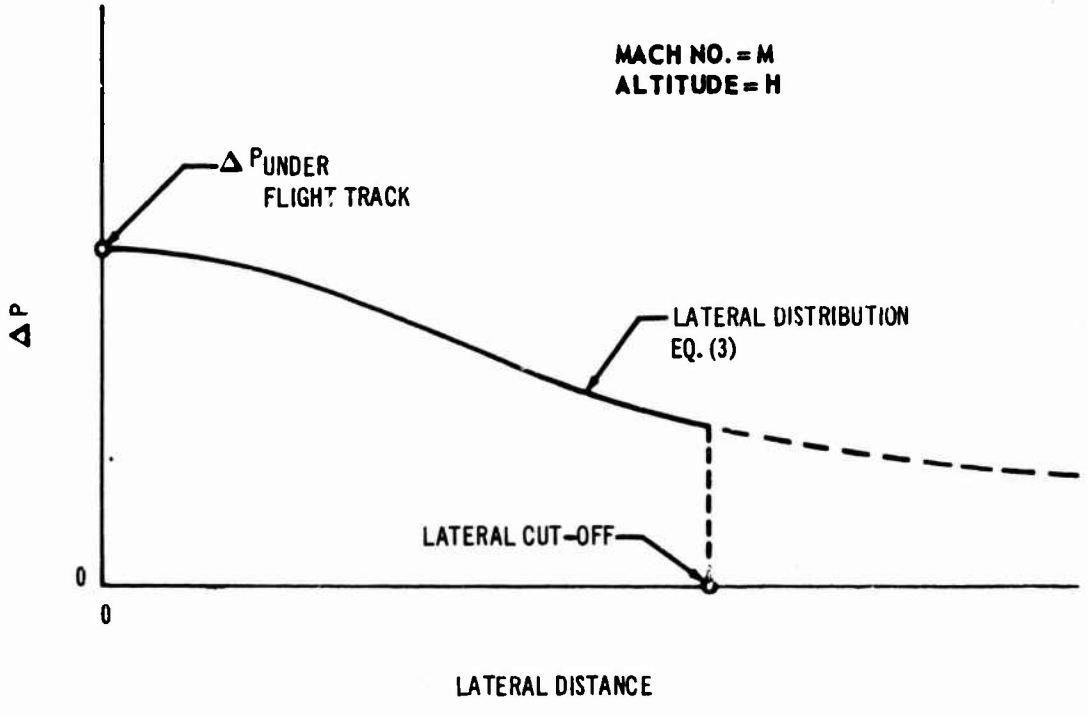

Fig. VIII-1 Routine Calculation of Sonic Boom.

APPENDIX IX DATA TRANSFORMATION FOR TURBULENT SCATTERING

The statistical study of sonic boom overpressures requires an appropriate transformation of the test data. The form of this transformation may be determined by finding the probability distribution of a randomly located set of measurements in an arbitrary plane from the mathematical description of the scattering of the shock wave by the turbulence. The geometry of finding the data transformation is shown in Fig. IX-1.

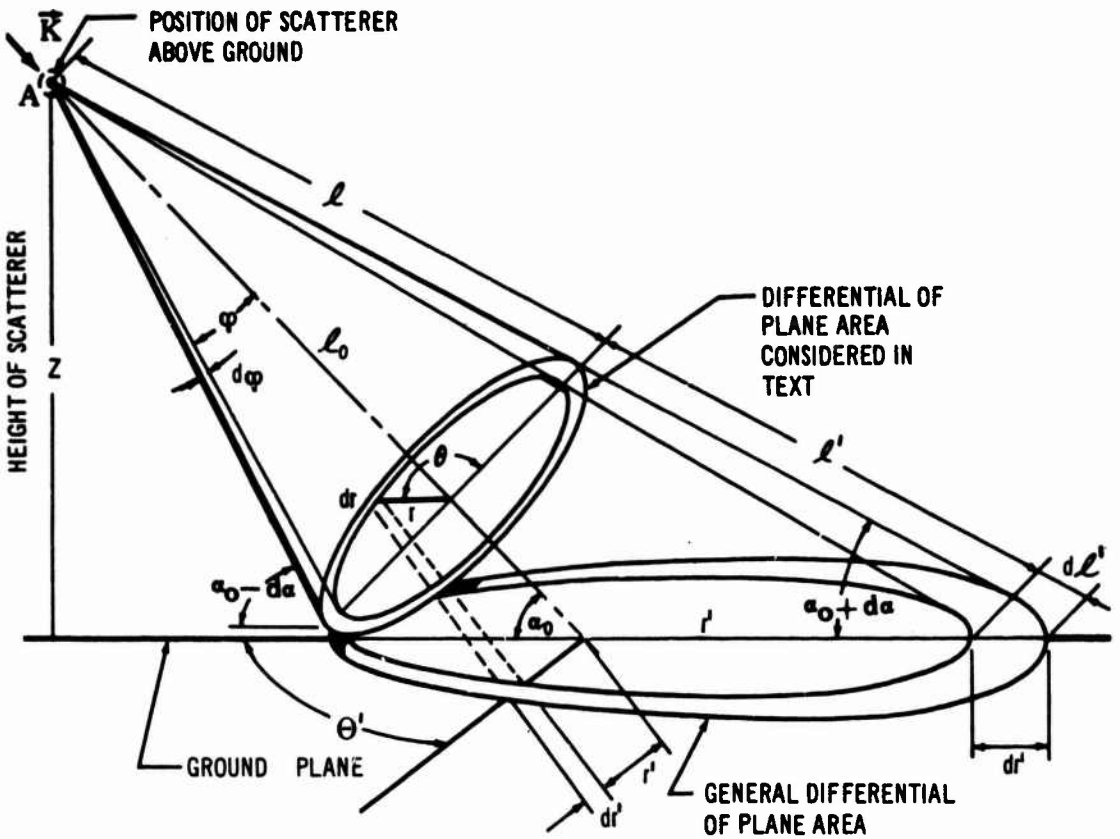

Fig. IX-1 Geometry for Determining Probability Distribution

In this figure a turbulent temperature or wind element at (A) has scattered the energy symmetrically in the angle φ about the direction of the shock propagation $\vec{K}$. A number of intensity measurements of the scattered field are made by microphones placed randomly in the (x,y)

or ground plane and it is desired to treat the measured data statistically. The actual form of the probability distribution of the measurements can be found from the probability theorem,

$$P(x,y) = \iint_R f(x,y)\, dx\, dy \qquad \text{Eq. (IX-1)}$$

which states that the joint probability $P(x,y)$ of a given value of a variate $f(x,y)$ occurring in the region R in the (x,y) plane is equal to the integral of $f(x,y)$ over the region R. The cross-section $\sigma(\vec{\ell})$ discussed in Section III-C-3 gives the distribution of the scattering intensity in terms of the solid angle. When this distribution is projected on the (x,y) plane, it gives the desired function $f(x,y)$, thus, the probability distribution becomes:

$$P\left(\frac{I}{I_o}\right) = \int_R \sigma(\vec{\ell}) \cdot \vec{dA} \qquad \text{Eq. (IX-2)}$$

where: I is the observed intensity of the scattered wave

I_o is the incident intensity of the original wave

$\vec{dA}$ is the vector differential area in the (x,y) plane

$\sigma(\vec{\ell})$ is the scattering cross-section discussed in Section III-C-3

If the definition of Eq. (IX-2) is extended to a number of scattering centers, randomly located in space above a single fixed microphone, the probability distribution becomes:

$$P\left(\frac{I}{I_o}\right) = \sum_i \int_{R_i} \sigma(\vec{\ell}_i) \cdot \vec{dA}_i \qquad \text{Eq. (IX-3)}$$

where the "i" subscript refers to one measurement taken of a single scattering event of an ensemble of such events.

Figure IX-1 shows that if the incident wave vector $\vec{K}$, is not perpendicular to the (x,y) plane of observation, the problem is geometrically complex, requiring the integration of elliptic functions. To illustrate how the form of the probability distribution of the measurements may be obtained, a simplified case of scattering by a turbulent

temperature field is developed where the N-wave is propagating in a direction perpendicular to the plane of observation (the ground). Substitution of the equation for the turbulent temperature cross-section from Section III-C

$$\sigma_T(\vec{\ell}) = \frac{\pi}{4} K^4 \cos^2\varphi \; \Phi(\vec{k})$$

into Eq. (IX-3) gives

$$P\left(\frac{I}{I_o}\right) = \frac{\pi}{4} \sum_{j=1}^{\infty} \sum_{i=1}^{N} K_j^4 \, \Phi(\vec{k}) \int_o^{2\pi} \int_o^{r_i} \frac{z_i^2 \, r_i \, d\, r_i \, d\, \Theta_i}{r_i^2 + z_i^2}$$

Eq. (IX-4)

where z_i is the height of the "i-th" scatterer above the ground

(r_i, θ_i) are polar coordinates in the horizontal, ground plane

N is the total number of observations

K_j is the "j-th" wave number, which contributes in an unspecified manner to the incident wave.

After performing the integrations, it follows that the measurements may be represented by the form of the probability distribution:

$$P\left(\frac{I}{I_o}\right) = \frac{\pi^2}{2} \sum_{j=1}^{\infty} \sum_{i=1}^{n} K_j^4 \, \Phi(\vec{k}) r_i^2 \, \ln\left(\frac{z_i^2 + r_i^2}{z_i^2}\right)$$

Eq. (IX-5)

The summation of logarithms in general can be written as:

$$\sum_i \alpha_i \ln b_i = \ln\left[\prod_i (b_i)^{\alpha_i}\right]$$

Eq. (IX-6)

which states that the sum of a set of logarithms of terms in (a_i, b_i) is equal to the logarithm of the product of terms in $(b_i)\alpha$. A reformulation of Eq. (IX-5) in these terms leads to the form of the probability distribution of the sonic boom measurements:

$$P\left(\frac{I}{I_o}\right) = \frac{\pi^2}{2} \sum_{j=1}^{\infty} K_j^4 \, \Phi(\vec{k}) \, \ln \left\{ \prod_{i=1}^{n} \left\{ \frac{z_i^2 + r_i^2}{z_i^2} \right\}^{r_i^2} \right\} \quad \text{Eq. (IX-7)}$$

Equation IX-7 shows that the form of the probability distribution is logarithmic and consequently a logarithmic transformation of the overpressure data would be appropriate for statistical purposes for this case.

ACKNOWLEDGEMENT

The authors would like to acknowledge the assistance of Messrs. C. S. Howell, A. Sigalla and S. Vanderleest during the preparation of this report, and also Mr. E. M. Hansen for gathering meteorological data.

REFERENCES

1. Champion, K.S.W., O'Sullivan, W.J.Jr., and Teweles, S., "U.S. Standard Atmosphere, 1962." U.S. Government Printing Office, Washington 25, D.C. December 1962

2. Whitham, G.B., "The Flow Pattern of a Supersonic Projectile." Communications on Pure and Applied Mathematics, Vol. V, pp. 301-348, 1952

3. Maglieri, D.J., and Hubbard, H.H., "Ground Measurements of the Shock-Wave Noise from Supersonic Bomber Airplanes in the Altitude Range from 30,000 to 50,000 feet." NASA TN D-880, July 1961

4. Lina, L.J., and Maglieri, D.J., "Ground Measurements of Airplane Shock-wave Noise at Mach Numbers to 2.0 and at Altitudes to 60,000 feet." NASA TN D-235, March 1960

5. Lina, L.J., and Maglieri, D.J., "Ground Measurements of Airplane Shock-wave Noise at Mach Numbers to 2.0 and at Altitudes to 60,000 feet." NASA TN D-235, March 1960

6. Friedman, M.P., Kane, E.J., and Sigalla, A. "Effects of Atmosphere and Aircraft Motion on the Location and Intensity of a Sonic Boom." AIAA Journal, Vol. I, No. 6, June 1963

7. Kane, E.J., "Propagation of Sonic Boom Through a Non-uniform Atmosphere." Boeing Document D6-8979, May 1962

8. Brown, J.R., "Sonic Boom Propagation -- Nonhomogeneous Atmosphere, TA-90." Boeing Document D6-2315TN, September 1964

9. Boynton, H.W., "Time of Formation and Burn-off of Nocturnal Inversions at Detroit," Journal of App. Meteor., V. 1, N.2, pp. 244-50, June 1962

10. Izumi, Y., "The Evolution of Temperature and Velocity Profiles During Breakdown of a Nocturnal Inversion and a Low-Level Jet." Journal of App. Meteor., V. 3, N.1, pp. 70-82, February 1964

11. Smith, J.W., "The Vertical Temperature Distribution and the Layer of Minimum Temperature," Journal of App. Meteor, V. 2, N. 5 pp. 655-67, October 1963

12. Izumi, T. and Barad, M.L., "Wind and Temperature Variations during Development of a Low-Level Jet." ibid pp. 668-673

13. Edinger, J.G., "Modification of the Marine Layer over Coastal Southern California," Journal of App. Meteor, V.Z. N.6, pp. 706-12, December 1963

14. Haurwitz, B., "Dynamic Meteorology," McGraw-Hill, New York, 1941

15. Sanders, F., "An Investigation of the Structure and Dynamics of an Intense Surface Frontal Zone." Journal of Meteor., V. 12, N. 6, pp. 542-52, December 1955

16. Ratner, B., "Upper-Air Climatology of the United States." Parts I, II, Tech. Paper No. 32, U.S. Weather Bureau, June 1957, Sept. 1958

17. Rasmussen, L.A., "Derivation of an Atmospheric Pressure-Height Curve from a Temperature-Height Curve." Boeing Document D6-9456TN, November 1963

18. Hering, W.S. and Borden, T.R., Jr., "Diurnal Variations in the Summer Wind Field over the Central United States," Journal of Atmos. Science, V. 19, N.1. pp. 81-86, January 1962

19. Gerhardt, J.R., "An Example of a Nocturnal Low-Level Jet Stream," ibid, pp 116-118

20. Pitchford, K.L. and London, J., "The Low-Level Jet as Related to Nocturnal Thunderstorms over Midwest United States." Journal of App. Meteor, V.1., N. 1, pp. 43-47, March 1962

21. Serebreny, S.M., Wiegman, E.J., and Hadfield, R.G., "Some Characteristic Features of the Jet Stream Complex during Selected Synoptic Conditions." Journal of App. Meteor, V. 1, N.2, pp. 137-153, June 1962

22. Brundidge, K.C., and Goldman, J.L., "Model Cross Sections Across the Jet Stream." Journal of App. Meteor., V. 1, N.3, pp. 303-317, September 1962

23. Gerhardt, J.R., "Mesoscale Association of a Low-Level Jet Stream with a Squal Line - Cold Front Situation," Journal of App. Meteor, V. 2, N.1, pp. 49-55, February 1963

24. Eddy, A., "A Statistical Model for the Mid-Latitude Tropopause and Jet Stream Layer." Journal of App. Meteor. V. 2, N.2, pp. 219-225, April 1963

25. Mantis, H., "Note on the Structure of the Stratospheric Easterlies of Midlatitude." Journal of App. Meteor., V. 2, N.3, pp. 427-29, June 1963

26. Hoecker, W.H.,Jr., "Three Southerly Low Level Jet-Systems Delineated by the Weather Bureau Special Pibal Network of 1961." Monthly Weather Review. V. 91, N. 10-12, pp. 573-82, Oct.-Dec. 1963

27. Crutcher, H.L., "Climatology of the Upper Air as Related to the Design and Operation of Supersonic Aircraft." U.S. Department of Commerce, U.S. Weather Bureau, March 1963

28. Berggren, R., Gibbs, W.J., and Newton, C.W., "Obervational Characteristics of the Jet Stream." Technical Note No. 19, World Meteor, Oregon Geneva 1958

29. Endlich, R.M., and McLean, G.S., "The Structure of the Jet Stream Core." Journal of Meteor, V. 14, N.6, pp.543-52, December 1957

30. Crossley, A.F., "Extremes of Wind Shear." Meteor, Office Scientific Paper No. 17, London, 1962

31. Reiter, E.R., "The Layer of Maximum Wind." Journal of Meteor, V. 15, N.1, pp. 27-43, February 1958

32. Reiter, E.R., "The Detailed Structure of the Wind Field Near the Jet Stream." Journal of Meteor, V. 18, N.1, pp. 9-30, February 1961

33. Blackadar, A.K., "Boundary Layer Wind Maxima and their Significance for the Growth of Nocturnal Inversions." Bulletin of American Meteor Soc., V. 38, N.5, pp. 283-90, May 1957

34. Reed, R.J., "Detailed Wind Structure in an Intense Frontal Zone." Bulletin of American Meteor Soc., V. 38, N.6, pp. 357-9, June 1957

35. Barad, M.L., "Low-Altitude Jet Stream." Scientific American. pp. 120-127, August 1961

36. Whitham, G.B., "A New Approach to Problems of Shock Dynamics, Part I, Two Dimensional Problems." Journal of Fluid Mechanics, Vol. 2, Part 2, March 1957

37. Maglieri, D.J., and Parrott, T.L., "Atmospheric Effects on Sonic Boom Pressure Signatures." Paper Presented to 63rd Meeting of Acoustical Society of America, New York, May 1962

38. Van Der Hoven, I., "Power Spectrum of Horizontal Wind Speed in the Frequency Range from 0.0007 to 900 cycles per hour." Journal of Meteorology 14, p. 160, 1957

39. Panofsky, H.A. and McCormick, R.A., "The Spectrum of Atmospheric Turbulence at 100 Meters." Quart. Journal Royal Meteorological Society 86, p. 495, 1960

40. Davenport, A.G., "The Spectrum of Horizontal Gustiness Near the Ground in High Winds." Quart. Journal Royal Meteorological Society 87, p. 194, 1961

41. Lumley, J.L. and Panofsky, H.A., "The Structure of Atmospheric Turbulence," Interscience, N.Y., 1964

42. Priestly, C.H.B., "Turbulent Transfer in the Lower Atmosphere," University Chicago Press, Chicago, 1959

43. Tsvang, L.R., "Measurements of Temperature Pulse Frequency Spectra in the Surface Layer." Izvestia ANSSSR Geo. Ser. No. 8, 1960

44. Batchelor, G.K., "Wave Scattering by Turbulence, Symp. on Naval Hydrodynamics." September 24-28, 1956, Washington, D.C., Pub. 515, National Academy of Sciences, NRC, Washington, D.C., 1957

45. Benkeris, C.L., "Note on Scattering of Radiation in an Inhomogen Medium." Physical Rev. 71, p. 268, 1947

46. Blokhintzev, D., "The Propagation of Sound in an Inhomogeneous and Moving Medium I." Journal Acoustical Society of America 18, p. 322, 1946

47. Blokhintzev, D., "The Propagation of Sound in an Inhomogeoneous and Moving Medium II." Journal Acoustical Society of America 18, p. 329, 1946

48. Lighthill, M.J., "On Sound Generated Aerodynamically, I General Theory, "Proc. Roy Soc Lond, A (211) p. 564, 1952

49. Lighthill, M.J., "On Sound Generated Aerodynamically, II Turbulence as a Source of Sound," Proc. Roy Soc London (222) p. 1, 1954

50. Kraichnan, R.H., "The Scattering of Sound in a Turbulent Medium," J. Acoustical Society of America 25, 1096, 1953

51 Tatarski, V.I., "Wave Propagation in a Turbulent Medium," McGraw-Hill, N.Y., 1961

52. Welkourtz, W.W., "Sound Fluctuations Caused by Turbulent Winds," Project Michigan Technical Report No. 2, Contract DA-36-039 SC 52654, 10 August 1955

53. Moriuchi, "Effects of Atmospheric Turbulence on the Propagation of Sound," Columbia University, Department of Electrical Engineering Technical Report No. 3, Contract No. 266123, March 1, 1954

54. Kallistratova, M.A., "Experimental Investigation of the Scattering of Sound in the Atmosphere," Proc. 3rd Int'l Congress on Acoustics Stuttgart, 1959, D. Cremer Ed. Vol. I, Principles, Elsevier Pub. Co., N.Y., P. 295, 1961

55. Harris, C.M., and Kirvida, L.B., "Phase Flucturations of Sound Propagated in an Inhomogeneous Atmosphere," Proc. 3rd Int'l Congress on Acoustics, Stuttgart, 1959, D. Cremer Ed. Vol. I, Principles, Elsevier Pub. Co., N.Y., p. 286, 1961

56. Lighthill, M.J., "On the Energy Scattered from the Interaction of Turbulence with Sound or Shockwaves," Proc. Cambridge Phil. Soc. 49, p. 531, 1953

57. Courant, R. and Hilbert, D., "Methods of Mathematical Physics Vol. II, Partial Differential Equations," Interscience, N.Y., pp. 206ff, 1962

58. Morse, P.M. and Feshbach, H., "Methods in Theoretical Physics," McGraw Hill, N.Y., 1953

59. Meecham, W.C. and Ford, G.W., "Acoustic Radiation from Isotropic Turbulence," Journal Acoustical Society of America 30, p. 318, 1958

60. Sears, W.R., "General Theory of High Speed Aerodynamics," Princeton University Press, Princeton, N.J., 1954

61 Jackson, J.D.,"Classical Electrodynamics," John Wiley, N.Y., 1962

62. Stratton, J.A., "Electromagnetic Theory," McGraw-Hill, N.Y., 1941

63. Aitchison, J. and Brown, J.A.C., "The Lognormal Distribution," Cambridge University Press, 1963

64. Johnson, N.L., "Systems of Frequency Curves Generated by Methods of Translation," Biometrika 36, p. 149, 1949

65. Johnson, N.L., "Bivariate Distributions Based on Simple Translation Systems," Biometrika 36, p. 297, 1949

66. Moshman, J., "Critical Values of the Log-normal Distribution," American Statistical Association Journal, p. 600, September 1953

67. Taylor, G.I., "Statistical Theory of Turbulence, Parts, I-IV," Proc. Roy. Soc. A151, p. 421-478 (1935) as reprinted in Turbulence, S.K. Friedlander and L. Topper ed. Interscience, N.Y., 1961

68. Taylor, G.I., "The Spectrum of Turbulence," Proc. Royal Society A164, p. 476-490 (1938) as reprinted in Turbulence, S.K. Friedlander and L. Topper ed. Interscience, N.Y., 1961

69. Kolmogoroff, A.N., "The Local Structure of Turbulence in Incompressible Viscous Fluid for Very Large Reynold' Numbers," Computes rendus (Doklady) de l'Acadamie Des Sciences de l'U.R.S.S. 30, 301-305 (1941) as reprinted in Turbulence, S.K. Friedlander and L. Topper ed. Interscience, N.Y., 1961

70. Kolmogoroff, A.N., "On Degeneration of Isotropic Turbulence in an Incompressible Viscous Liquid," Computes rendus (Doklady) de l'Acadamie des Sciences de l'U.R.S.S. 31 538-540 (1941) as reprinted in Turbulence, S.K. Friedlander and L. Topper ed. Interscience, N.Y., 1961

71. "Equations, Tables, and Charts for Compressible Flow." NACA Report 1135, 1953

72. Von Rues, D.and Böttger, P., "An Approximate Solution for Mach Reflections (Eine Näherungslösung Für Machreflexionen)." Zeitschrift Fur Angewandte Mathematik und Mechanik, Vol. 43, pp. 167-168, 1963

73. Liepmann, H.W. and Roshko, A., "Elements of Gas Dynamics," John Wiley & Sons, 1958

74. Pack, D.C., "The Reflection and Diffraction of Shock Waves." Journal of Fluid Mechanics," Vol. 18, Part 4, 1964

75. Whitham, G.B., "Flow Pattern of a Supersonic Projectile." Communications on Pure and Applied Mathematics," Vol. V, p. 301-348, 1952

76. Brown, J.R., "Radiosonde Meteorological Data Reduction - TA-108," Boeing Document D6-2387TN, September 1964

77. Friedman, M.P., "A Study of Atmospheric Effects on Sonic Booms." MIT Aerophysics Laboratory Technical Report 89, April 1964

78. Lansing, D.L., "Some Effects of Flight Maneuvers on the Distribution of Sonic Booms." Paper presented to Symposium on Atmospheric Acoustic Propagation, El Paso, Texas, June 1961

79. Prandtl, L. and Tiejens, O.G., "Applied Hydro and Aeromechanics." Dover Publications, Inc.

80. Carlson, H.W., "Influence of Airplane Configuration on Sonic Boom Characteristics." Journal of Aircraft, Vol. 1, No. 2, March-April 1964

81. Palmer, T.Y., "Effects of Turbulence on the Sonic Boom." Paper presented to Fifth Conference on Applied Meteorology of the American Meteorological Society, March, 1964

82. Sternberg, J. "Triple-Shock-Wave Intersections." The Physics of Fluids, Vol. 2, No. 2, p. 179, Mar.-Apr. 1959

83. Friedman, M.P., "A Study of Atmospheric Effects on Sonic Booms". NASA CR-157, 1965 (Digital computer program available from NASA Langley, Dynamic Loads Division.)

84. Hubbard, H.H., Maglieri, D.J., Huckel, V., and Hilton, D.A., "Ground Measurements of Sonic Boom Pressures for the Altitude Range of 10,000 to 75,000 Feet." NASA Technical Report R-198, July, 1964

85. Cox, E.F., "Sound Propagation in Air." Handbuch der Physic, Vol. 48, Chapter 22, Springer, Berlin, 1958

86. Lamb, H. "Hydrodynamics." Dover Publications, Sixth Edition, New York, 1945

GPO 887-279

The Boeing Company, Airplane Division, Renton, Wash.
METEOROLOGICAL ASPECTS OF THE SONIC BOOM by
E. J. Kane and T. T. Palmer. Final Report, Sept. 1964,
134 pp. , incl. illustrations, includes Bibliography, (86 refs).
(Contract No. FA-WA-4717. Project No. 206-003-R.
Report No. RD-64-160

Unclassified Report

This report is a study of the effect of changing meteorological conditions on the sonic boom produced during steady level flight. The influence of variations in atmospheric temperature, pressure, and wind on this noise are investigated. Simplified methods are established for estimating the effect of these variations. Combinations of meteorological conditions which can produce anomalous propagation such as complete cut-off, focusing, and extreme lateral spread are discussed. The effect of air turbulence near the ground is considered. A number of comparisons with test data measured at Oklahoma City (1964) are presented, and recommendations for additional experimental and theoretical work are outlined.

UNCLASSIFIED

I. Kane, E. J.
Palmer, T. Y.
II. Contract No. FA-WA-4717
III. Project No. 206-003-R
IV. Report No. RD-64-160

DESCRIPTORS

Cut-Off
Focusing
Lateral Distribution
Meteorology
Noise
Pressure
Sonic Boom
Supersonic
Temperature
Turbulence
Wind

UNCLASSIFIED

The Boeing Company, Airplane Division, Renton, Wash.
METEOROLOGICAL ASPECTS OF THE SONIC BOOM by
E. J. Kane and T. Y. Palmer. Final Report, Sept. 1964,
134 pp. , incl. illustrations, includes Bibliography, (86 refs).
(Contract No. FA-WA-4717. Project No. 206-003-R.
Report No. RD-64-160

Unclassified Report

This report is a study of the effect of changing meteorological conditions on the sonic boom produced during steady level flight. The influence of variations in atmospheric temperature, pressure, and wind on this noise are investigated. Simplified methods are established for estimating the effect of these variations. Combinations of meteorological conditions which can produce anomalous propagation such as complete cut-off, focusing, and extreme lateral spread are discussed. The effect of air turbulence near the ground is considered. A number of comparisons with test data measured at Oklahoma City (1964) are presented, and recommendations for additional experimental and theoretical work are outlined.

UNCLASSIFIED

I. Kane, E. J.
Palmer, T. Y.
II. Contract No. FA-WA-4717
III. Project No. 206-003-R
IV. Report No. RD-64-160

DESCRIPTORS

Cut-Off
Focusing
Lateral Distribution
Meteorology
Noise
Pressure
Sonic Boom
Supersonic
Temperature
Turbulence
Wind

UNCLASSIFIED

The Boeing Company, Airplane Division, Renton, Wash.
METEOROLOGICAL ASPECTS OF THE SONIC BOOM by
E. J. Kane and T. T. Palmer. Final Report, Sept. 1964,
134 pp. , incl. illustrations, includes Bibliography, (86 refs).
(Contract No. FA-WA-4717. Project No. 206-003-R.
Report No. RD-64-160

Unclassified Report

This report is a study of the effect of changing meteorological conditions on the sonic boom produced during steady level flight. The influence of variations in atmospheric temperature, pressure, and wind on this noise are investigated. Simplified methods are established for estimating the effect of these variations. Combinations of meteorological conditions which can produce anomalous propagation such as complete cut-off, focusing, and extreme lateral spread are discussed. The effect of air turbulence near the ground is considered. A number of comparisons with test data measured at Oklahoma City (1964) are presented, and recommendations for additional experimental and theoretical work are outlined.

UNCLASSIFIED

I. Kane, E. J.
Palmer, T. Y.
II. Contract No. FA-WA-4717
III. Project No. 206-003-R
IV. Report No. RD-64-160

DESCRIPTORS

Cut-Off
Focusing
Lateral Distribution
Meteorology
Noise
Pressure
Sonic Boom
Supersonic
Temperature
Turbulence
Wind

UNCLASSIFIED

The Boeing Company, Airplane Division, Renton, Wash.
METEOROLOGICAL ASPECTS OF THE SONIC BOOM by
E. J. Kane and T. Y. Palmer. Final Report, Sept. 1964,
134 pp. , incl. illustrations, includes Bibliography, (86 refs).
(Contract No. FA-WA-4717. Project No. 206-003-R.
Report No. RD-64-160

Unclassified Report

This report is a study of the effect of changing meteorological conditions on the sonic boom produced during steady level flight. The influence of variations in atmospheric temperature, pressure, and wind on this noise are investigated. Simplified methods are established for estimating the effect of these variations. Combinations of meteorological conditions which can produce anomalous propagation such as complete cut-off, focusing, and extreme lateral spread are discussed. The effect of air turbulence near the ground is considered. A number of comparisons with test data measured at Oklahoma City (1964) are presented, and recommendations for additional experimental and theoretical work are outlined.

UNCLASSIFIED

I. Kane, E. J.
Palmer, T. Y.
II. Contract No. FA-WA-4717
III. Project No. 206-003-R
IV. Report No. RD-64-160

DESCRIPTORS

Cut-Off
Focusing
Lateral Distribution
Meteorology
Noise
Pressure
Sonic Boom
Supersonic
Temperature
Turbulence
Wind

UNCLASSIFIED

The Boeing Company, Airplane Division, Renton, Wash.
METEOROLOGICAL ASPECTS OF THE SONIC BOOM by
E. J. Kane and T. T. Palmer. Final Report, Sept. 1964.
134 pp., incl. illustrations, includes Bibliography. (86 refs).
(Contract No. FA-WA-4717. Project No. 206-003-R.
Report No. RD-64-160

Unclassified Report

This report is a study of the effect of changing meteorological conditions on the sonic boom produced during steady level flight. The influence of variations in atmospheric temperature, pressure, and wind on this noise are investigated. Simplified methods are established for estimating the effect of these variations. Combinations of meteorological conditions which can produce anomalous propagation such as complete cut-off, focusing, and extreme lateral spread are discussed. The effect of air turbulence near the ground is considered. A number of comparisons with test data measured at Oklahoma City (1964) are presented, and recommendations for additional experimental and theoretical work are outlined.

UNCLASSIFIED

I. Kane, E. J.
Palmer, T. Y.
II. Contract No. FA-WA-4717
III. Project No. 206-003-R
IV. Report No. RD-64-160

DESCRIPTORS

Cut-Off
Focusing
Lateral Distribution
Meteorology
Noise
Pressure
Sonic Boom
Supersonic
Temperature
Turbulence
Wind

UNCLASSIFIED

The Boeing Company, Airplane Division, Renton, Wash.
METEOROLOGICAL ASPECTS OF THE SONIC BOOM by
E. J. Kane and T. Y. Palmer. Final Report, Sept. 1964.
134 pp., incl. illustrations, includes Bibliography. (86 refs).
(Contract No. FA-WA-4717. Project No. 206-003-R.
Report No. RD-64-160

Unclassified Report

This report is a study of the effect of changing meteorological conditions on the sonic boom produced during steady level flight. The influence of variations in atmospheric temperature, pressure, and wind on this noise are investigated. Simplified methods are established for estimating the effect of these variations. Combinations of meteorological conditions which can produce anomalous propagation such as complete cut-off, focusing, and extreme lateral spread are discussed. The effect of air turbulence near the ground is considered. A number of comparisons with test data measured at Oklahoma City (1964) are presented, and recommendations for additional experimental and theoretical work are outlined.

UNCLASSIFIED

I. Kane, E. J.
Palmer, T. Y.
II. Contract No. FA-WA-4717
III. Project No. 206-003-R
IV. Report No. RD-64-160

DESCRIPTORS

Cut-Off
Focusing
Lateral Distribution
Meteorology
Noise
Pressure
Sonic Boom
Supersonic
Temperature
Turbulence
Wind

UNCLASSIFIED

The Boeing Company, Airplane Division, Renton, Wash.
METEOROLOGICAL ASPECTS OF THE SONIC BOOM by
E. J. Kane and T. T. Palmer. Final Report, Sept. 1964.
134 pp., incl. illustrations, includes Bibliography. (86 refs).
(Contract No. FA-WA-4717. Project No. 206-003-R.
Report No. RD-64-160

Unclassified Report

This report is a study of the effect of changing meteorological conditions on the sonic boom produced during steady level flight. The influence of variations in atmospheric temperature, pressure, and wind on this noise are investigated. Simplified methods are established for estimating the effect of these variations. Combinations of meteorological conditions which can produce anomalous propagation such as complete cut-off, focusing, and extreme lateral spread are discussed. The effect of air turbulence near the ground is considered. A number of comparisons with test data measured at Oklahoma City (1964) are presented, and recommendations for additional experimental and theoretical work are outlined.

UNCLASSIFIED

I. Kane, E. J.
Palmer, T. Y.
II. Contract No. FA-WA-4717
III. Project No. 206-003-R
IV. Report No. RD-64-160

DESCRIPTORS

Cut-Off
Focusing
Lateral Distribution
Meteorology
Noise
Pressure
Sonic Boom
Supersonic
Temperature
Turbulence
Wind

UNCLASSIFIED

The Boeing Company, Airplane Division, Renton, Wash.
METEOROLOGICAL ASPECTS OF THE SONIC BOOM by
E. J. Kane and T. Y. Palmer. Final Report, Sept. 1964.
134 pp., incl. illustrations, includes Bibliography. (86 refs).
(Contract No. FA-WA-4717. Project No. 206-003-R.
Report No. RD-64-160

Unclassified Report

This report is a study of the effect of changing meteorological conditions on the sonic boom produced during steady level flight. The influence of variations in atmospheric temperature, pressure, and wind on this noise are investigated. Simplified methods are established for estimating the effect of these variations. Combinations of meteorological conditions which can produce anomalous propagation such as complete cut-off, focusing, and extreme lateral spread are discussed. The effect of air turbulence near the ground is considered. A number of comparisons with test data measured at Oklahoma City (1964) are presented, and recommendations for additional experimental and theoretical work are outlined.

UNCLASSIFIED

I. Kane, E. J.
Palmer, T. Y.
II. Contract No. FA-WA-4717
III. Project No. 206-003-R
IV. Report No. RD-64-160

DESCRIPTORS

Cut-Off
Focusing
Lateral Distribution
Meteorology
Noise
Pressure
Sonic Boom
Supersonic
Temperature
Turbulence
Wind

UNCLASSIFIED